Stable isotopic studies on monsoon vapour/clouds and precipitation over Kerala

A THESIS

submitted for the Award of Ph.D degree of

MOHANLAL SUKHADIA UNIVERSITY

in the

Faculty of Science

by

Lekshmy P R

Under the Supervision of

Dr. R. Ramesh

Outstanding Scientist

Geoscience Division

Physical Research Laboratory, Ahmedabad, India

DEPARTMENT OF PHYSICS

MOHANLAL SUKHADIA UNIVERSITY,

UDAIPUR, INDIA

2015

CERTIFICATE

I certify that the thesis entitled "Stable isotopic studies on monsoon vapour/clouds and precipitation over Kerala" by Mrs Lekshmy P R was prepared under my guidance. She has completed the following requirements as per Ph.D. regulations of the University

(a) Course work as per the university rules.

(b) Residential requirements of the university.

(c) Presented her work in the departmental committee.

(d) Published/accepted minimum of one research paper in referred research journals,

I am satisfied with the analysis of data, interpretation of results and conclusions drawn. I recommend the submission of the thesis.

Date:

Prof. R. Ramesh
(Supervisor)
Outstanding Scientist
Physical Research Laboratory
Ahmedabad, India.

Countersigned by
Head of the Department

DECLARATION

I Lekshmy P R, d/o Mr. P. V. Ravisankar, resident of A-5, PRL residences, Navrangpura, Ahmedabad - 380009, hereby declare that the research work incorporated in the present thesis entitled "Stable isotopic studies on monsoon vapour/clouds and precipitation over Kerala" is my own work and is original. This work (in part or in full) has not been submitted to any university or institute for the award of a Degree or a Diploma. I have properly acknowledged the material collected from secondary sources wherever required. I solely own the responsibility for the originality of the entire content.

Date:

Lekshmy P R

(Author)

Dedicating to

Amma, Achan and Hari

Acknowledgements

First and foremost I express my gratitude to my supervisors Prof R.Ramesh and Dr. M.G.Yadava for their supervision, invaluable advices and guidance. I would like to extend my deepest gratitude to Prof R.Ramesh for giving me freedom to work on my plans during the last 5 years. I am thankful to him for patiently correcting the unlimited mistakes I used to make in manuscripts also. It is only because of him I could complete my thesis. I really enjoyed working with him with great inspiration and I am indebted to him more than he knows.

I am specially thankful to Dr. Sanjeev Kumar and Dr. J.S. Ray for their most supporting words and the scientific suggestions and discussions. I thank R.A. Jani for discussions and introducing me to the mass spectrometer analyses in the stable isotope lab. I also thank N.B Vaghela Bhai for his all support and help in lab.

I thank all my teachers in PRL, Prof. M.M Sarin, Dr. A.K. Singal, Dr. Dibyendu Chakrabarty, Dr.S. Ramachandran, Dr. Kuljeet Marhas, Dr. Vinay K Ray, Dr. Varun Sheel and Dr. Jitesh Bhatt for their nice lectures during the course work period. I thank Dr. Lokesh Sahu for guiding me to do a project during the course work. Discussions with Dr. R.D. Deshpande and encouragement from him helped me a lot in the thesis work. The generous support from Dr. Sunil Singh, Dr. Shyam Lal, S. Venkataramani, T.A. Rajesh, D.K Rao, Virendra, Dr. Neeraj Rastogi, Dr. Bhushit and Dr. Navin Juyal is greatly appreciated.

I also acknowledge people from different sections of PRL: Pauline, Parulben, Sasi Kumar, Dr. Nishita Ma'am, Tejas, Sivadasan, Nandiniben, Pritiben, Richa, Sentil Babu, Manan Shah, Lakhan Bhai, M.P.K Kurup, Bankim Bhai, G.P Patel, Ranganathan, Jayashree, Prabha Ben, Nilesh Bhai, Ubale, Jayati Patel and Jaldhi for their helps at various stages. I also acknowledge those people who all helped

me in shifting, packing and cleaning the heavy scientific luggage and stuffs. I can never forget the lovely support and help from late Abdul Bhai. I am thankful to Pappu Bhai for making tasty egg 'omelets' and 'full fries' that made me survive during this period. Manoj Tank deserves a special thanks for solving the mass spectrometer problems.

I thank Lathika, Sreenivas, Abraham Baby, Sugunan, Rekha, Sivadasan, Adarsh, Smruthy, Asokan and PC Sreedharan for help in collecting the samples. I also acknowledge Rajiv Gandhi Centre for Biotechnology, Thiruvananthapuram and Centre for Water Resources Development and Management, Kozhikode, for providing Liquid Nitrogen for the water vapour collection.

I would also like to say thanks to all my dear batch mates, Gangi, Aathi, Girish, Gaurav, Monojith, Gulab, Yashpal, Dilip Nandi, Arko, Damorad, Naveen Negi, Avdesh, Tanmoy, Priyanka, Anjali, Upendra, Dinesh, Wageesh, Rajeev, Gorav Sharma and Nigam for creating a wonderful time in hostel and PRL. I sincerely thank Manu, Anirban, Ikshu, Abhaya, Arun, Girish, Tanmoy, Guruprasad, Ashim, Lalit, Deepak, Dipti, Ali, Jabir, Nijil, Vishnudath and Niharika and many others for making a memorable atmosphere in hostel and PRL. I deeply express my thanks to all my dear seniors Chinmay, Susanta, Prasant,Vineeth, Srinivas, Sunil, Arun Awasthi Fazlul, Shashi, and friends Balaji, Ejaz, Sneha, Upasana, Subha Anand, Komal, Rajlaxmi, Nisha and many others.

Together with Bhavya, Shraddha, Rupa, Niharika, Trina and Midhun, I had a very nice time in the stable isotope lab with lots of unforgettable memories. I was fortunate to have very good seniors in our lab. Amzad, Naveen and Arvind were really supportive and a good source of encouragement and knowledge.

Sometimes the word 'thank' cannot convey the complete feeling that I really mean in my mind. I will gratefully remember Blesson, Ranjith and Linto for *their love, care and the energy they gave me to wake up from my falls. I thank Chithrabhanu, Swapna for sharing a wonderful time in my life. A special thanks to Bivin Geo George for a good friendship and all support. The moments shared with Anju, Apurv, Neetha, Sreeja, Nita, Aswathi and my lovely angels Gargi, Allen and Aaron were really sweet and memorable. If I say thanks to Bhavya, she will definitely laugh on it, I know. But I should mention that she has gifted me many wonderful moments in the past 7 years; the loveliest were the peacock feather hunts in 'Thaltej forest', which I used to like more than isotopes, indeed. I keep the memories of continuous support from my dear friend Sudha in my mind all the time.*

Last but not least, I thank my amma, achan and Hari for their love, giving me strength in my weaknesses, putting a lot of efforts in the sample collections in Kerala and above all for motivating me to reach here. Midhun was there with me in all my happiness and sorrows with a lot of efforts from his side to complete my thesis. I thank midhun's parents and Chinchu as well for their continuous support.

I have been fighting with pigeons for the last 5 years, for disturbing me in my sleep and making nests in my windows and balcony. 'I have destroyed your hundreds of nests, thrown your lovely eggs to the garden without any mercy. But, you again made new nests and laid eggs. I express my great affection to you here, though I know you are neither going to read this nor I will stop the fight. I thank you for encouraging me in the silent fights, for teaching me to enjoy the happiness of small victories and above all for teaching me that there can be no permanent hatred in mind.' Otherwise they would have never come back to my balcony again.....

Lekshmy PR

Abstract

Stable isotopes of water provide a tool for studying the hydrological cycle and reconstructing past climate from proxies such as tree rings, speleothems, ice cores etc. It is important to understand the responses of the stable isotopic composition of rain and water vapour to various climate conditions for accurate paleoclimate reconstruction. In India, due to lack of sufficient observations, such studies were limited. The hydrological processes determining the isotopic composition of rain and water vapour and their importance in paleomonsoon reconstruction are studied here.

High resolution (spatial and temporal) rain and water vapour isotopic observations were done from the Kerala, south western peninsular India. The new results obtained from this work are as under: though the rainfall showed a large spatial heterogeneity in the study area, its isotopic composition remained coherent during the Indian summer monsoon period. The amount of rain had a very weak role in determining the isotopic composition of rain. Stronger ^{18}O and D depletion of rain is associated with large scale organised convection occurring in the south eastern Arabian Sea, near the Kerala coast. The intense moisture recycling occurring in the large scale convective area is responsible for the higher ^{18}O and D depletion of rain. Water vapour and rain are in isotopic equilibrium during Indian summer monsoon season and deviate more from equilibrium mainly during such large scale organised convective events. The fraction of stratiform rain from large scale convective area shows a significant negative correlation with the

$\delta^{18}O$ of vapour and rain; this signifies the role of stratiform clouds in moisture recycling during such events.

Varying seasonal rainfall amounts in peninsular India and Sri Lanka lead to a large spatial variation in the slopes of the rainfall amount -$\delta^{18}O$ relations. The stronger ^{18}O depletion of north east monsoon rainfall is likely caused by increased cyclonic activity over the Bay of Bengal, in addition to ^{18}O depletion of its surface waters by river discharge. This leads to significant negative correlations between monthly rainfall and its $\delta^{18}O$ chiefly in regions where the north east monsoon contributes more than, or at least as much rain as the Indian summer monsoon. Interannual variations in the amount effect due to varying interannual contributions of Indian summer monsoon and north east monsoon rainfall is also noted. Thus, a careful choice of sites for ^{18}O based monsoon proxies can be made so as to minimise noise in the paleomonsoon signal that could arise at sites with inverse amount effects. Using proxies capable of providing annual resolution (e.g., fast growing trees) past annual monsoon rainfall can be reconstructed at sites where the ratio of Indian summer monsoon season to north east monsoon rain continues to remain less than or comparable to unity, using the local amount effect.

Key words: Indian Summer monsoon, Oxygen and Hydrogen isotopes, large scale organised convection, amount effect.

Abbreviations

α	Isotopic fractionation factor between product and source
$\delta^{18}O$	Oxygen isotopic composition of water relative to VSMOW standard
δD	Deuterium isotopic composition of water relative to VSMOW standard
ϵ	Isotopic enrichment factor i.e, $(\alpha - 1) \times 10^3$
‰	per mil (parts per thousand)
AS	Arabian Sea
BoB	Bay of Bengal
CRU	Climate Research Unit
EKM	Ernakulam
ENSO	El Nino Southern Oscillation
GDAS	Global Data Assimilation System
GDP	Gross domestic product
GISP	Greenland Ice Sheet Precipitation
GMWL	Global Meteoric Water Line
GNIP	Global Network of Isotopes in Precipitation
GPCP	Global Precipitation Climatology Project
HYSPLIT	Hybrid Single-Particle Lagrangian Integrated Trajectory
IAEA	International Atomic Energy Agency
IDK	Idukki
IRMS	Isotope Ratio Mass Spectrometer
ISM	Indian Summer Monsoon

IST	Indian Standard Time
ITCZ	Inter Tropical Convergence Zone
JJAS	June, July, August, September
KKD	Kozhikode
LLJ	Low Level Jet
LMWL	Local Meteoric Water Line
MCZ	Maximum Cloud Zone
MERRA	Modern Era Retrospective-Analysis for Research and Application
NARM	Narmada water standard
NBR	Nilambur
NOAA	National Oceanic and Atmospheric Administration
NCEP	National Centers for Environmental Prediction
NEM	North East Monsoon
OLR	Outgoing Longwave Radiation
OND	October, November, December
PKD	Palakkadu
PND	Ponmudi
PRL	Physical Research Laboratory
QBO	Quasi Biennial Oscillation
SL	Subcloud Layer
SLAP	Southern Light Antarctic Precipitation
SST	Sea Surface Temperature
TCR	Thrissur
TRMM	Tropical Rainfall Measuring Mission
TVM	Thiruvananthapuram
VSMOW	Vienna Standard Mean Ocean Water (IAEA water standard)
WICO	Interlaboratory comparison exercise for δ^2H and $\delta^{18}O$ analysis of water samples
WYD	Wayanad

Contents

List of Figures **xiii**

List of Tables **xv**

1 Introduction **1**

1.1 Indian Summer Monsoon (ISM) 2

1.1.1 Mechanism 2

1.1.2 Variability 4

1.1.3 Paleo-monsoon reconstruction 4

1.2 Stable isotopologues of water 5

1.2.1 Notations 6

1.2.2 Isotopic Fractionation 7

1.2.3 Rayleigh model for isotopic fractionation 8

1.2.4 Global Meteoric Water Line (GMWL) 10

1.2.5 Deuterium-excess 10

1.2.6 Observed isotopic effects 11

1.3 Previous studies in India 17

1.4 Outline of the thesis 19

1.5 Major Questions addressed in the present study 20

2 Materials and Methods **21**

2.1 Sample collection 22

2.1.1 Rain water collection 23
2.1.2 Water vapour collection 24
2.2 Isotopic analysis 25
2.2.1 Isotope ratio mass spectrometry 25
2.2.2 $\delta^{18}O$ and δD measurements 28
2.2.3 Calibration of laboratory standards 30
2.3 Additional data used 32
2.3.1 Global Network of Isotopes in Precipitation (GNIP) 32
2.3.2 Hybrid Single-Particle Lagrangian Integrated Trajectory (HYSPLIT) 33
2.3.3 Satellite/ reanalysis/ model data 33

3 Investigation of the cause of amount effect in tropical rain 35

3.1 Monsoon performance during 2012 and 2013 36
3.2 Spatial variation of rainfall and $\delta^{18}O$ 38
3.3 Intra-seasonal variations of $\delta^{18}O$ 41
3.4 Amount effect 44
3.5 Role of convective activity 47
3.6 ^{18}O and D depleted and enriched rain events 50
3.7 Influence of spatially extended rain events 53
3.8 Moisture source variation 54
3.9 Anomalous events 54
3.10 Monsoon withdrawal 56
3.11 Conclusion 57

4 Water vapour- rain isotopic interactions over Kerala 59

4.1 Back trajectory analysis 61
4.2 Variations of δD and $\delta^{18}O$ of Vapour 64
4.3 Rain-vapour isotopic interaction 67
4.4 Moisture recycling during the Indian summer monsoon 70

4.5 Conclusions 72

5 'Amount effect' in peninsular India and Sri Lanka 73

5.1 The amount effect in peninsular India and Sri Lanka 75

5.2 Controls on NEM rainfall $\delta^{18}O$ 81

5.2.1 ^{18}O depletion in BoB surface water 82

5.2.2 Continental effect 84

5.2.3 Effect of cyclonic disturbances in BoB 85

5.3 Rainfall- $\delta^{18}O$ relation on a seasonal scale 87

5.4 Conclusion 89

6 Summary and recommendations 91

6.1 Results from the study of stable isotopes of monsoon rainfall . . . 91

6.2 Results from rain and vapour interaction studies 92

6.3 Results from studies on the rainfall-$\delta^{18}O$ relations 93

6.4 Recommendations 95

References 96

List of Publications 107

List of Figures

1.1 Meteorological conditions during ISM . . . 3
1.2 Rayleigh isotopic distillation curve . . . 9
1.3 Global temperature- $\delta^{18}O$ relationship in precipitation . . . 11
1.4 Relation between rainfall and its $\delta^{18}O$ . . . 12
1.5 Schematic representation of a convective cloud system . . . 13
1.6 $\delta^{18}O$ variation with altitude . . . 15
1.7 Latitude effect . . . 16
1.8 Continental effect . . . 16

2.1 Sampling locations . . . 22
2.2 Rainfall collection system . . . 23
2.3 Water vapour collection system . . . 24
2.4 Isotope ratio mass spectrometer . . . 26
2.5 Measured and reported values of the international standards . . . 31

3.1 Seasonal rainfall and $\delta^{18}O$ over each station . . . 37
3.2 Local meteoric water line of rainfall in Kerala . . . 38
3.3 Time series of the amount of rain, $\delta^{18}O$ and convective activity during 2012 . . . 41
3.4 Time series of the amount of rain, $\delta^{18}O$ and convective activity during 2013 . . . 42
3.5 Relation between monthly rainfall and its $\delta^{18}O$ . . . 45

3.6 Relation between daily rainfall and its $\delta^{18}O$ 46

3.7 Correlation between rain amount and its $\delta^{18}O$ in TVM and TCR 48

3.8 Relation between $\delta^{18}O$ and proxies of large scale convection 49

3.9 Co-occurrence of large scale convection and isotopically depleted rain during 2012 51

3.10 Co-occurrence of large scale convection and isotopically depleted rain during 2013 52

3.11 Spatial correlation pattern of the daily $\delta^{18}O$ and rainfall 53

3.12 Back trajectory analyses 55

4.1 Back trajectories and $\delta^{18}O$-δD relations of rain and vapour during different seasons 62

4.2 Time series of heavy isotopic concentration of rainfall and vapour 65

4.3 The relation between $\delta^{18}O$ of vapour and the $\delta^{18}O$ of vapour in isotopic equilibrium with the rain 68

4.4 Schematic representation of wind pattern over Peninsular India during ISM and NEM seasons 69

4.5 Relation between stratiform rain and the $\delta^{18}O$ of rain and vapour 71

5.1 Spatial pattern of the ratio of ISM to NEM rainfall and correlation coefficients between monthly rain and their $\delta^{18}O$ 78

5.2 Linear correlation coefficient (R) between rainfall and $\delta^{18}O$ plotted as a function of the number of monthly data 81

5.3 Monthly mean rainfall $\delta^{18}O$ at Kozhikode, Mumbai, Hyderabad and Kakinada 85

5.4 Co-occurance of ^{18}O depleted NEM rain and cyclones in BoB . . . 86

5.5 $\delta^{18}O$ variation of a low pressure cyclonic storm 86

5.6 a) Relation between ISM rainfall anomaly at peninsular India and $\delta^{18}O$ of rain at Kozhikode. b) Relation between all India ISM rainfall anomaly and $\delta^{18}O$ of rain at Kozhikode. 89

List of Tables

1.1 Stable isotopes of hydrogen and oxygen 5

2.1 Sample preparation methods and mass spectrometric parameters . 29

2.2 Measured and reported values of the international standards . . . 31

2.3 Calibrated values of laboratory standards; calculated with respect to the international standards. 32

2.4 Details of different satellite data used in the present study 34

3.1 Number of common rain events between different stations during 2012 and 2013 39

3.2 Linear cross correlation coefficients of rainfall and $\delta^{18}O$ between different stations 40

4.1 Seasonal mean $\delta^{18}O$, δD and $d-$excess values of water vapour and rain 66

5.1 Rainfall-$\delta^{18}O$ relations in different stations at peninsular India and Sri Lanka 76

5.2 Table 5.1 cont'd 77

5.3 Correlation coefficients between monthly rainfall and its $\delta^{18}O$ calculated for every 2 consecutive years 80

5.4 $\delta^{18}O$ of vapour flux from BoB 83

5.5 Relation between rainfall and its $\delta^{18}O$ at Kozhikode on monthly and seasonal scales 88

Chapter 1

Introduction

Earth's climate has been changing throughout its past history [*Augustin et al.*, 2004; *Dansgaard et al.*, 1993; *Masson-Delmotte et al.*, 2013]. Both natural and anthropogenic factors are known to be responsible for this [*Crowley*, 2000; *Forster et al.*, 2007]. The last two centuries experienced severe changes in climate, especially the rise in global temperature, which is due to the anthropogenic CO_2 emissions. The present day hydrological cycle, on which the world population is highly dependent, is also highly susceptible to the climate change. In particular, in the Indian context, melting of Himalayan glaciers [*Singh et al.*, 2014] extreme rain events [*Goswami et al.*, 2006] show an increasing trend. Our knowledge about the past climatic variations are limited because instrumental weather records are short. Since it is necessary to understand the past climate variability for the future climate projection, we make use of paleoclimate proxies to reconstruct past climate. *The present study is an attempt to understand the response of stable isotopes of water to the climate change for a better reconstruction of paleoclimate from climatic proxies.*

This chapter is a brief introduction about the Indian Summer Monsoon (ISM), emphasising on its mechanism and variability. The stable isotopologues of water (*see p.5*) used for the study of hydrological cycle and paleoclimatic reconstruction are also explained in detail, followed by a review of most previous stable isotopic studies carried out on rain and water vapour in India.

1.1 Indian Summer Monsoon (ISM)

ISM refers to the seasonal reversal of prevailing north easterly winter wind into south westerly summer wind over the Indian domain and the subsequent enhanced rain over India and the nearby countries during June- September every year. Since ISM contributes to ∼80% of the annual total rainfall in India, the economy of the country depends upon the performance of the monsoon [*Gadgil and Gadgil*, 2006]. Abnormal fluctuations of the date of onset of the monsoon (starting day of monsoon rainfall) and the total quantum of rainfall thus lead to severe economic burden on the government. Understanding the fluctuation of ISM for accurate forecasting and projection is therefore very important in the context of recent climate change.

1.1.1 Mechanism

There are mainly two hypotheses regarding the mechanism of monsoon. In 1686 CE, Halley proposed that the differential heating of land and ocean causes monsoon and thus it is a gigantic sea breeze. Currently, many scientists consider monsoon as the seasonal migration of Inter Tropical Convergence Zone (ITCZ) onto the continental south western Asia [*Gadgil*, 2003; *Wang*, 2006].

ISM has different spatial components that extend from the southern to the northern hemisphere [Fig 1.1(a)]. During the boreal summer, due to the intense heating of continents in the northern hemisphere, a low pressure area forms over northern India. The low pressure associated with this heating is called heat low (<999 mb). It extends from northern Rajasthan to Kolkata at the surface level, known as the monsoon trough. Simultaneously, austral winter leads to the formation of a high pressure area over the southern hemispheric subtropical Indian ocean ($\sim 30^{o}$S), also called the Mascarene High (>1023 mb). This pressure difference drives a strong wind across the equator, the maximum of which has a curved path (due to Coriolis force) [Fig 1.1(a)]. This is called the Low Level Jet stream (LLJ). A huge moisture uptake takes place along the path of LLJ over Arabian Sea (AS) which leads to copious rainfall over India [Fig 1.1(b)]. Rainfall peaks are observed along the mountain ranges of Western Ghats and eastern end of Himalaya extending to the south along Myanmar [*Wang*, 2006].

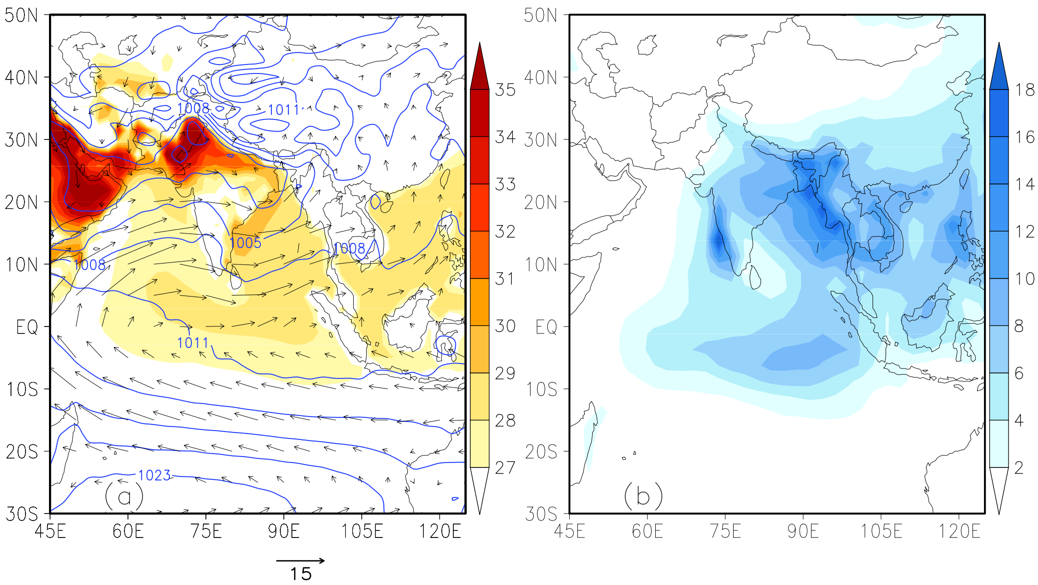

Figure 1.1: (a) The climatological average surface air temperature (gradient shown in shades of red and yellow), surface pressure pattern (contours of isobars in blue colour at 3mb intervals) and the surface wind vectors (black arrows) (b) the observed climatological (1979-2010 CE) total rainfall during June- September [Data sources: NCEP Climate Forecast System Reanalysis temperature, wind and surface pressure data and Global Precipitation Climatology Project (GPCP) rainfall data].

1.1.2 Variability

Instrumental records and the available paleo monsoon archives show that ISM varies on different time scales from intraseasonal to interannual, decadal, centennial and millennial time scales [*e.g., Gadgil*, 2003; *Ramesh et al.*, 2010]. The intra seasonal variability of monsoon observed by the 30-60 day oscillations, associated with the active and break cycles of monsoon [*Rajeevan et al.*, 2010] and the 10-20 day oscillations, associated with the propagation of weather disturbances from Western equatorial Pacific Ocean [*Goswami and Mathew*, 1994] are mainly determined by the internal dynamics. The interannual variability of monsoon rainfall is mainly controlled by both the internal dynamics as well as the external controls such as El Niño Southern Oscillations (ENSO) [*Kumar et al.*, 2006], snow cover anomalies [*Fasullo*, 2004], stratospheric Quasi Biennial Oscillations (QBO) [*Bhalme et al.*, 1987], the solar cycle etc. The longer time scale variability (decadal to millennial) is controlled by the changes in incoming solar radiation (insolation) associated with changes in the Earth's orbital parameters along with the changes in circulation pattern [*Leuschner and Sirocko*, 2003].

1.1.3 Paleo-monsoon reconstruction

Past instrumental records of rainfall over India are limited up to the mid 19^{th} century, which is not sufficient to study the variability of monsoon on longer time scales. So retrieval of past rainfall variations from different rainfall proxies is needed. Many methods are used for paleoclimate reconstruction *viz.,* study of ancient manuscripts, dentroclimatology [*e.g., Esper et al.*, 2002] and stable isotope proxies to reconstruct the past climate. Stable isotopes of water (hydrogen and oxygen) are good tools to reconstruct continuous past climate variations on longer time scales. Continental proxies such as tree rings [*e.g., Managave et al.*, 2011; *Ramesh et al.*, 1989; *Sano et al.*, 2011], cave calcites [*e.g., Sinha et al.*, 2015; *Yadava et al.*, 2004], ice cores [*e.g., Petit et al.*, 1999; *Thompson et al.*, 1997] and marine sediments [*e.g., Overpeck et al.*, 1996; *Tiwari et al.*, 2006], corals [*e.g., Chakraborty and Ramesh*, 1993; *Charles et al.*, 1997] etc are used for paleoclimate reconstruction through stable isotopic analyses. For this, a good understanding of the isotopic responses of the proxies to different climatic parameters at the present climate is required (i.e. calibration).

1.2 Stable isotopologues of water

Isotopes are nuclides with the same atomic number (i.e., proton number) and different masses (different neutron numbers). Radioactive isotopes show certain probability of decay while, stable isotopes do not spontaneously disintegrate by any known mode of decay.

Table 1.1: Stable isotopes of hydrogen and oxygen and their different combinations to form water isotopologues, along with their natural abundances [*source: Clark and Fritz*, 1997].

Isotope	Abundance (%)	Water isotopologues	Abundance (%)
H	99.98	$H_2{}^{16}O$	99.73
D	0.015	HD^{16}O	0.015
^{16}O	99.76	$D_2{}^{16}O$	2.24×10^{-6}
^{17}O	0.035	$H_2{}^{17}O$	0.035
^{18}O	0.205	HD^{17}O	5.2510^{-6}
		$D_2{}^{17}O$	7.88×10^{-10}
		$H_2{}^{18}O$	0.20
		HD^{18}O	3.07×10^{-5}
		$D_2{}^{18}O$	4.6×10^{-6}

Different combinations of these isotopes form water molecules with different masses, called water isotopologues. The natural abundances of hydrogen and oxygen isotopes and water isotopologues are given in Table 1.1. In the hydrological cycle, water undergoes phase transitions (mainly evaporation, condensation and freezing). Due to the different rates of participation of isotopologues in the processes (mainly due to their mass difference), their relative abundance changes during different processes of the hydrological cycle. Monitoring the variations in the abundances of water isotopologues ($H_2^{18}O$ and HDO) can provide detailed knowledge on the hydrological cycle.

1.2.1 Notations

The relative abundance of any heavier isotope is conveniently represented as its ratio with that of the lighter one.

$$R = \frac{\text{Abundance of the heavier isotope}}{\text{Abundance of the lighter isotope}}$$

Since the absolute ratios of isotopes are difficult to measure and only relative variations are important, isotopic ratios are expressed as deviations (δ) from that of an international standard. Water isotopic compositions are mostly reported with respect to the standard provided by the International Atomic Energy Agency (IAEA): Vienna Standard Mean Ocean Water (VSMOW) [*Clark and Fritz*, 1997]. For example, the deuterium or oxygen-18 abundances in a sample are commonly reported as

$$\delta D = \left(\frac{R_{Sample}}{R_{Standard}} - 1\right) \times 10^3 ‰$$

and

$$\delta^{18}O = \left(\frac{R_{Sample}}{R_{Standard}} - 1\right) \times 10^3 ‰,$$

respectively.

1.2.2 Isotopic Fractionation

Abundance of water isotopologues changes during phase transitions due to their difference in vapour pressures. Lighter isotopologues of water preferentially evaporate while the heavier ones preferentially condense. This differential participation of isotopologues leads to isotopic fractionation. The fractionation factor is expressed as the ratio of isotopic ratios in two coexisting phases.

$$\text{Fractionation factor,}\alpha_{Liquid}^{Vapour} = \frac{R_{Vapour}}{R_{Liquid}}$$

Fractionation during physical or chemical processes can occur in two ways.

1. **Equilibrium fractionation:** Equilibrium fractionation occurs at thermodynamic equilibrium conditions. e.g., condensation, equilibration of water vapour and water in a closed system. The empirically determined formula for equilibrium fractionation factor is

$$\ln \alpha_{eq} = \frac{C_1}{T^2} + \frac{C_2}{T} + C_3$$

   Where, for ^{18}O, $C_1 = 1.137 \times 10^3$, $C_2 = -0.4156$ and $C_3 = -2.066 \times 10^{-3}$ and for D, $C_1 = 24.884 \times 10^3, C_2 = -76.248$ and $C_3 = 52.612 \times 10^{-3}$ [*Majoube*, 1971] for temperature (T in Kelvin) above 0°C. Equilibrium fractionation is more for $HD^{16}O$ than $H_2^{18}O$ due to the quantum mechanical effects of the molecules during phase transitions.

2. **Kinetic fractionation:** Kinetic (or non-equilibrium) fractionation occurs in processes which are mostly unidirectional and fast (e.g., evaporation, vapour deposition etc). The different rates of diffusion of isotopologues is the reason for kinetic fractionation [*Craig and Gordon*, 1965; *Merlivat and Jouzel*, 1979]. Molecular diffusivity of a gas (i) through air (e.g., water vapour through air) given by the gas kinetic theory is,

$$D_{i,Air} \propto \frac{(\frac{1}{M_i} + \frac{1}{M_{Air}})T^3}{P\sigma_{i,Air}^2 \Omega_{i,Air}}$$

Where M = molecular mass, T= absolute temperature, P= total pressure, σ = sum of atomic radii and Ω =interactive correction term [*Chapman and Cowling*, 1951].

Thus, the kinetic fractionation factors depend on the ratio of diffusivities, i.e., $\frac{D_{HDO}}{D_{H_2O}}$ and $\frac{D_{H_2^{18}O}}{D_{H_2O}}$

1.2.3 Rayleigh model for isotopic fractionation

The Rayleigh model can be used to understand the isotopic variation of a system from which a substance is continuously removed [*Mook*, 2006]. Consider a vapour mass (reservoir) from which rain is been continuously removed by condensation. Due to fractionation, the remaining vapour gets depleted in ^{18}O (and D) and the rain is enriched in ^{18}O (and D). Here we assume that, i) the abundance of heavier isotopes is much less than that of the lighter ($N^* \ll N$), ii) the isotopic fractionation occurs with instantaneous isotopic equilibrium, iii) the process is isothermal and iv) the reservoir is homogeneous (no isotopic gradient across the reservoir). At any instant, the stable isotope ratio of the vapour is given by

$$R = \frac{N^*}{N}$$

Where N* and N are the number of heavier and lighter molecules. Differentiating the equation gives,

$$dR = \frac{dN^*}{N} - \frac{RdN}{N}$$

By solving the equation with $\alpha = \frac{dN*}{dN}/R$, we get

$$R = R_0 f^{\alpha-1}$$

Where, R_0 is the initial isotopic ratio, f is the fraction of substance remaining in the reservoir and α is the isotopic fractionation factor. In δ notations, Rayleigh equation can be expressed as

$$\delta = \delta_0 + (\alpha - 1)10^3 \ln f$$

The variation of isotopic composition of the water vapour, rain and the accumulated rain formed from the vapour at any instant according to Rayleigh fractionation theory are shown in Fig 1.2 [*Clark and Fritz*, 1997]. In permil notation α is represented as the separation factor,

$$\epsilon = (\alpha - 1).10^3‰$$

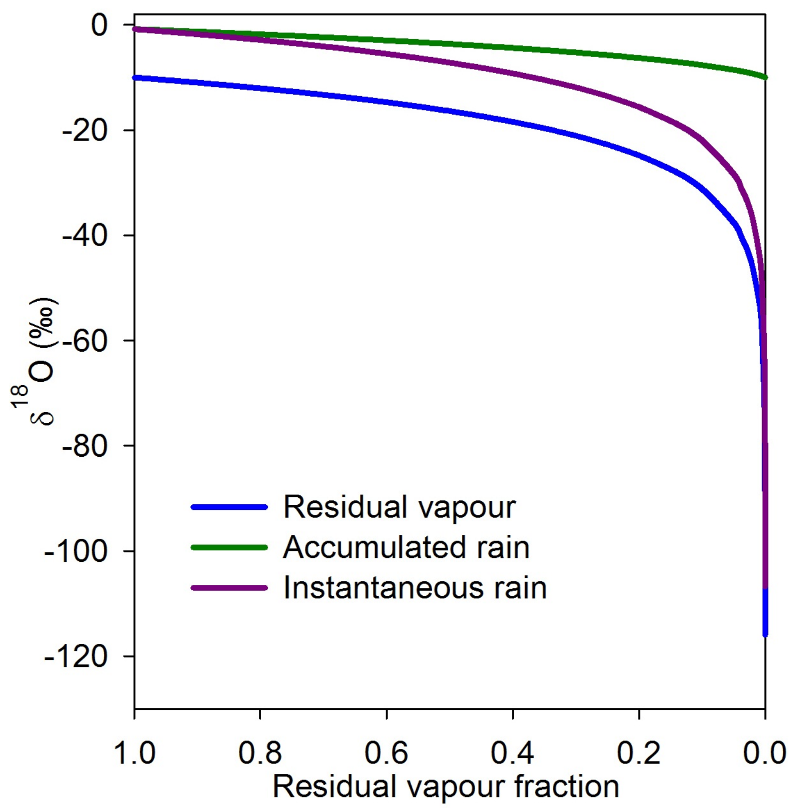

Figure 1.2: The change in the $\delta^{18}O$ of the water vapour, instantaneous rain and the accumulated rain formed from the water vapour versus the fraction of vapour remaining in the system, according to the Rayleigh isotopic distillation.

1.2.4 Global Meteoric Water Line (GMWL)

GMWL is the observed linear relation between $\delta^{18}O$ and δD in global precipitation [*Rozanski et al.*, 1993]. It is observed as,

$$\delta D = (8.20 \pm 0.07)\delta^{18}O + (11.3 \pm 0.6)‰$$

The slope of the GMWL is a result of the difference in equilibrium isotopic fractionation factors of ^{18}O and D ($\epsilon_D/\epsilon_{^{18}O} \approx 8.22$ to 9.59, at 30^OC to 0^OC). The $\sim$ 10‰ intercept is due to the kinetic fractionation that occurs during the formation of the vapour. The slope and intercept of this relation can vary according to the degree of kinetic fractionation. Kinetic fractionation during evaporation (consider rain drop re-evaporation) leads to less ^{18}O in the evaporated vapour compared to D, while more ^{18}O in the remaining water (since $\alpha_{k(^{18}O)} > \alpha_{k(D)}$) [*Clark and Fritz*, 1997].

1.2.5 Deuterium-excess

Deuterium-excess (d) is defined as $d = \delta D - 8 \times \delta^{18}O$, which gives information about the kinetic fractionation that occurs during evaporation of the source moisture or re-evaporation from the raindrops. Evaporation under low humidity leads to kinetic fractionation. Since kinetic fractionation is more for ^{18}O than D, the vapour has relatively less ^{18}O leading to higher d-excess in the vapour. At the same time, the remaining water (reservoir or raindrop) has a lesser d-excess. Thus, a negative relation is observed between the d-excess and the relative humidity. During condensation, according to the Rayleigh model, the d-excess is invariant (equilibrium process) and hence preserves the d-excess of the source moisture. But moisture recycling such as rain drop re-evaporation leads to changes in the d-excess of rainfall.

1.2.6 Observed isotopic effects

Stable isotopes of global precipitation shows large variations due to isotopic effects and geography.

1. **Temperature effect:**

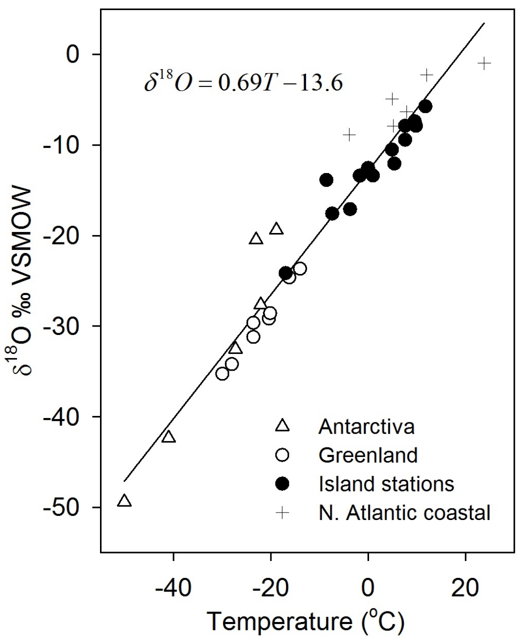

Figure 1.3: Global temperature- $\delta^{18}O$ relationship in precipitation. [*source: Clark and Fritz*, 1997]

An observed linear relationship between the mean annual surface air temperature and the mean annual precipitation isotopic composition is the temperature effect. This relation has been established using the data collected by the Global Network of Isotopes in Precipitation (GNIP) and the mean annual air temperature at each station [e.g., *Dansgaard*, 1964; *Rozanski et al.*, 1993],

$$\delta^{18}O = 0.695T_{annual} - 13.6‰$$

$$\delta D = 5.6 T_{annual} - 100‰$$

2. **Amount effect:**

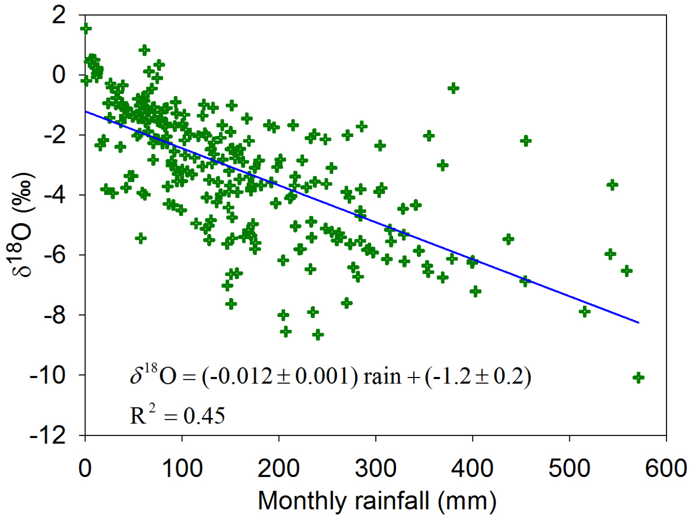

Figure 1.4: Relation between monthly rainfall and its $\delta^{18}O$ in tropical island stations around the globe [*source: GNIP data*].

In the tropics, precipitation isotopic composition does not show any relation with the temperature (especially where the mean annual surface air temperature is > 15^{o}C); but it is related to the amount of rainfall. This is known as the amount effect [*Dansgaard*, 1964]. It is the negative relation between the precipitation isotopic ratio and rainfall [Fig 1.4]. *Dansgaard* [1964] reported it as -1.5 ‰/ 100 mm of monthly rain. The reasons for the amount effect are: i) newly formed condensate is enriched in ^{18}O (and D) according to the theory of Rayleigh isotopic fractionation ii) lighter rain reevaporates at the bottom of the cloud because of lower humidity. So the increase of rainfall reduces the ^{18}O and D in rain. The exact mechanisms which lead to the observed amount effect are yet to be completely understood.

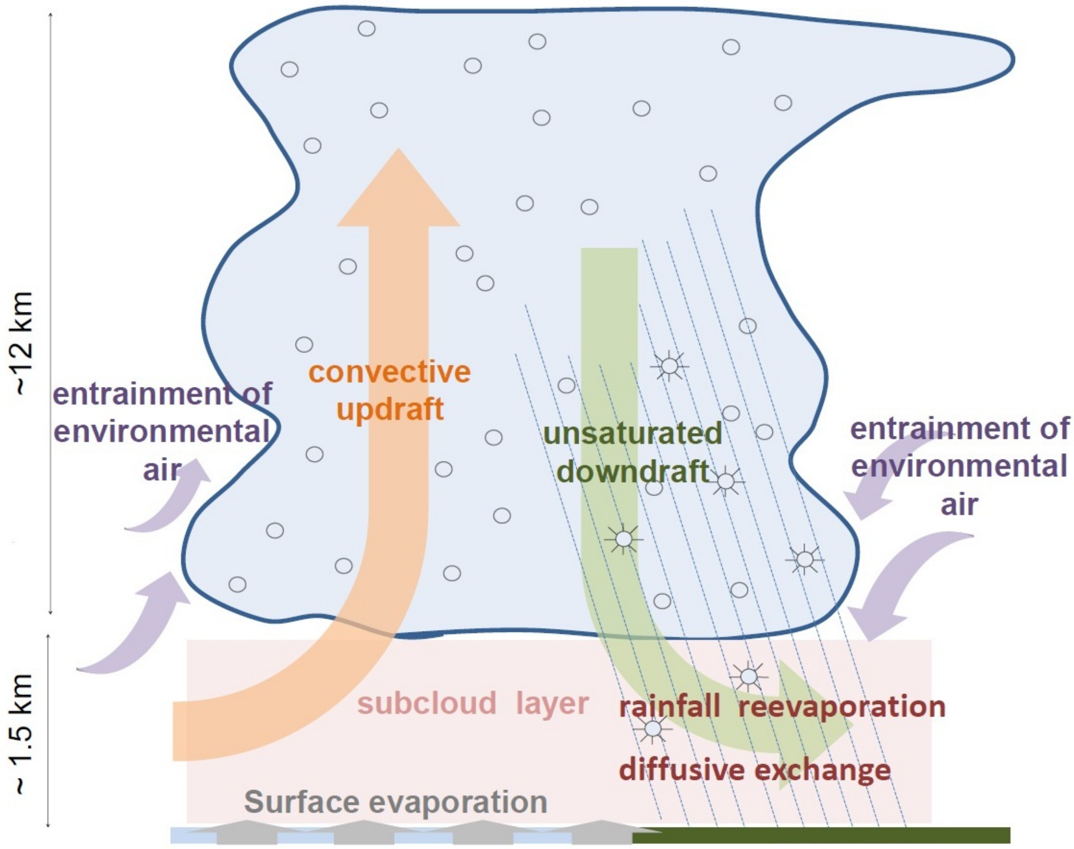

Figure 1.5: Schematic representation of a convective cloud system [modified from *Risi et al.*, 2008].

The current understanding of the amount effect is as follows. Most precipitation in the tropics is derived from atmospheric convection. Fig 1.5 shows a schematic representation of different components of a convective cloud system. The moisture which feeds the system is primarily from the sub-cloud layer (SL), which is constituted by the surface evaporation, recycled moisture from the cloud and the entrainment of the environmental moisture. If the convection is intense, more SL vapour is taken into the cloud along with the entrainment of environmental air, which is more depleted in the heavier isotopes. The condensation inside the cloud leaves

^{18}O and D depleted water vapour (unsaturated) which reaches the SL by downdraft (mass movement of air from the cloud due to the drag from the falling rain drops). The re evaporation of falling rain drops also feeds isotopically depleted vapour to the SL vapour. Thus for intense convective activity (more rain), this feedback mechanism leads to effective recycling of the moisture in the system and thus depletion of ^{18}O and D of rainfall [*Risi et al.*, 2008].

Recent studies point out the equal contributions of both convective and stratiform clouds to organized convection in determining the rainfall [*Houze J R*, 1997]. The larger spatial extent of stratiform clouds leads to mesoscale subsidence of depleted background vapour into the sub-cloud layer. ^{18}O and D depletion of stratiform clouds by mixing with the environmental air (due to its large residence time) could also be an additional reason for the observed heavier isotopic depletion in the heavy rainfall events. The ^{18}O and D depleted remnant vapour after the condensation also reaches the sub-cloud layer along with the mesoscale subsidence and downdrafts. During the convective updraft, this ^{18}O and D depleted vapour is also taken up into the cloud from the sub-cloud layer and thus the rain becomes more depleted in the heavier isotopes [*Kurita*, 2013].

3. **Altitude effect:**

Orographic precipitation occurs as a vapour mass rises over a mountain and cools adiabatically. Precipitation starts at a particular height of the mountain and continues till the top. The continuous precipitation from the bottom to top of the mountain results in the ^{18}O and D enrichment in rain in at the initial stages (lower altitude) and their depletion in rain at higher altitude. This is manifested as the altitude effect (negative relation between $\delta^{18}O$ and δD of rain and the altitude) as seen in Fig 1.6.

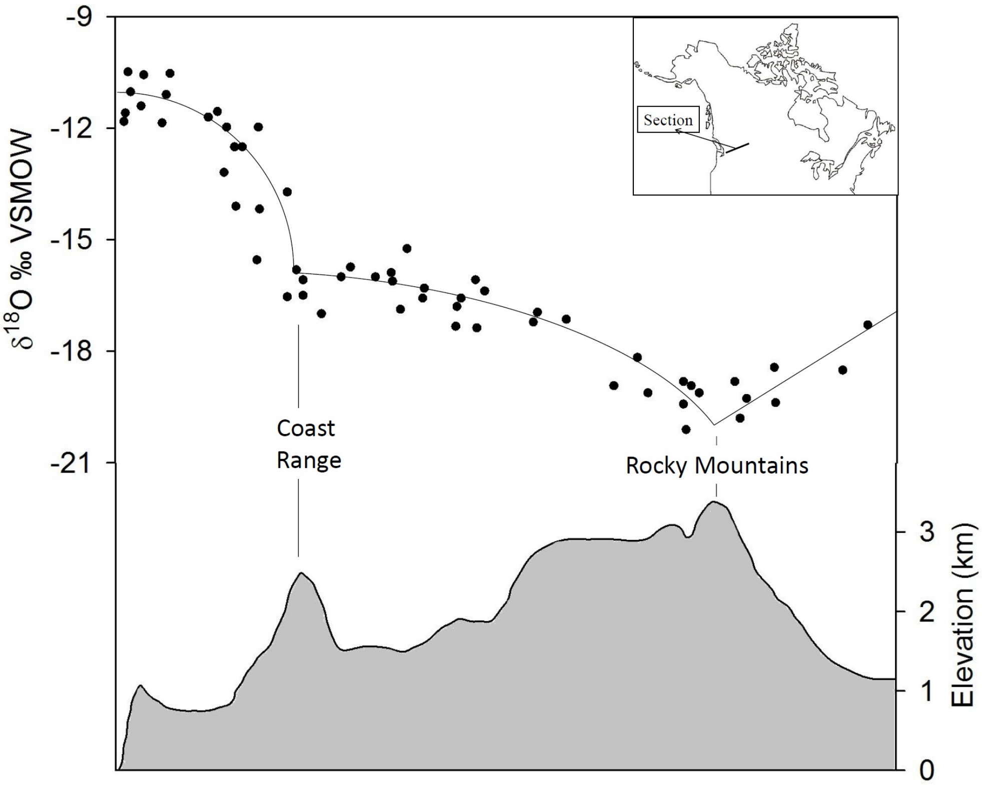

Figure 1.6: $\delta^{18}O$ variation along a high altitude mountain region [source: *Yonge et al.*, 1989].

4. **Latitude effect:**

Global map of stable isotopes of precipitation show that, the most ^{18}O and D enriched precipitation occurs generally in the equatorial region, whereas the most ^{18}O and D depleted precipitation is received by the polar region. This is mainly due to (i) latitudinal variation of temperature (temperature effect) and (ii) the general atmospheric circulation. The latter brings a significant amount of vapour from the tropical region (a region of excess evaporation over precipitation) to the polar region which becomes depleted in ^{18}O and D due to the precipitation history along its meridional path.

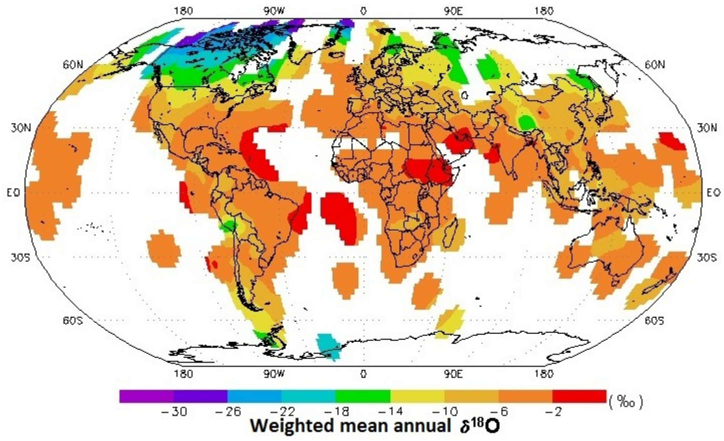

Figure 1.7: Spatial pattern of $\delta^{18}O$ (*source: GNIP dataset,* `http://www-naweb.iaea.org/napc/ih/documents/userupdate/Waterloo`).

5. **Continental effect:**

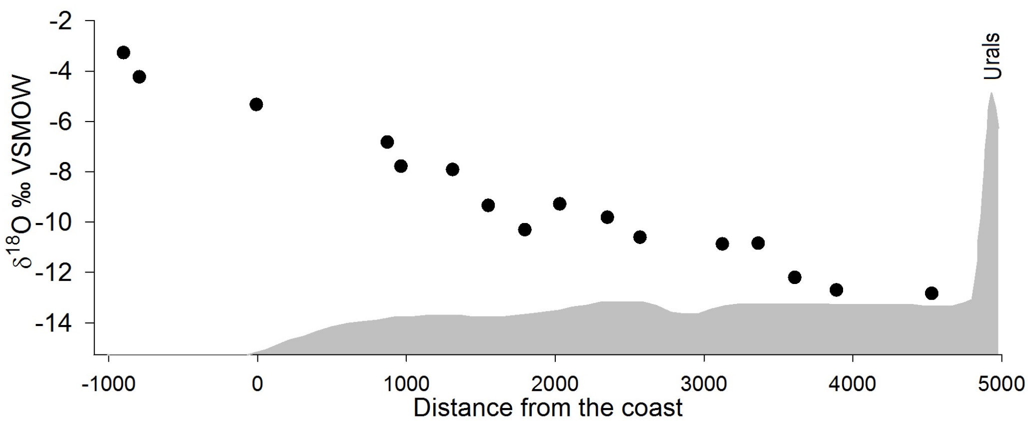

Figure 1.8: Variation of $\delta^{18}O$ from oceanic (southwest coast of Ireland) to inland region (Perm) over Europe [*source: Rozanski et al.*, 1993].

As a vapour mass moves from its source region (generally oceanic) to inland, continuous rain out leads to the expulsion of the heavier isotopes present in the initial vapour mass. So a gradual depletion of the heavier isotopes can be observed in precipitation towards the interior of continents, which is known as the continental effect. Fig 1.8 shows an example of continental effect observed on the long term annual $\delta^{18}O$ of precipitation in Europe.

1.3 Previous studies in India

The vast area and diverse geography of India provide different rainy seasons in different parts. The ISM contributes to 80% of the annual rainfall in the Indian plains during June to September. Peninsular India gets significant amount of rain during October- December, through the North East monsoon (NEM) rainfall. North-east coastal region and north east India receive moderate amounts of thunderstorm rainfall during the pre-monsoon period (March- May). These are called as Nor'westers (locally known as *Kalbaishakhi*). Northern India gets rain during January- May from extra tropical storms from the Mediterranean, known as Western disturbances. Due to these seasonal differences in the source of moisture and their different moisture transport pathways (and hence different precipitation histories), large spatial and seasonal variations are observed in the stable isotopic composition of rainfall over India.

Global Network of Isotopes in Precipitation (GNIP) provides isotopic data of 35 locations all over India, of which only 5 stations have at least 5 years of data. Thus, isotopic studies of precipitation in India are limited. *Datta et al.* [1991] have shown that the long term mean temperature and rainfall amount explain ∼ 80-95% of the long term mean variability of $\delta^{18}O$ in New Delhi, while the monthly rainfall $\delta^{18}O$ is likely to be controlled by the different circulation patterns during different seasons. *Araguás-Araguás et al.* [1998] pointed out the distinct isotopic signatures of summer and winter monsoon rainfall in India; the summer monsoon rainfall in Mumbai is enriched in ^{18}O due to the local source of moisture (Arabian Sea) while the southward movement of Inter Tropical Convergence Zone (ITCZ) brings moisture from different sources during winter time. *Bhattacharya et al.*

[2003] figured out the importance of north-west moving depressions from head Bay of Bengal with diverse routes and their variable transit times in determining the monsoon rainfall $\delta^{18}O$ in New Delhi. In contrast, the monsoon rainfall $\delta^{18}O$ in Mumbai is explained by the continuous supply of oceanic moisture from cyclonic activity over the west coast of India, which leads to negligible stable isotopic variations (and thus no amount effect). *Pang et al.* [2004] figured out a significant correlation between the *d*-excess in rainfall of Delhi with the relative humidity over the western Arabian Sea suggesting that the rainfall in New Delhi is driven by moisture from Arabian sea. But later *Sengupta and Sarkar* [2006] found that, 45% of rain at New Delhi is contributed by the evapo-transpirated water vapour along the path of monsoon depression (from head BoB, north westward) while, moisture from Arabian Sea also contributes to a significant amount of rainfall (20%) at New Delhi. *Yadava et al.* [2007] observed a positive relation between monthly rainfall amount and its ^{18}O in south west coast India (Mangalore). The most ^{18}O-depleted events are mainly observed in the latter period of monsoon (September- October) with less amount of rainfall. This ^{18}O depletion of post monsoon season rainfall in south west coast of India (Kozhikode) was explained in terms of moisture source difference as well as the different rain out histories of the moist air parcel compared to the summer monsoon by *Warrier et al.* [2010]. *Breitenbach et al.* [2010] reports the amount independence of rainfall $\delta^{18}O$ in north east India (Meghalaya). They suggest that, the ^{18}O- depletion of post monsoon rainfall is due to the depletion of evaporative flux from BoB contributed by the ^{18}O-depleted fresh water influx from Ganga Brahmaputra river systems. A comparative study of Local Meteoric Water Lines (LMWL) of 30 stations in India by *Kumar et al.* [2010] suggested the despite of the control by temperature, relative humidity and rainfall amount, change in vapour sources plays an important role in regulating the temporal and spatial variations of rainfall $\delta^{18}O$.

Stable isotopic studies of water vapour are even less in India perhaps due to logistics. It is observed that, the ground level water vapour at Ahmedabad is not in isotopic equilibrium with the rainfall, and reflect the contributions from evaporation from non-local moisture sources (under less humid conditions)[*Deshpande et al.*, 2010; *Srivastava et al.*, 2015].

1.4 Outline of the thesis

This thesis is divided into six chapters, as detailed below:

Chapter 1: Introduction

This chapter introduces the importance and mechanism of Indian Summer Monsoon and the necessity to reconstruct the past monsoon variations. It also discusses the stable isotopic technique used for the study of the hydrological cycle and paleoclimate reconstruction. The main findings of the earlier studies on this subject in this region are also briefly presented.

Chapter 2: Materials and Methods

This chapter is a brief description about the sampling sites and the rain and water vapour sampling techniques. We also discuss the isotopic analysis of the samples, and associated precision and accuracy. The satellite and *in-situ* observational data utilized for the present study are also described.

Chapter 3: Investigation of the cause of amount effect in tropical rain

The controls of the Indian summer monsoon rainfall isotopic variability in the south west coast of India is discussed.

Chapter 4: Water vapour- rain isotopic interactions over Kerala

Rain- water vapour isotopic interactions in the south west coast of India during pre monsoon, summer monsoon and post monsoon seasons are detailed.

Chapter 5: 'Amount effect' in peninsular India

The spatial and temporal variability of rainfall- $\delta^{18}O$ relation in peninsular India is assessed in this chapter and the controls of NEM rainfall $\delta^{18}O$ are discussed.

Chapter 6: Summary and recommendations

The results obtained are summarised in this chapter and scope for future work is detailed.

1.5 Major Questions addressed in the present study

1. What controls the heavier isotopic variations of the ISM rainfall in the south west coast of India?
2. What are the type of isotopic interaction occurring between the rainfall and water vapour in the south west coast of India?
3. What controls the spatial and temporal variations of rainfall- $\delta^{18}O$ relation in peninsular India?
4. What are the factors responsible for rainfall $\delta^{18}O$ variability during the NEM season ?

Chapter 2

Materials and Methods

The experimental methodology followed in the present work is described in three major sections. In the first section, the rain water and water vapour collection methods are presented. The second discusses the mass spectrometry techniques and isotopic analysis of the water samples while the third describes the available online data additionally utilised for the present work.

2.1 Sample collection

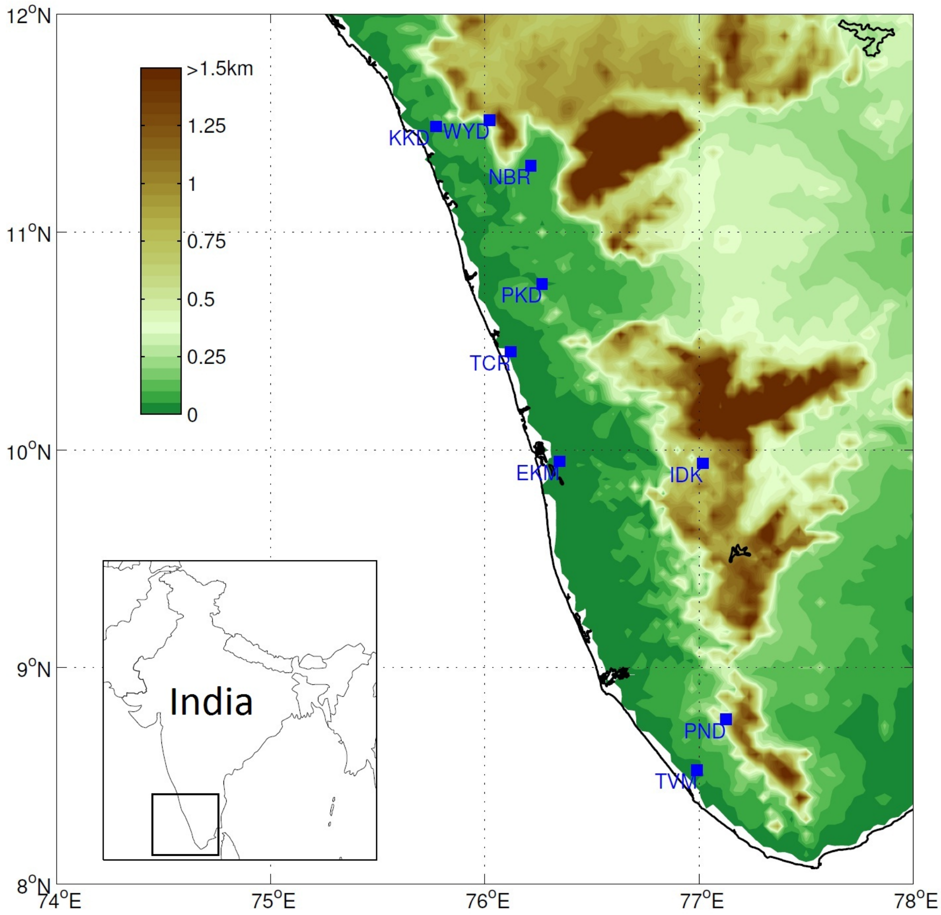

Figure 2.1: Sampling locations: 1- Thiruvananthapuram (TVM, 53 m asl), 2- Ponmudi (PND, 780 m asl), 3- Idukki (IDK, 700 m asl), 4- Ernakulam (EKM, 6 m asl), 5- Thrissur (TCR 12 m asl), 6- Palakkad (erstwhile Palghat) (PKD, 26 m asl), 7- Nilambur (NBR, 35 m asl), 8- Kozhikode (KKD, 30 m asl), 9- Wayanadu (WYD, 800 m asl). Water vapour samples were collected from PND and WYD.

Sampling was restricted to the state of Kerala, southwestern India. Rain water was collected daily (whenever it rained) from 9 stations of Kerala [Fig 2.1] between 8 to 13^{o}N, 75 to 77.5^{o}E and 0 to 850 m above mean sea level, during 2012-2013

CE. All the stations are located to the west of the Western Ghats (which has a maximum height of 2700 m above m.s.l in Kerala). A total of 1681 such rain water samples were collected. In addition, ∼310 atmospheric water vapour samples were also collected from Ponmudi and Wayanad during April-October 2012 CE.

2.1.1 Rain water collection

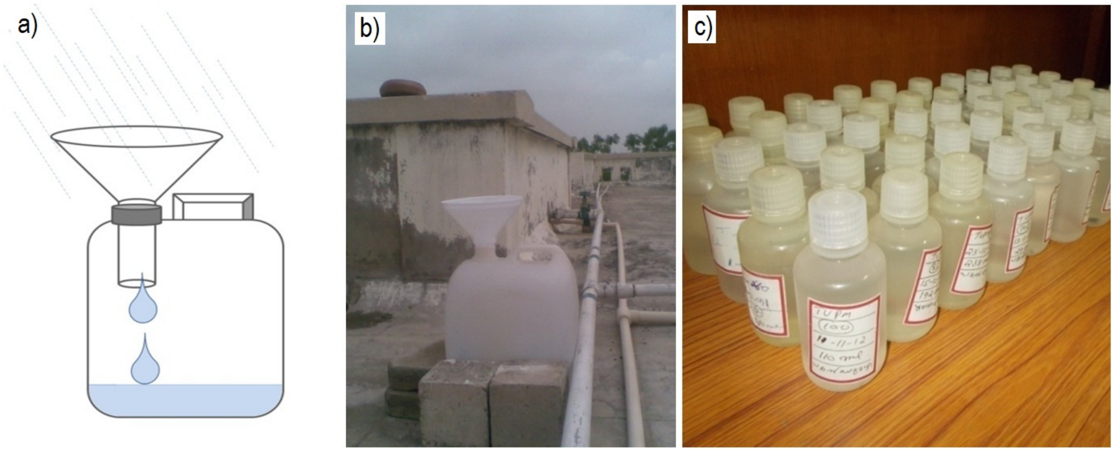

Figure 2.2: a) shows the schematic diagram of rain water collection system, b) is the photograph of the same and c) is the photograph of samples in Tarson bottles.

The protocol proposed by the International Atomic Energy Agency (IAEA) was adopted for rain water sample collection [`http://www-naweb.iaea.org/napc/ih/documents/other/gnip_manual_v2.02_en_hq.pdf`]. A carboy connected with a funnel was kept in an open space to aid the unobtrusive collection of rain for 24 hours. Care was taken to avoid re-evaporation of the samples at every stage, by covering the sides of the carboy with a white cloth (to prevent direct heating) and placing a plastic ball in the mouth of the funnel (to prevent the re-evaporation of the water from the carboy). Samples were collected everyday at 09.00 am (IST) and the amount of rain was measured. Small amounts of samples was transferred to leak-proof plastic (polypropylene) bottles filling them up to the brim to avoid re-evaporation and taken to the lab for further analysis.

2.1.2 Water vapour collection

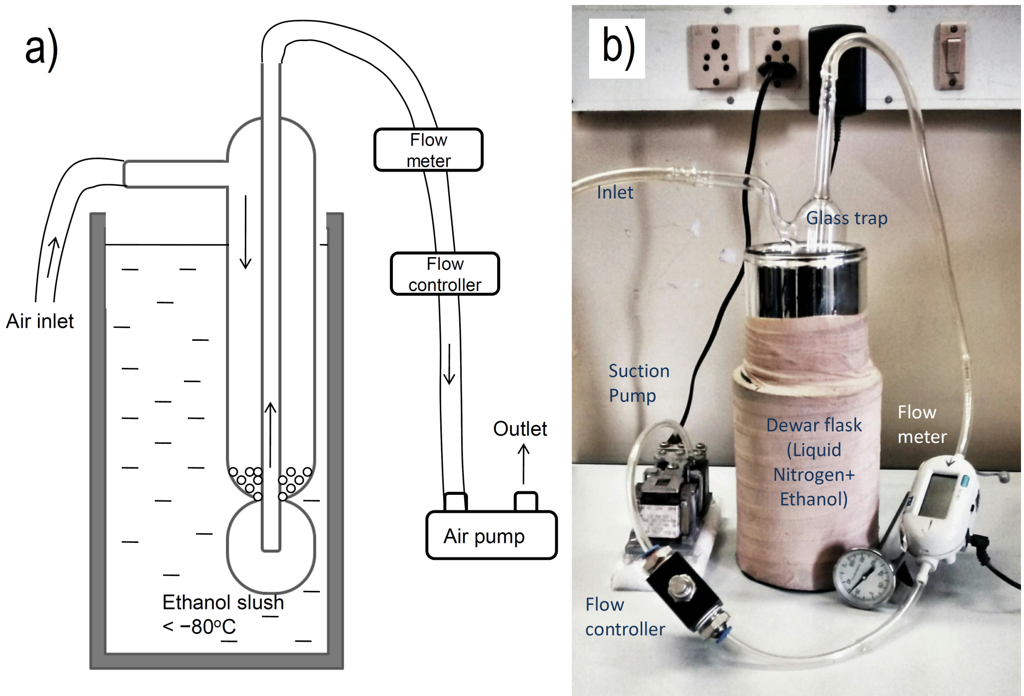

Figure 2.3: a) Schematic diagram of water vapour collection system and b) is the photograph of the same.

Water vapour samples are collected from two hill stations in Kerala; Ponmudi and Wayanad [see Fig 2.1]. Push and trap method, proposed by the IAEA was followed for the vapour collection [`http://www-naweb.iaea.org/napc/ih/documents/miba/water_vapour_protocol.pdf`]. Atmospheric air was sucked using an air pump from 2 m above the ground level and passed through a glass trap kept below -80^{o}C (by a cooled mixture of ethanol and liquid nitrogen) for $\sim$3 hours [Fig 2.3]. The flow rate was kept below 500 ml/min and glass beads were put inside the glass trap to ensure efficient trapping. The efficiency of the trap was checked by connecting an extra cold trap to the outlet of the first trap, and no significant condensate was found in it. Samples were taken out from the trap using a pipette (with a rubber suction ball) and transferred into leak proof vials.

2.2 Isotopic analysis

2.2.1 Isotope ratio mass spectrometry

Mass spectrometry is a technique of separating ions according to their mass to charge ratio. For the isotopic analysis of water samples, we use Isotope Ratio Mass Spectrometer (IRMS). Inside the mass spectrometer, gaseous samples are ionised and accelerated by an electric field, passed through a magnetic field in a perpendicular direction, which leads to the separation of ion beams according to their mass to charge ratio. These separated ion beams are then collected by different detectors (Faraday cups) and the isotope ratios are calculated according to the respective ion currents.

Isotopic analysis of the water samples was done using mass spectrometers: Initially with Sercon Geo 20-20 Dual Inlet IRMS [Fig 2.4(b)] and later with Thermo Fisher Delta V-plus continuous flow IRMS [Fig 2.4(c)]. Dual inlet IRMS contains two individual inlets for sample and reference gases and works at a vacuum level of $\sim 10^{-8}$ Torr. Continuous gas flow systems use a carrier gas (Helium) to carry the gas into the ion source chamber. The sample and the reference gases are injected into the carrier gas flow for the isotopic analysis.

A mass spectrometer contains mainly 3 parts for the preparation, separation and for the detection of ions [Fig 2.4(a)].

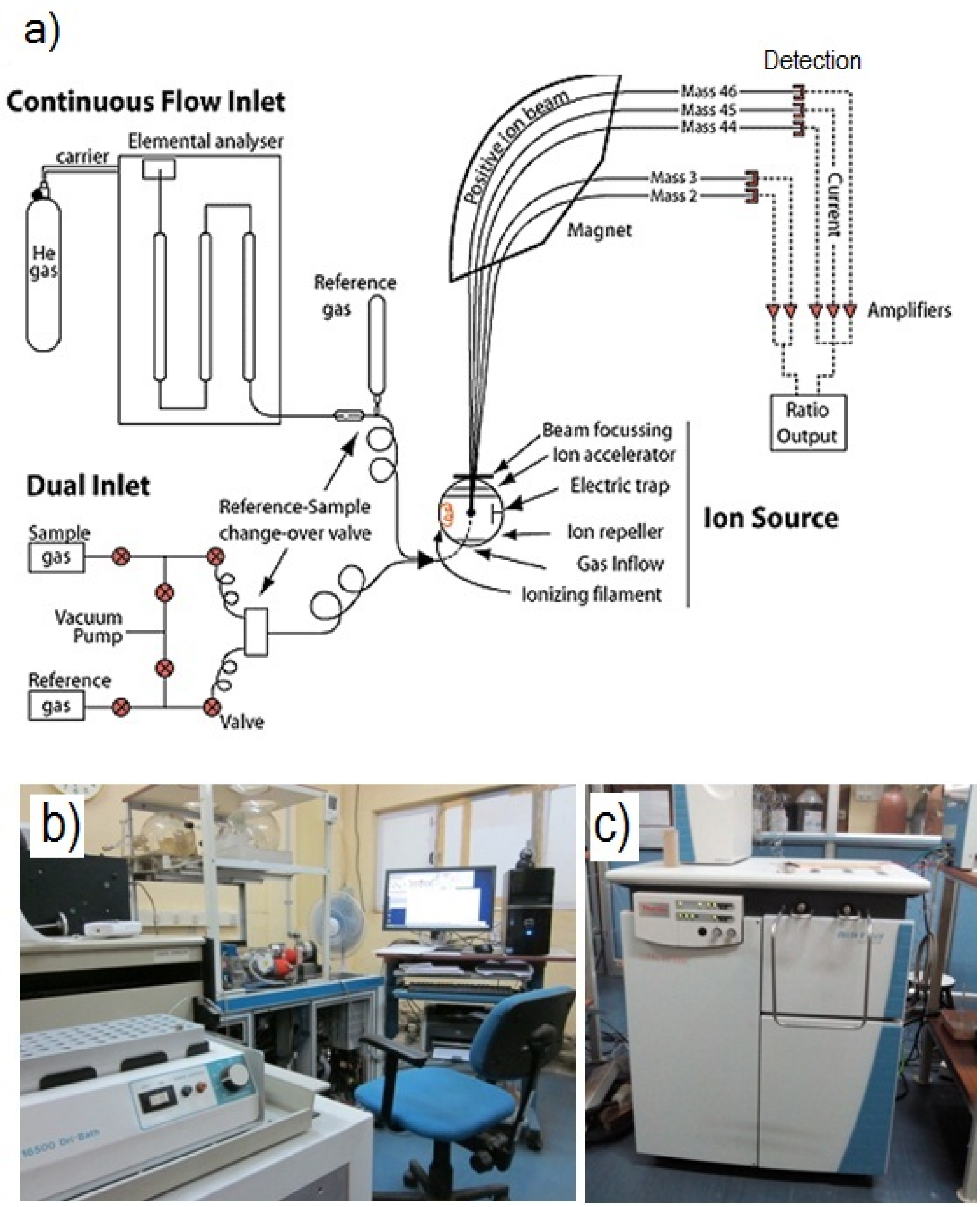

Figure 2.4: a)Schematic diagram of a mass spectrometer with both dual inlet and continuous modes of operation, [*source: Clark and Fritz*, 1997]. b) Sercon Geo 20-20 mass spectrometer. c) Thermo Fisher Delta Vplus mass spectrometer.

1. **Source:** A thorium coated tungsten filament produces electrons (accelerated to ∼70 eV energy) when ∼3.5A current is passed through it. These electrons ionise the gas (CO_2 or H_2) with an efficiency of 0.1%. In order to increase the ionisation efficiency, a low magnetic field is applied to make the path of electrons spiral. The positively ionised gas molecules are then accelerated by a high voltage (∼2.5 kV) and focused using collimating plates into the analyser.

   A charged (q) molecule in an accelerating voltage (V) obtain kinetic energy.

$$qV = \frac{1}{2}mv^2$$

2. **Analyser:** A magnetic field of ∼3.8 kG for CO_2 (∼1 kG for H_2) is applied perpendicular to the ion path around the flight tube; it splits the ionized beam into 3 (for CO_2) according to their mass/charge ratio which travel in a curved path. The Lorentz force experienced by the ion while entering perpendicular to the magnetic field imparts a centripetal force (with radius of curvature r).

$$q(\mathbf{v} \times \mathbf{B}) = \frac{mv^2}{r}$$

   Thus the radius of curvature of the ion is,

$$r = \sqrt{\frac{2Vm}{\mathbf{B}^2 q}}$$

   So for a constant V, B and q, the radius of curvature of the singly charged ion is directly proportional to the square root of its mass.

3. **Collector:**The currents due to the split ion beams are measured using detectors (Faraday cups), which are attached to very high resistances $\sim 10^9 \Omega$.

Ions produce a voltage across the resistance, which is measured. This is proportional to the number of ionised isotopologues entering into the cup in unit time.

2.2.2 $\delta^{18}O$ and δD measurements

Since the mass spectrometer analyzes only gaseous samples, water samples have to be converted into a suitable gaseous form before being let in to the source. We use the gas equilibration method [*Epstein and Mayeda*, 1953] to prepare the gaseous sample which takes on the isotopic signature of the water sample to be analysed.

For this, water sample is filled in standard glass vials. A threaded cap having neoprene septum seals the bottle preventing any vacuum leak. A sharp needle with two holes pierces the septum and flushes the vial with either CO_2 (or H_2) for $\delta^{18}O$ (for δD) analyses. The needle moves up and the neoprene septum get closed immediately. After a certain time of equilibration, the gaseous sample is analysed [Table 2.1]. Standard water samples (whose isotopic composition in known) are also analysed in between, for an accurate measurement of the sample isotopic composition.

Because of the limited availability of the international standard, a laboratory standard (Narmada river water, NARM), which has been already calibrated using the international standard, is used for the analysis of the samples. Finally the sample isotopic abundances are reported with respect to VSMOW (Vienna Standard Mean Ocean water) using the following conversion equation [*Clark and Fritz*, 1997].

$$\delta^{18}O_{VSMOW}^{Sample} = \delta^{18}O_{VSMOW}^{NARM} + \delta^{18}O_{NARM}^{Sample} + \delta^{18}O_{VSMOW}^{NARM} \times \delta^{18}O_{NARM}^{Sample} \times 10^{-3}‰$$

Table 2.1: Sample preparation methods and mass spectrometric parameters used in the measurement of $\delta^{18}O$ and $|deltaD$ in Geo 20-20 and Delta V plus mass spectrometers.

	$\delta^{18}O$		δD	
	Geo 20-20	Delta V^+	Geo 20-20	Delta V^+
Sample amount	1.0 ml	0.3 ml	1.0 ml	0.3 ml
Vial volume	5.9 ml	12.0 ml	5.9 ml	12.0 ml
Flushing gas	CO_2 (99.999 %)	He (99 %)+CO_2 (1 %)	H_2 (99.999%)	He (99 %)+H_2 (1 %)
Flush time	1 minute	10 minutes	40 seconds	10 minutes
Equilibration time	6 hours	20 hours	2 hours	40 minutes
Equilibration temperature	35^{o}C	22^{o}C	35^{o}C	22^{o}C
Catalyst	-	Hocko beads	-	Platinum sticks
Electron energy	80 eV	110 eV	70 eV	90 eV
High voltage	2.5 kV	3 kV	3.5 kV	3.3 kV
Separated ion beams	$_{12}C_{16}O_{16}O(\mathbf{44})$, $_{13}C_{16}O_{16}O$+$_{12}C_{16}O_{17}O(\mathbf{45})$ $_{12}C_{16}O_{18}O$ +$_{13}C_{16}O_{17}O$+$_{12}C_{17}O_{17}O$ (**46**)		HH (**2**) HD (**3**)	
Correction	Craig correction		H_3 correction	
Precision	0.1‰	0.1‰	1‰	1‰

For $\delta^{18}O$ analyses, ions masses 44, 45 and 46 of CO_2 [*Epstein and Mayeda*, 1953] are utilized and for the δD analyses ion masses 2 and 3 of H_2 are used. The details of sample preparation, equilibration and mass spectrometer conditions are listed in Table 2.1. While the calculation of the isotopic composition of the samples, isobaric interference is corrected by applying corrections as explained below.

1. **Craig correction:** The mass of 45 and 46 beams is contributed to both by ^{13}C and ^{17}O. When these molecular ratios are converted into atomic ratios, a correction is required to eliminate the effect of $^{13}C^{16}O^{17}O$ from $^{12}C^{16}O^{18}O$ ($\delta^{18}O$), which is called as Craig correction [*Craig*, 1957].

$$\delta^{13}C = 1.0676\delta_{45} - 0.0338\delta_{46}$$

$$\delta^{18}O = 1.0010\delta_{46} - 0.0021\delta_{45}$$

2. H_3 **correction:** During ionization, H_3^+ ions are also produced and get measured along with HD^+ ions. The formation of H_3^+ current (I) is directly proportional to the concentration of H_2^+ ions. The effect of H_3^+ ion can be removed by calculating $\frac{I_3'/I_2}{I_2}$ i.e.,$(HD^+ + H_3^+)/H_2^+$ ratio for different H_2^+ ion currents.

2.2.3 Calibration of laboratory standards

The Narmada river water standards (NARM), used for the accurate calculation of sample isotopic composition, has been calibrated using international standards provided by IAEA. Our laboratory has also participated in an inter comparison exercise conducted by IAEA during 2011 and values reported by us are in good agreement with the IAEA consensus values [*WICO-2011, Ahmad et al.*, 2012]. We have calibrated the NARM standards again during the September 2014 and the results are given in the Table 2.2, Fig 2.5 and Table 2.3. We measured the

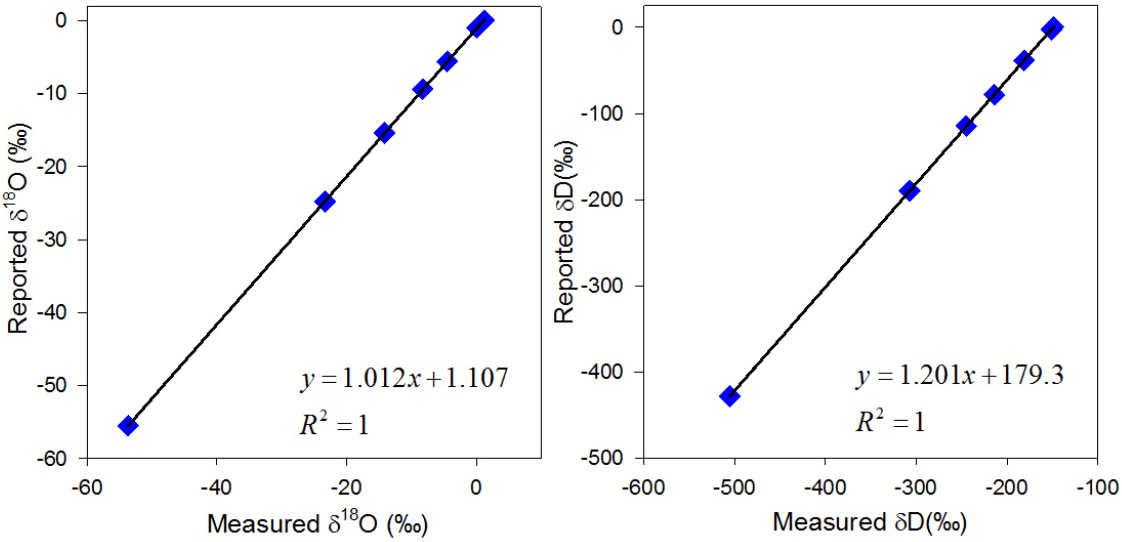

Figure 2.5: The reported and measured raw values of δD and $\delta^{18}O$. The best fit equation are given at the bottom of the graphs.

Table 2.2: Measured and reported values of the international standards.

International standards	Measured $\delta^{18}O$	Reported $\delta^{18}O$	Measured δD	Reported δD
VSMOW	0.06 ± 0.07	0.0	0.1 ± 0.2	0.0
SLAP	-55.5 ± 0.1	-55.5	-427.7 ± 1.4	-428.0
GISP	-24.8 ± 0.07	-24.8	-190.5 ± 0.4	-189.5
OH-13	-1.0 ± 0.1	-0.96	-2.5 ± 0.4	-2.8
OH-14	-5.63 ± 0.1	-5.6	-38.4 ± 0.1	-38.3
OH-15	-9.47 ± 0.1	-9.4	-78.0 ± 0.3	-78.2
OH-16	-15.48 ± 0.1	-15.4	-114.9 ± 0.2	-114.6

Table 2.3: Calibrated values of laboratory standards; calculated with respect to the international standards.

Laboratory standard	$\delta^{18}O$ ‰	δD ‰
NARM	-4.55 ± 0.07	-33.5 ± 0.3
NARM new	-4.63 ± 0.1	-33.8 ± 0.4

laboratory standard and the international standards together in a single batch. We use 6 international water standards for the calibration; viz., VSMOW, SLAP (Southern Light Antarctic Precipitation), GISP (Greenland Ice Sheet Precipitation), OH-13, OH-14, OH-15 and OH-16, provided by IAEA. The linear regression equation is calculated from the relation between the measured and reported values of the 6 international standards which has a correlation coefficient of R = 1 (Fig. 2.5). This equation is then used to calculate the value of NARM standards w.r.t VSMOW. Since we use 2 sets of NARM water standards (running NARM standard for daily measurements and a NARM reservoir), both of them are calibrated to monitor measurements.

2.3 Additional data used

The present study utilises many observations, satellite and model data to understand the isotopic variability of monsoon rainfall over Kerala. These are detailed below.

2.3.1 Global Network of Isotopes in Precipitation (GNIP)

The IAEA's Water Resources Programme and the World Meteorological Organization (WMO) have been surveying the stable hydrogen and oxygen isotopic and tritium compositions in precipitation around the globe since 1961 CE. In the present study, we choose monthly precipitation amounts and their $\delta^{18}O$ and δD from GNIP data, for peninsular India and Sri Lanka.

2.3.2 Hybrid Single-Particle Lagrangian Integrated Trajectory (HYSPLIT)

HYSPLIT model is used to calculate the trajectories of air parcel in the atmosphere; it is forced using Global Data Assimilation System (GDAS) [*Draxler and Rolph*, 2003]. Trajectory (forward or backward) of any air parcel is calculated using the position (grid point) and three dimensional velocity at a time interval of 1 minute to 1 hour. At each time step, the model calculates a guess position and the velocity vectors are linearly interpolated in both space and time. The first guess position is

$$P'_{t+\Delta t} = P_t + V_{P,t}\Delta t$$

and the final position is,

$$P_{t+\Delta t} = P_t + 0.5(V_{P,t} + V_{P',t+\Delta t})\Delta t$$

In the present study, we use the back trajectories, which give an idea about the route of the air parcel before it reaches the final position and hence the probable locations of the moisture origin. The model also provides meteorological parameters such as temperature, potential temperature, relative humidity and height of the parcel above the mean sea level along the trajectory.

2.3.3 Satellite/ reanalysis/ model data

The spatial and temporal variation of meteorological parameters such as rainfall, Outgoing Longwave Radiation (OLR), wind velocity etc are studied using satellite and reanalysis data. Details of the data used in the present study are given in the Table 2.4.

Table 2.4: Details of different satellite data used in the present study.

Resolution	Data type	Parameter	Unit	Reference
Tropical Rainfall Measurement Mission (TRMM)				
0.25 × 0.25	Daily	Rainfall	mm/day	*Huffman et al.* [2007]
NOAA interpolated Outgoing Longwave Radiation (OLR)				
2.5 × 2.5	Daily	OLR	W/m2	*Liebmann* [1996]
Modern-Era Retrospective Analysis for Research and Applications (MERRA)				
2.5 × 2.5	Daily, 300-600 hPa levels	Vertical velocity	mb/s	*Rienecker et al.* [2011]
Climatic Research Unit (CRU)				
0.5 × 0.5	Climatological monthly mean	Rainfall	mm/day/month	*New et al.* [2002]
Global Precipitation Climatology Project (GPCP)				
2.5 × 2.5	Climatological monthly mean	Rainfall	mm/day/month	*Adler et al.* [2003]

Chapter 3

Investigation of the cause of amount effect in tropical rain

This chapter deals with the factors that control stable isotope variations in the Indian summer monsoon rainfall over Kerala, where the monsoon rain starts first over India. First we compare the rainfall and its isotopic composition between the stations. The next part includes discussion on the role of convective activity and variation in moisture source in determining the stable isotopic composition of rainfall.

Most annual rain in India is contributed by Indian Summer Monsoon (ISM). South western India (Kerala, known as the gateway of monsoon in India) gets the first rains during ISM, from the moist air masses originating in the southern Indian Ocean and the Arabian Sea. ISM rainfall in Kerala is known to be well modulated by the 30-60 day mode of intra seasonal oscillations of ISM [*Joseph et al.*, 2004]. Here, ISM rain has the advantage of minimal isotopic alteration by continental recycled water (e.g., soil re-evaporation and transpiration from vegetation), and thus is a good region for examining the characteristics of the moisture source and the effect of cloud processes on the stable isotopes of monsoon rainfall.

3.1 Monsoon performance during 2012 and 2013

Daily rain was collected at 9 stations between 8 to 13^{o}N, 75 to 77.5^{o}E and 0 to 850 m above sea level (above m.s.l) during mid-May to October, 2012 and again in 2013 (at 7 stations only). Barring events of less than 2 mm/day rain, a total of 654 samples were collected during 2012 from all the 9 stations and 646 samples during 2013 from 7 stations. Seasonal total rain during 2012 over Kerala was 24% less than its climatological mean ($\sim$2040 mm), and 26% higher during 2013; but individual stations recorded both higher and lower values than their respective climatological means.

The seasonal total rainfall values at all the stations show [Fig 3.1] large differences during 2012 with a general increasing trend towards the north (with the exception of NBR, located leeward) similar to the climatological rainfall pattern. The climatological rainfall pattern shows a peak over Mangalore (north of our sampling stations). But the excess monsoon rainfall of 2013 produced comparable amounts of rainfall in all the 7 stations. The orographic features of Western Ghats play a significant role in modulating ISM rain, since the mountain ranges are per-

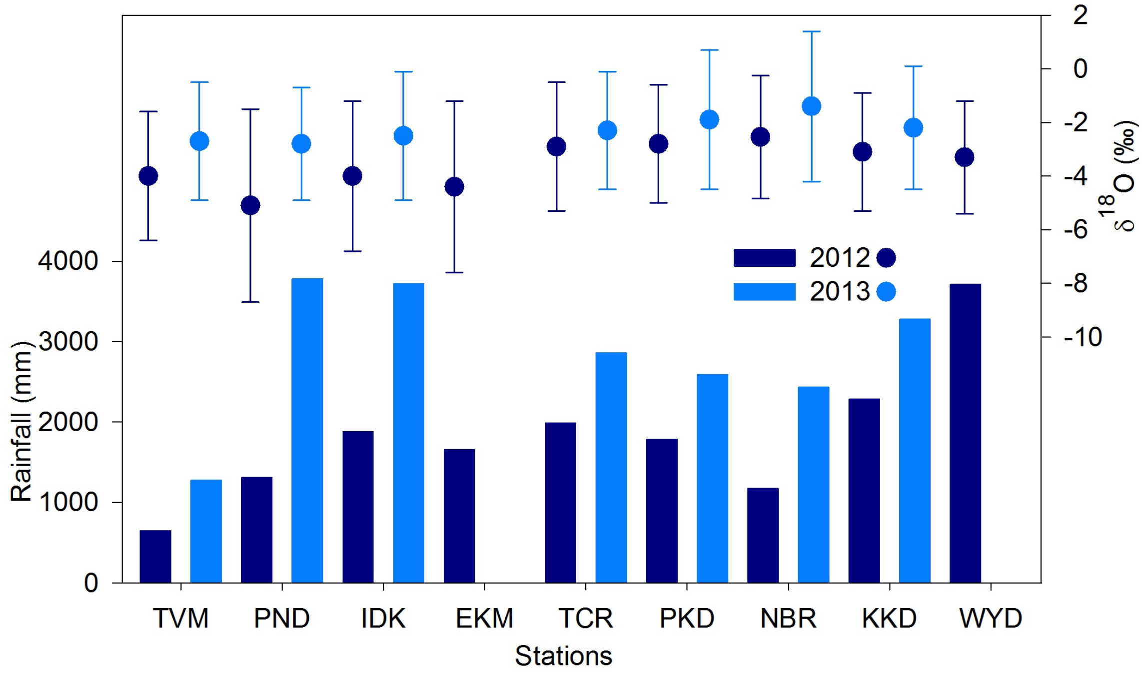

Figure 3.1: Total rainfall (mm, vertical bars) during June to October - 2012 and 2013, and the corresponding seasonal average $\delta^{18}O$ of rain (filled circles) with 1 σ spread, over each station. Samples were not collected from EKM and WYD during 2013. The abbreviations of station name are given in Chapter 2.

pendicular to the prevailing ISM winds. The spatial variation of the amount of rainfall is mainly induced by the changing orography [*Rajendran et al.*, 2012].

Local Meteoric Water Line (LMWL) of rainfall in Kerala is close to the Global Meteoric Water Line (GMWL). The slope the LMWL is close to 8 (that of GMWL) implying isotopic equilibrium condensation occurred at above 90% relative humidity values over the region. The intercept, 13.0±0.2 is slightly higher than that of GMWL [Fig 3.2].

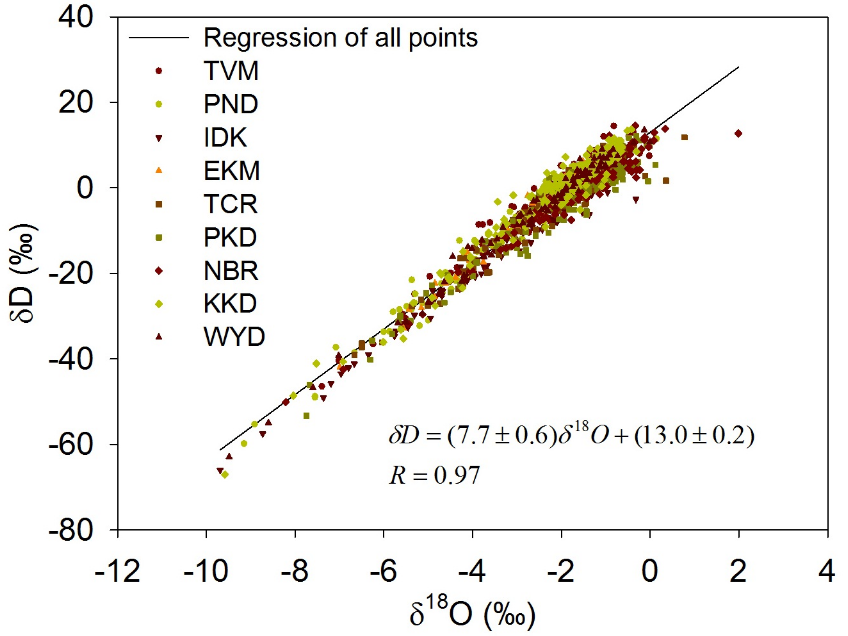

Figure 3.2: Local meteoric water line of rainfall in Kerala (June- September, 2012-2013). The best fit equation is shown below the LMWL. R is the linear correlation coefficient. The abbreviations of station name are given in Chapter 2.

3.2 Spatial variation of rainfall and $\delta^{18}O$

The daily rainfall also shows large variation among the stations. Table 3.2 shows the linear cross correlation coefficients of rainfall and $\delta^{18}O$ of rain among the stations. The correlation coefficients of daily rainfall between all the stations are mostly insignificant. But the daily variation of $\delta^{18}O$ of rain at the stations shows very good coherence among each other (significant at $P < 0.05$ level). This implies that the rain at different stations is from a single vapour/ cloud mass which has spread over Kerala. Similarly the seasonal average isotopic composition (Fig 3.1) of total rainfall does not show a significant variation between the stations. The variation fall within one standard deviation of the distribution. The seasonal total rainfalls, however, are different. Thus, despite of the large variations in the daily as well as the seasonal total rainfall, the isotopic composition of rainfall remained the same in all the stations indicating that the rainfall - $\delta^{18}O$ relation is not controlled by the intensity (i.e., amount) of rain.

Table 3.1: Lower left triangular matrix shows the number of common rain events between different stations during 2012 and the upper right triangle shows the same for 2013. The abbreviations of station name are given in Chapter 2.

	TVM	**PND**	**IDK**	**EKM**	**TCR**	**PKD**	**NBR**	**KKD**	**WYD**
TVM	-	65	54	-	51	59	37	58	-
PND	37	-	74	-	75	81	51	80	-
IDK	36	53	-		63	71	48	72	-
EKM	26	32	40	-	-	-	-	-	-
TCR	35	49	57	35	-	79	50	78	-
PKD	34	45	60	41	58	-	57	84	-
NBR	28	33	48	35	43	50	-	55	-
KKD	30	38	47	31	51	56	41	-	-
WYD	38	49	63	40	63	66	51	61	-

Table 3.2: Linear cross correlation coefficients between the rainfall at different stations (upper right triangle); and between rain $\delta^{18}O$ at different stations (lower left triangle) during (a) 2012 and (b) 2013. Bold fonts represent statistically significant correlations at P = 0.05. The abbreviations of station name are given in Chapter 2.

a)	**TVM**	**PND**	**IDK**	**EKM**	**TCR**	**PKD**	**NBR**	**KKD**	**WYD**
TVM	-	**0.65**	**0.37**	−0.20	0.03	−0.18	0.23	0.20	0.07
PND	**0.87**	-	0.16	−0.01	0.08	0.10	−0.07	-0.12	0.10
IDK	**0.86**	**0.87**	-	**−0.22**	0.10	0.19	0.15	**0.36**	**0.29**
EKM	**0.76**	**0.75**	**0.67**	-	0.08	**0.28**	−0.16	-0.05	0.05
TCR	**0.70**	**0.83**	**0.80**	**0.83**	-	**0.22**	0.05	0.02	0.13
PKD	**0.62**	**0.68**	**0.70**	**0.86**	**0.75**	-	**0.34**	0.22	0.08
NBR	**0.64**	**0.36**	**0.55**	**0.78**	**0.46**	**0.71**	-	-0.03	0.18
KKD	**0.72**	**0.74**	**0.81**	**0.79**	**0.89**	**0.76**	**0.53**	-	**0.26**
WYD	**0.62**	**0.64**	**0.78**	**0.66**	**0.78**	**0.74**	**0.51**	**0.89**	-

b)	**TVM**	**PND**	**IDK**	**EKM**	**TCR**	**PKD**	**NBR**	**KKD**	**WYD**
TVM	-	**0.36**	0.15	-	0.06	-0.12	0.04	0.14	-
PND	**0.52**	-	**0.41**	-	0.20	-0.09	**0.41**	0.01	-
IDK	**0.50**	**0.62**	-	-	**0.28**	0.04	**0.61**	0.05	-
EKM	-	-	-	-	-	-	-	-	-
TCR	**0.32**	**0.50**	**0.68**	-	-	**0.28**	**0.28**	**0.34**	-
PKD	**0.46**	**0.38**	**0.54**	-	**0.64**	-	0.23	**0.31**	-
NBR	**0.30**	**0.25**	**0.48**	-	**0.50**	**0.37**	-	**0.26**	-
KKD	**0.43**	**0.41**	**0.71**	-	**0.70**	**0.57**	**0.78**	-	-
WYD	-	-	-	-	-	-	-	-	-

3.3 Intra-seasonal variations of $\delta^{18}O$

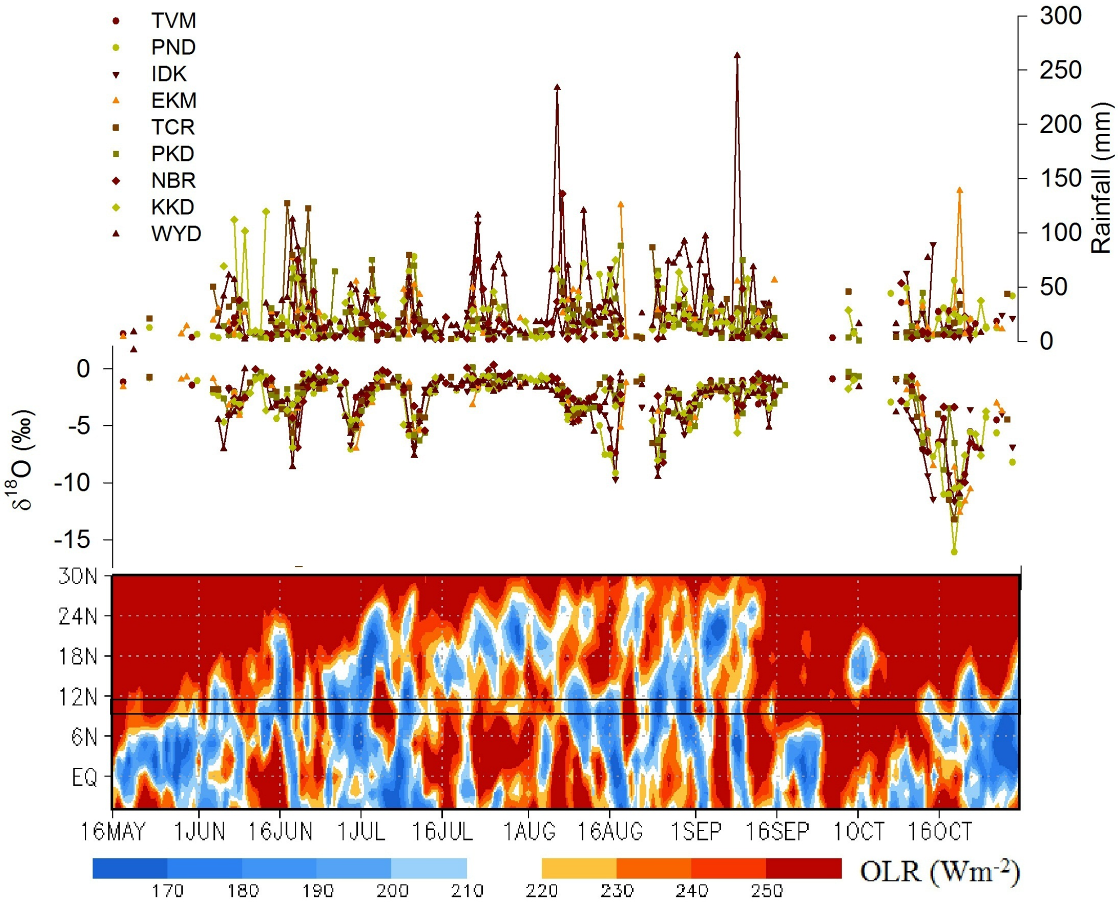

Figure 3.3: (a) Time series of measured amount of daily rain (mm). (b) rain $\delta^{18}O$ (‰) and (c) Hovmöller diagram of average NOAA interpolated OLR over 65° E 77.5° E for the year 2012. Solid parallel lines in (c) depict the latitude range of the sampling stations.

Figures 3.3 and 3.4 respectively show the time series of rainfall and the corresponding rain $\delta^{18}O$ during 2012 and 2013. The daily rainfall over the stations varies from 0 to 263 mm (0 to 225 mm) whereas the rainfall $\delta^{18}O$ varies from 0.3 to -9.7 ‰ (2.0 to -9.6 ‰) from the onset to the withdrawal of the monsoon

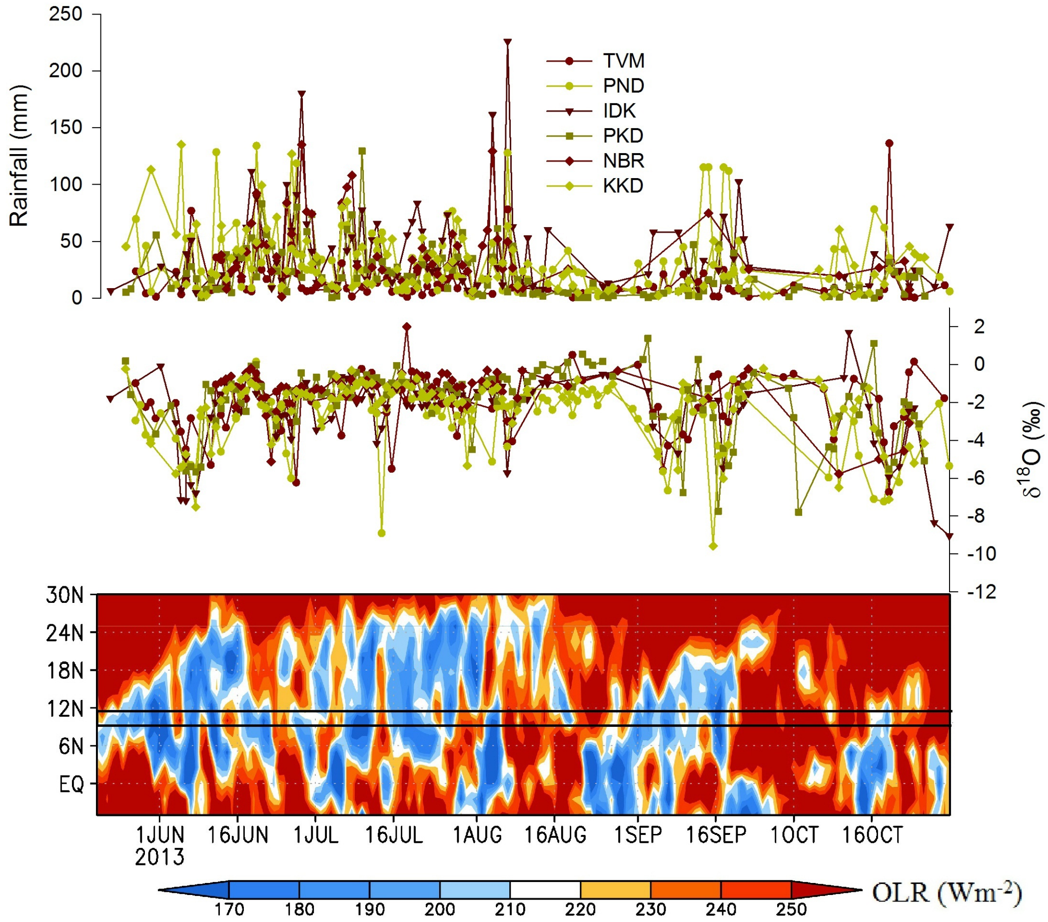

Figure 3.4: (a) Time series of measured amount of daily rain (mm). (b) rain $\delta^{18}O$ (‰) and (c) Hovmöller diagram of average NOAA interpolated OLR over 65° E 77.5° E for the year 2013. Solid parallel lines in (c) depict the latitude range of the sampling stations. The abbreviations of station name are given in Chapter 2.

during 2012 (2013); the amount weighted average $\delta^{18}O$ of all the stations is -2.8 ± 1.6 ‰ (-2.3 ± 2.1 ‰). Hovmöller diagrams i.e., latitude versus time plot of Outgoing Longwave Radiation (OLR), averaged over 65.0 to 77.5^{o}E, [Fig 3.3 and 3.4 (c)] indicate the relevance of organized convective activity, in determining the temporal variability of rain $\delta^{18}O$. Low values of OLR represent intense convective activity (thick clouds) and high values represent a clear sky. Figures 3.3 and 3.4 show that, relatively stronger ^{18}O-depletion is seen to correspond mainly with the presence of clouds over larger spatial extent, when OLR is low.

In 2012, four ^{18}O-depleted events were observed from the first day of the monsoon season until mid-July. During July 15 to August 5, the spatial extent of clouds is limited, yet continuous rain was recorded in most stations with a peak during July 25th. The average amount weighted $\delta^{18}O$ of rain during this period is -1.3±0.3‰, with no corresponding ^{18}O-depletion with increased rainfall; this shows that the rainfall $\delta^{18}O$ is independent on rain amount. From August 6th onwards movement of another large cloud cover occurred: 5-6 additional, high ^{18}O-depletion events were then recorded. After a dry period from mid September to 8th October, rain got re-established. This was the period of monsoon withdrawal and the change in wind direction, which brought moisture from the Bay of Bengal (BoB). ^{18}O was much more depleted in the rain [Fig 3.3].

Similarly, during 2013 too, such strong ^{18}O-depleted events were observed, though they were not as prominent as during 2012. The strong ^{18}O-depleted event associated with the onset of 2013 monsoon persisted for ~7 days followed by 3 more such events. During July 16 to 26, OLR was minimum, moderate rain was recorded in all the stations, but the rainfall ^{18}O remained within -1.7±0.2‰. This was again followed by two more strong ^{18}O-depleted events. Less rain events were recorded during 7 to 30 August with no organized convective activity, and the $\delta^{18}O$ of rain remained comparatively higher. Thereafter, two more strong ^{18}O

depleted events were recorded in association with organized convective activity. During October, rainfall ^{18}O was much more depleted (due to a different moisture source) even though there was no organized convection in the region [Fig 3.4].

Though the rainfall amounts during 2012 and 2013 monsoon seasons were significantly different, the average $\delta^{18}O$ of rainfall were not significantly different (-2.8 ± 1.6 ‰ and -2.3 ± 2.1 ‰ respectively). This is supported by the average convective activity occurred in the region during the season (June to September,). The average OLR during the monsoon season (67.5 - 75^{o}E and 5 - 12.5^{o}N grid box) was 219.9 ± 31.6 W/m^2 during 2012 and 215.0 ± 30.4 W/m^2 during 2013.

3.4 Amount effect

The canonical definition of the amount effect is the negative relation between the monthly rainfall and its $\delta^{18}O$ [*Dansgaard*, 1964]. In Kerala, no significant amount effect is observed during ISM months of 2012 and 2013 (Fig 3.5). The slopes of the rainfall amount- $\delta^{18}O$ relation show a large spatial variation. Positive relations (i.e., inverse amount effect) are observed at most of the stations. No relation is significant at P=0.05 level. These observations are consistent with the long-term (11 years) observation at the GNIP station Kozhikode. On a daily scale too, the slopes of the rainfall - $\delta^{18}O$ relation show a large spatial variation [Fig 3.6]. 5 out of 9 stations show significant negative correlations ($P < 0.05$ level) between daily rainfall and $\delta^{18}O$ of rain. But among these stations except at EKM, only 4-7% (R^2) of the daily rain $\delta^{18}O$ variability is explained by the rainfall. While in EKM, 32% (R^2) of the total variability of $\delta^{18}O$ is explained by rainfall.

The large spatial variability of rainfall- $\delta^{18}O$ relation is due to the coherent variations of daily rain $\delta^{18}O$ among the stations and the incoherent daily rainfall

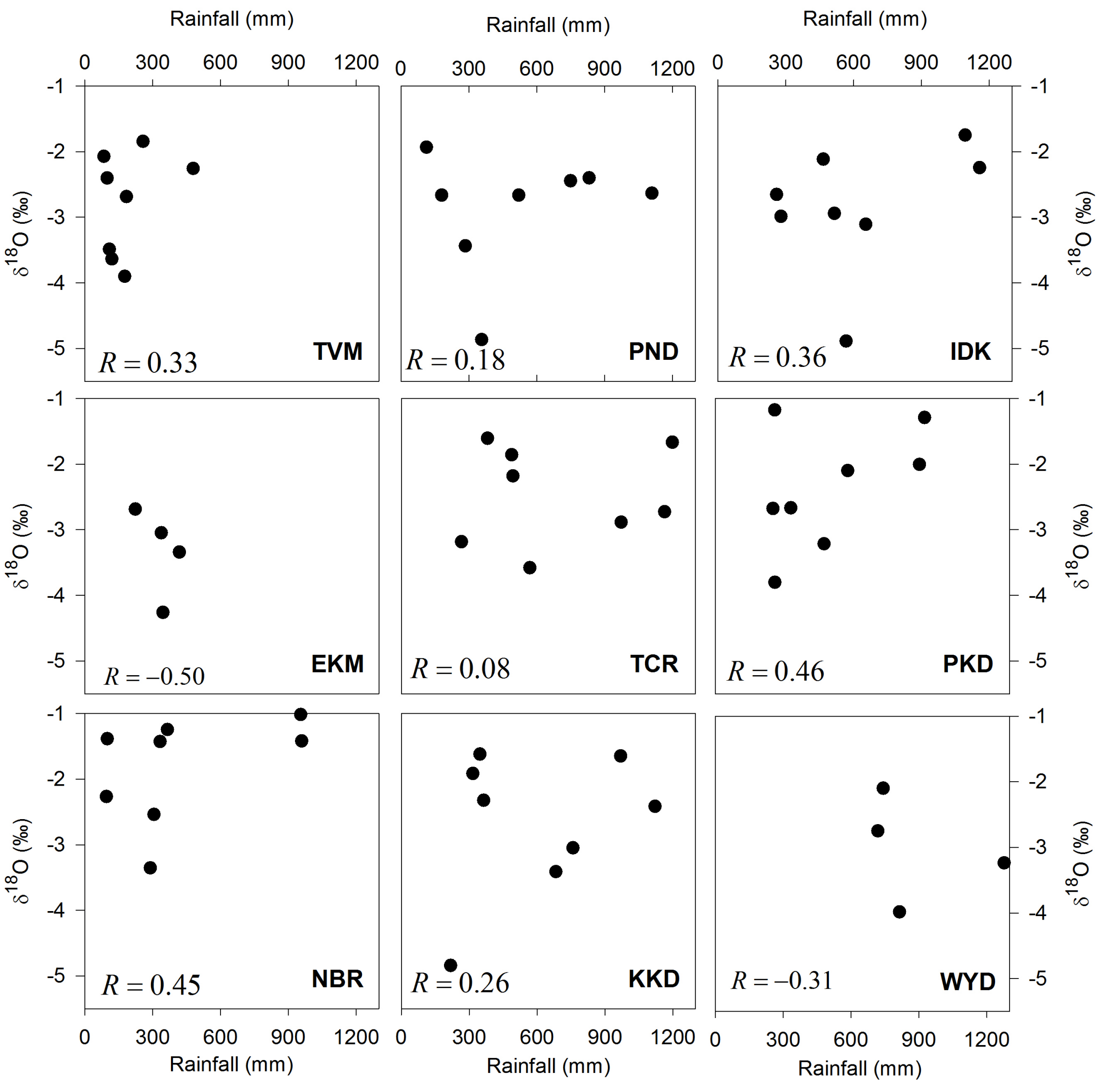

Figure 3.5: Relation between monthly rainfall and its $\delta^{18}O$ at different staions for June- September, 2012-2013 CE. No relation is significant at P=0.05 level.

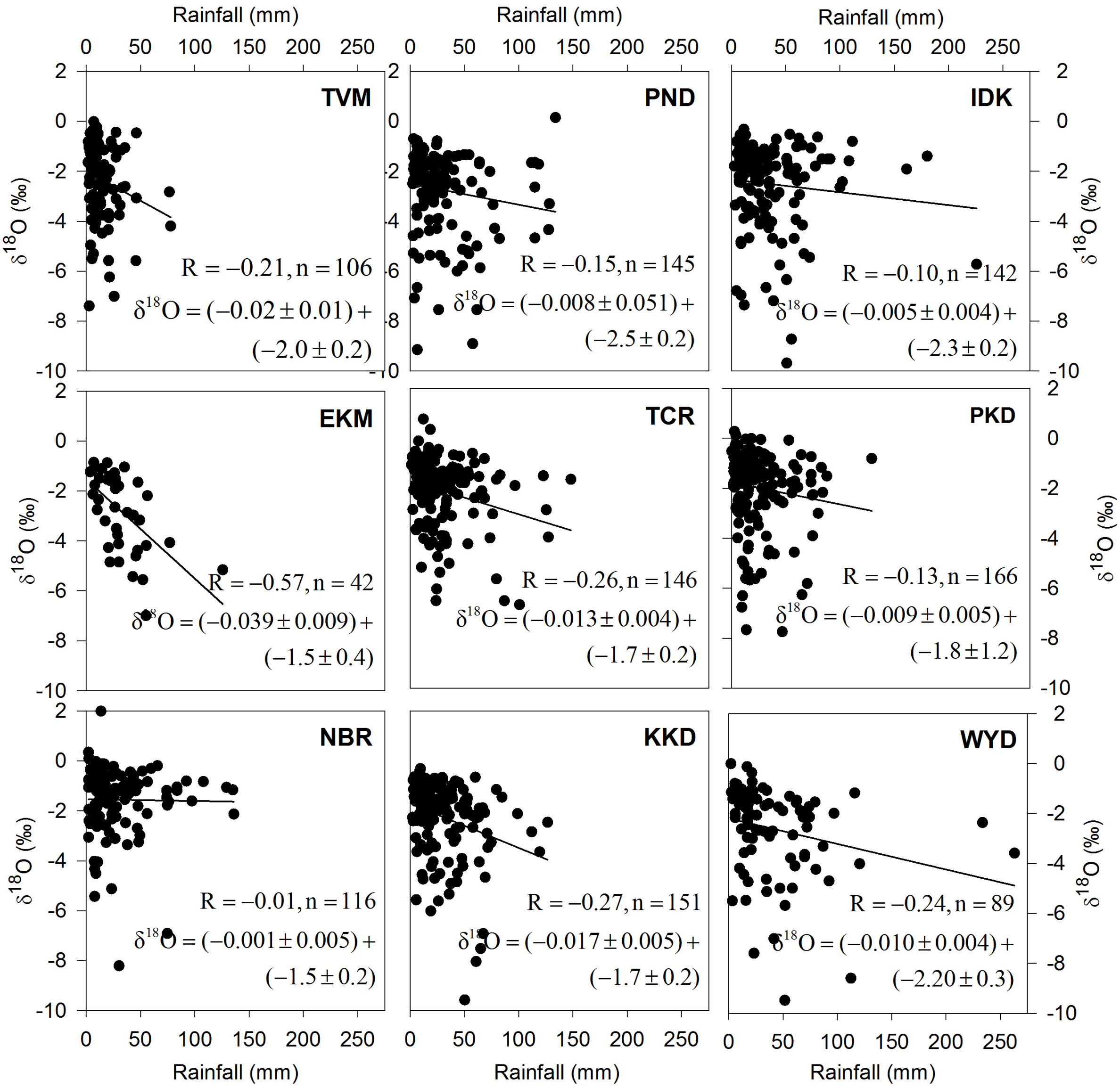

Figure 3.6: Relation between daily rainfall and its $\delta^{18}O$ at different stations for June- September (ISM), 2012-2013 CE.

variations. For example, the number of rainy days and the JJAS rainfall amount are remarkably less in TVM (53 rainy days, 465 mm rain) compared to TCR (77 rain events, 1864 mm rain) during 2012. No correlation is observed between the daily rainfall in these two stations (R=−0.02). But the daily variation of the rain $\delta^{18}O$ at TVM follows that of the station TCR with a correlation of 0.70 for the 38 common rainy days in 2012. The average $\delta^{18}O$ of JJAS rainfall in these stations do not show a significant difference as the rainfall does [Fig 3.1]. The relation between rainfall and its $\delta^{18}O$ has similar intercept values at both the stations. Generally, the intercept of rainfall - $\delta^{18}O$ relation is an indicative of the isotopic composition of the first condensate from the moist air mass [*Ramesh and Yadava*, 2005]. This reinforces the concept of same moisture source in both the stations. The slope of the regression line shows a higher value at TVM than at TCR [Fig 3.7]. Thus the different slopes are due to the contrast in rain amounts and the similarity in stable isotopic compositions.

3.5 Role of convective activity

Gadgil [2003] noted that OLR values significantly less than 240 W/m^2 and SST greater than 27.5^{o}C are indicative of large scale organized convection. Intense convective activity leads to increased rain. We observe a correlation of $R = -0.37$ ($n = 232$, $P < 0.0001$) between the OLR and the daily rainfall amount. At the same time, the correlation between OLR and the rain $\delta^{18}O$ is $R = 0.60$ ($P < 0.0001$).Thus the pronounced signature of organized convection is well captured as a high ^{18}O depletion of rain rather, than that of amount [Fig 3.8]. The observed correlation between daily rainfall and $\delta^{18}O$ ($R = -0.30$) is thus possibly manifested because of the OLR (convective activity)-rainfall relation.

Strong convection usually occurs in association with strong mid tropospheric convergence of moist air and thus vertical velocity too is a good surrogate for con-

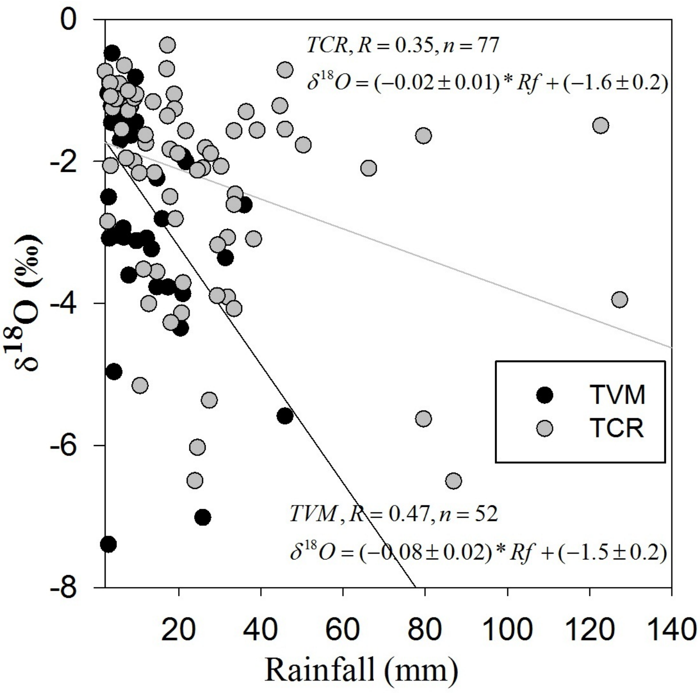

Figure 3.7: Correlation between rain amounts and its $\delta^{18}O$ in TVM and TCR during 2012 monsoon season.

vective activity. Back-trajectory analysis to the mean location (∼10.5^{o}N, 76.5^{o}E) of the sampling stations shows [Fig 3.12] a general upward motion of air masses during events of stronger ^{18}O-depletion, while downward or horizontal wind motion is seen during weaker ^{18}O-depletion rain events. The average trajectory height during weaker ^{18}O-depletion events is 2 km, and air parcels do not move vertically up when they reach Kerala; in contrast, during stronger ^{18}O-depletion events, the average trajectory height is below 1.5 km. This enables effective entrainment of additional moisture from the sub-cloud layer and the warm ocean below, before ascending over the rainfall site. At 4 pressure levels between 300 hPa and 600 hPa over a grid box of 75 - 77.5^{o}E and 7.5 - 12.5^{o}N [Fig 3.8], a linear correlation coefficient of 0.37 (n = 232, P $<$ 0.001) is observed between rain $\delta^{18}O$ and the average vertical velocity (ω, hPa/s) up to the time of monsoon withdrawal.

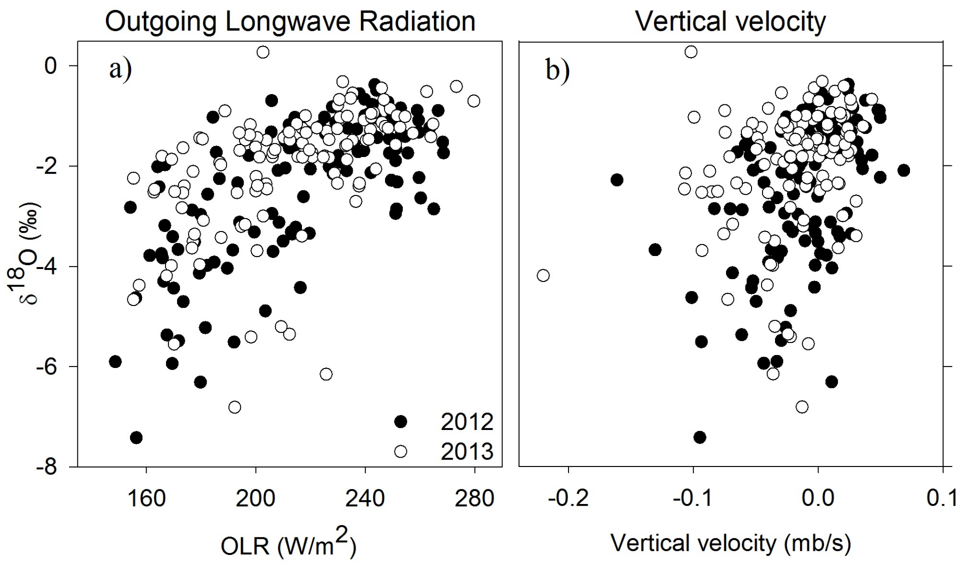

Figure 3.8: (a) Average OLR (67.5 - 75^o E and 5 - 12.5^{o}N grid box) versus $\delta^{18}O$ of rain and (b) average vertical wind velocity (MERRA, average of 300 hPa to 600 hPa pressure levels and 75-77.5^{o}E, 7.5-12.5^{o}N grid box) versus $\delta^{18}O$ of rain for June 1st to September 30, 2012 ans 2013.

Recent studies indicate the equal contributions of both convective and stratiform clouds in the Maximum Cloud Zone (MCZ) of ISM in determining the rainfall [*Chattopadhyay et al.*, 2009]. The large spatial extent of stratiform cloud leads to mesoscale subsidence of background vapour depleted in ^{18}O and D into the sub-cloud layer. ^{18}O depletion of stratiform clouds by this mixing of environmental air could also be an additional reason for the observed variability of rain ^{18}O and D. The ^{18}O and D depleted remnant vapour after the condensation also reaches the sub-cloud layer along with the mesoscale subsidence and downdraft. During the convective updraft, this vapour is also taken up into the cloud from the sub-cloud layer and thus the rain becomes more depleted in ^{18}O and D. Hence, for large scale convective events, along with the other factors, recycling of ^{18}O and D depleted vapour from stratiform clouds during the MCZ activity too leads to rain ^{18}O depletion [*Kurita*, 2013; *Risi et al.*, 2008].

3.6 ^{18}O and D depleted and enriched rain events

We have seen that the $\delta^{18}O$ of rain is unrelated to the local rain amount and it is related to large scale convection. Then $\delta^{18}O$ values of rain should be comparable with large scale rain as measured by TRMM (Tropical Rainfall Measuring Mission). The difference in the spatial patterns of TRMM derived rainfall and OLR during stronger and weaker ^{18}O-depletion rain events (the latter events are not associated with large scale convection) are shown in Fig 3.9 and 3.10. Intense rains [Fig 3.9(b) and 3.10 (b)] from clusters of clouds [Fig 3.9(d) and 3.10 (d)] with a large spatial extent over the eastern Arabian Sea, including southern peninsular India, are observed during stronger ^{18}O-depletion rain events. In contrast, weaker ^{18}O-depletion rain events (Fig 3.9(a) and 3.10 (a)) are characterized by isolated clouds with smaller spatial extent [Fig 3.9(c) and 3.10 (c)].

The average OLR values over the region of convection (5 - 12.5^{o}N and 67.5 - 75^{o}E grid box) during high and low ^{18}O-depletion events are 180 ± 19 W/m^2 and 235 ± 19W/m^2 (184 ± 24 W/m^2 and 228 ± 26 W/m^2), respectively during 2012 (2013). The corresponding average TRMM rainfall values for the same are 15 ± 7 mm/ day and 2 ± 4 mm/day (17 ± 11 mm/ day and 3 ± 4 mm/day during 2013), respectively.

Thus, the OLR and TRMM rainfall are significantly different during weak and strong ^{18}O-depletion events. Presence of clouds with large spatial extent leads to stronger ^{18}O-depletion because (i) fresh condensate is enriched in ^{18}O relative to the vapour according to the Rayleigh distillation theory [*Clark and Fritz*, 1997], and so the increased condensation (higher rain amount) reduces ^{18}O in the rain, (ii) rain drops re-evaporate to a lesser extent at the cloud base due to higher ambient humidity and thus less enrichment of ^{18}O compared to events of lesser rain [*Dansgaard*, 1964]; and (iii) unsaturated downdraft vapour and re-evaporated vapour (both relatively depleted in ^{18}O) during rain events feed the sub-cloud

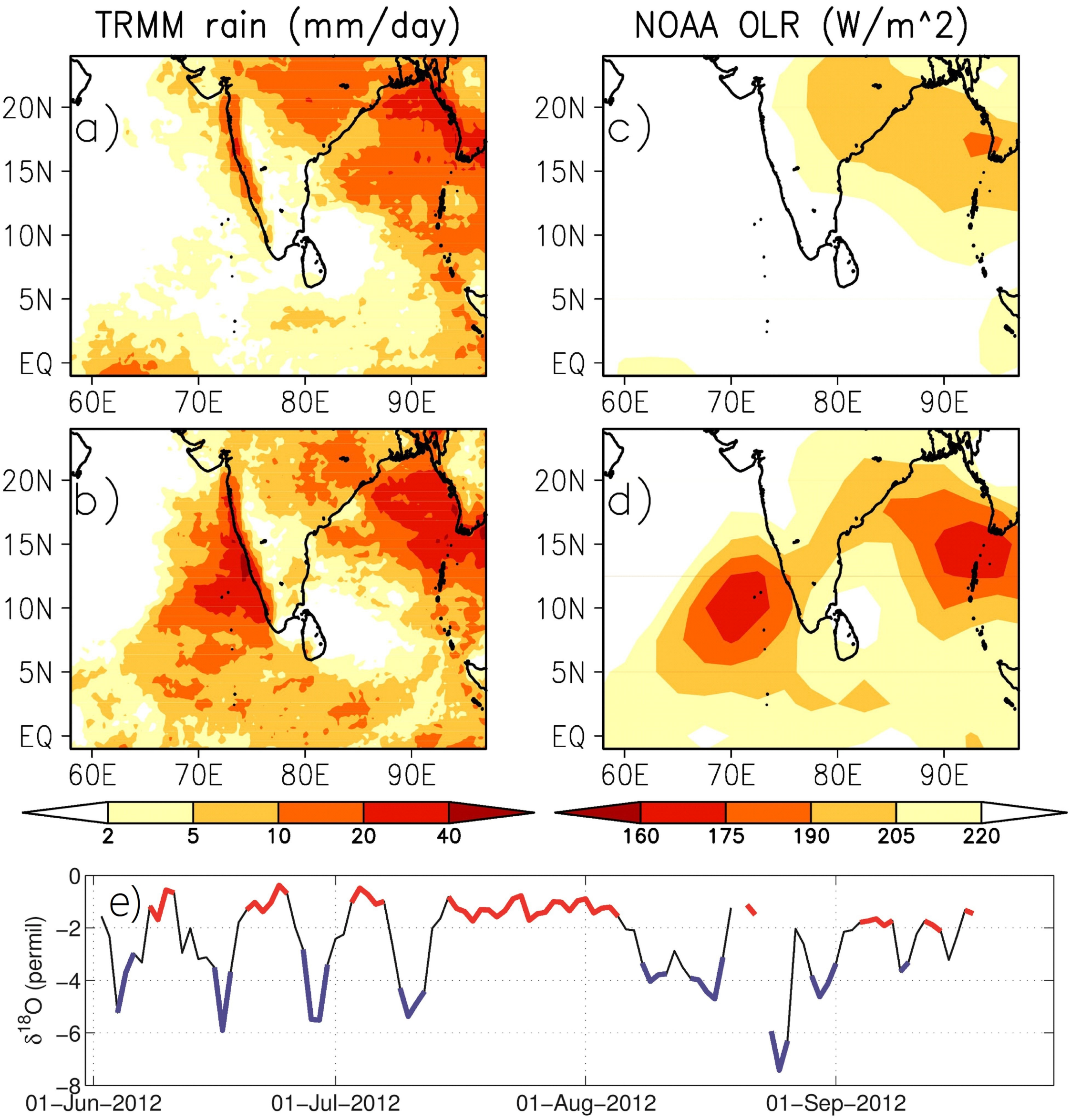

Figure 3.9: Composite of rainfall (TRMM 3B42) and OLR (NOAA) pattern during stronger ^{18}O depletion (b,d) and weaker ^{18}O depletion (a,c) rain events. e) Shows the days chosen to plot the composite of stronger ^{18}O depletion (blue) and weaker ^{18}O depletion (red) rain events during 2012 CE.

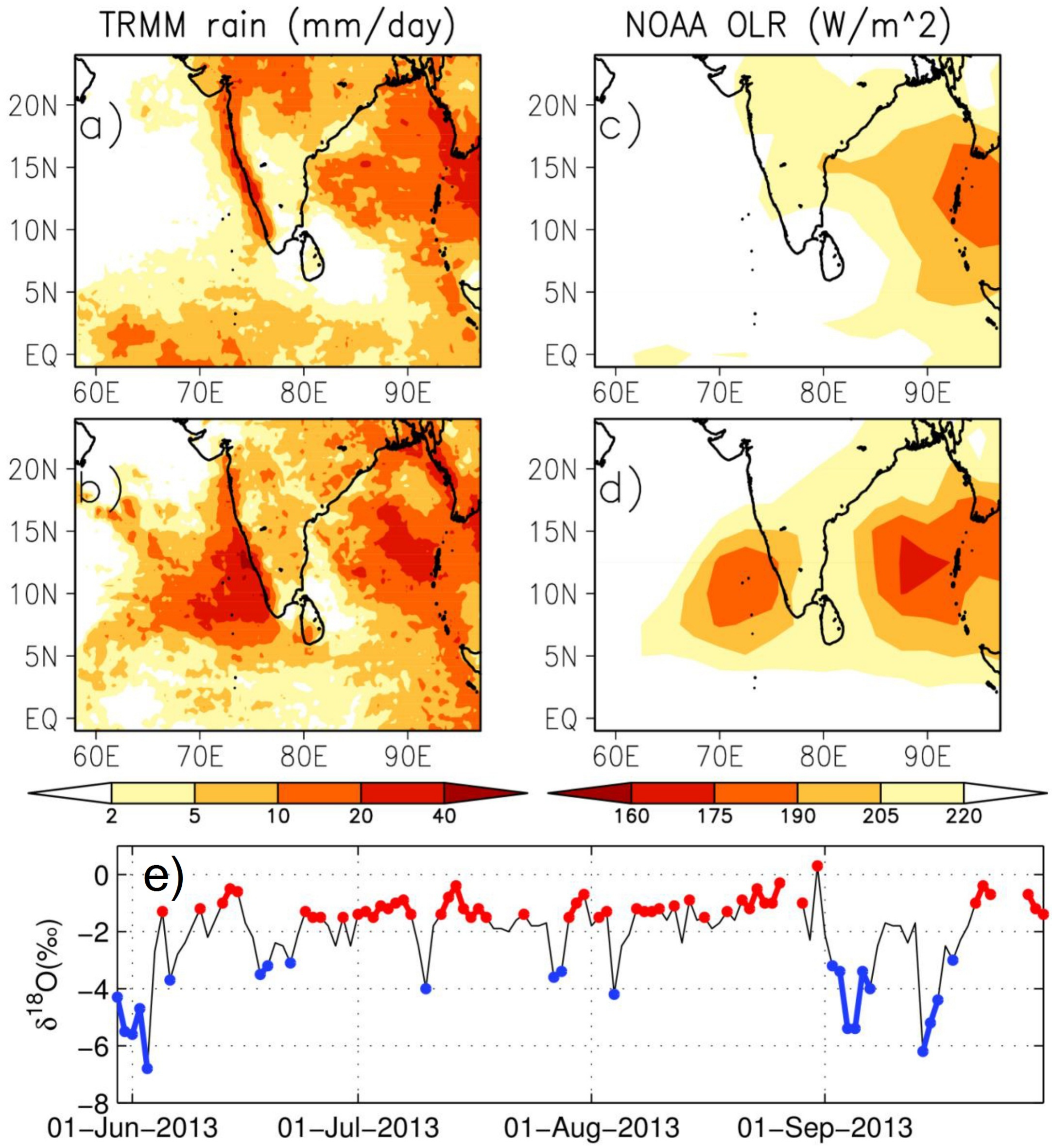

Figure 3.10: Composite of rainfall (TRMM 3B42) and OLR (NOAA) pattern during stronger ^{18}O depletion (b,d) and weaker ^{18}O depletion (a,c) rain events. e) Shows the days chosen to plot the composite of stronger ^{18}O depletion (blue) and weaker ^{18}O depletion (red) rain events during 2013 CE.

layer vapour [*Kurita et al.*, 2011; *Midhun et al.*, 2013], which will entrain to the convective clouds through updraft and the rain is further depleted in ^{18}O.

3.7 Influence of spatially extended rain events

The daily amount-weighted all-station average $\delta^{18}O$ of rain and grid-wise ($0.25^o \times 0.25^o$) daily TRMM-derived rainfall show a statistically significant (R > 0.25; P > 0.01) negative correlation over the south eastern Arabian Sea, including the Kerala coast [Fig 3.11]. This region of high correlation is more intense in 2012 relative to 2013. The spatial correlation pattern is similar to the OLR and TRMM rainfall pattern during strong ^{18}O depletion events [Fig 3.9(b) and (d) and 3.10 (b) and (d)] . This reinforces our conclusion that this negative relationship is not due to the canonical 'amount effect' (which is local) but rather due to large scale convection and the cloud spread.

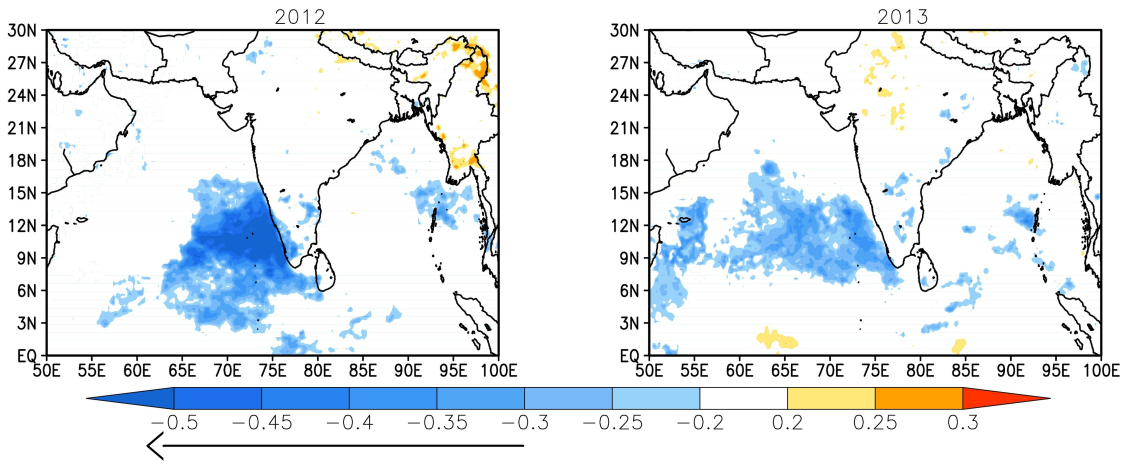

Figure 3.11: Spatial correlation pattern of the daily average $\delta^{18}O$ of rain at all stations with the TRMM3B42 rainfall over the south Asian region at each $0.25^o \times 0.25^o$ grid for the period June to mid October. Values statistically significant at 0.001 level (R > 0.30) are indicated with an arrow at the bottom of the colour bar.

3.8 Moisture source variation

During ISM, equatorially asymmetric pressure pattern leads to cross equatorial flow, also known as the Low Level Jet Stream (LLJ), which connects the Mascarene High in the Southern Hemisphere and the Monsoon Trough over India and transports moisture from the southern Indian Ocean to south Asia. Intra seasonal variability of LLJ is also seen associated with the active/break cycles of ISM as per the pressure fluctuation between the two hemispheres. Back trajectory analysis (see methods) shows that during days of strong ^{18}O -depletion, air mass travels longer distances from maritime locations from the south of the equator in 2012. In contrast, during the 3 days prior to the weak ^{18}O -depletion events, the air mass moves zonally from the western Arabian Sea, as well as the inland locations of northern Somalia.

During 2013, this pattern of dual moisture transport pathways of strongly and weakly ^{18}O depleted events are not clearly observed. Out of ten strong ^{18}O depleted events, 6 show a cross equatorial flow similar to that observed during 2012. 2 events show trajectories from Somali coast, still a clear upward motion from the off Kerala shore can be seen and the trajectory height was below 500m until rise of the air parcel. Similarly, out of the nine weakly ^{18}O depleted events, 4 events show a cross equatorial flow. Nevertheless, the height of the parcel shows a descending motion towards Kerala. Thus, large scale organised convection over Kerala is seen mostly in association with a cross equatorial flow of wind. While the isolated events are mainly associated with zonal wind from Somali coast region. Thus more observations are needed to further confirm this.

3.9 Anomalous events

An anomalous high rain event occurred during 18 - 28th of July with low ^{18}O-depletion all over Kerala. The rain amount was quite high in many stations,

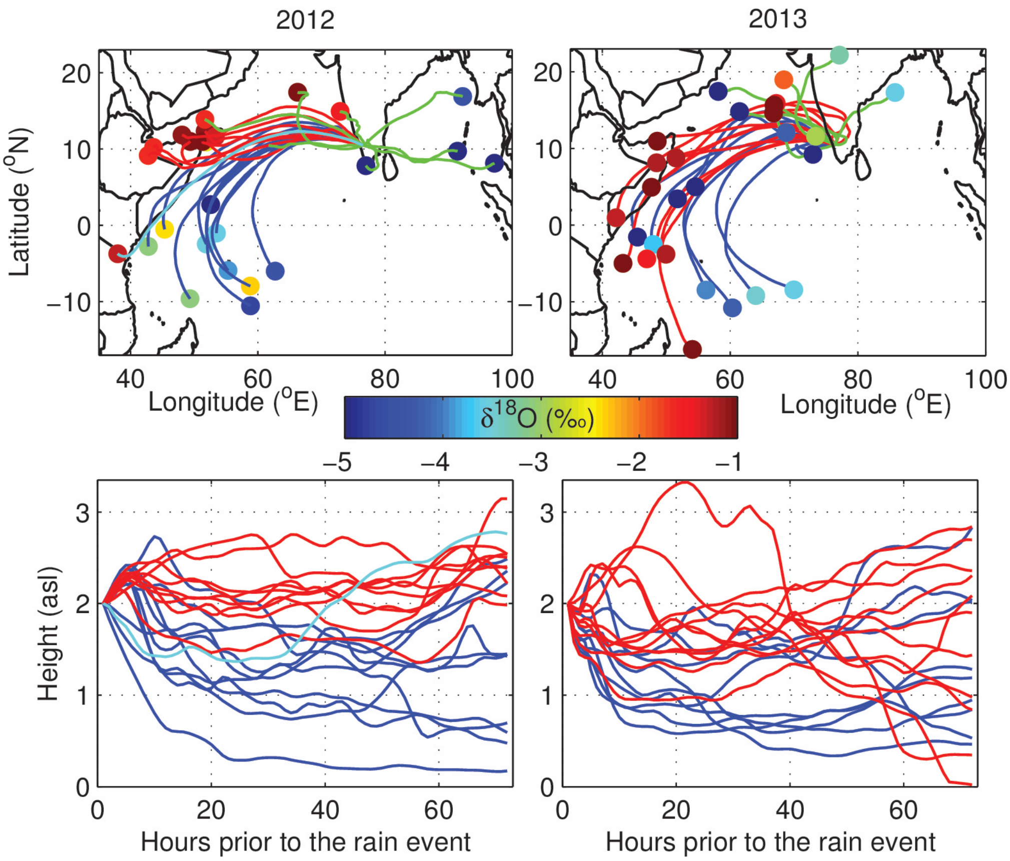

Figure 3.12: a) Three-days back trajectory to the mean location of sampling stations (10.50^{o}N, 76.50^{o}E), derived from the HYSPLIT model, for weak ^{18}O depletion events (red lines), strong ^{18}O depletion events (blue lines) and rain events during October (green lines), the month of monsoon withdrawal. Cyan line shows the back trajectory ending on 25th July, 2012, when weak ^{18}O depletion events with heavy rainfall occurred in the absence of organised convection. The filled circles indicate the position of the air mass 72 hours prior to rain, and their colours indicate the $\delta^{18}O$ of rain at the final station (plotted at the initial point to avoid clustering at the end point); refer to colour code on the right. b) Change in the height of the air mass en-route during strong ^{18}O depletion (blue) and weak ^{18}O depletion events (red), and on during 25th July (cyan) to the mean cloud base altitude at the sampling station (2 km).

particularly in the north. Organized convective activity was absent [Figs 3.3]. Yet, the location of origin of the air mass [Fig 3.12] does not show significant difference (taking into account the associated model uncertainty) from those during strong ^{18}O-depletion rain events. Air mass back trajectory of 25^{th} July shows a descending motion up to 1.5 km (above m.s.l) till the previous 30 hours and subsequently an ascending motion [Fig 3.12]. Therefore the dominant vapour source is likely confined to the atmosphere over the Arabian Sea (with a little contribution from south of the equator), though the parcel had an apparent cross equatorial flow. Thus, along with the absence of large scale clouds during this event, this could also be a reason for the observed anomaly.

During June 16-26, 2013, no ^{18}O depletion was observed though the OLR values were low [Fig 3.4]. The daily spatial pattern of rainfall and OLR show that the location of large scale organized convection was mostly east of the sampling location, with a small extension towards Kerala. The rain obtained in the stations during this period could be from the moisture brought by the south westerly wind, with very little contribution from the recycled moisture from convective area. This could be the reason for the observed isotopic enrichment of the rain water.

3.10 Monsoon withdrawal

The withdrawal of monsoon after ISM, leads to the change in wind direction from south-westerly to north-easterly. The $\delta^{18}O$ of rain is much more negative ($\sim$ 3 ‰ depletion in ^{18}O; -2.2 ± 1.9‰ during ISM and -4.9 ± 2.9‰ during October) during this period when the wind travels from BoB. The suggested reasons are: (i) the air mass travels a longer distance from the BoB, effectively depleting the rain ^{18}O over Kerala, due to rainfall extraction en route (the continental effect), (ii) Relatively lower $\delta^{18}O$ of surface BoB due to seasonal run-off from the

Ganga- Brahmaputra river system [*Breitenbach et al.*, 2010; *Singh et al.*, 2010]. This isotopic depletion after the monsoon withdrawal is clearly observed during 2012 and 2013. These will be discussed in more detailed in Chapter 5.

3.11 Conclusion

To summarise, the presence of large scale cloud bands during ISM leads to a strong ^{18}O-depletion in the monsoon rain. This signature of convective activity is well captured in rain $\delta^{18}O$ rather than in the local rainfall. This is confirmed by an analysis of the spatial pattern of clouds using OLR and the TRMM derived rainfall. Intense cloud activity with a large spatial extent is associated with a strong cross equatorial flow and high moist air convergence over Kerala during all the high ^{18}O-depletion rain events. Analyses of proxies of convection such as OLR, vertical wind velocity and the air mass back trajectory show high moisture convergence and heavy convection in the southern Peninsular India which can effectively take the recycled strong ^{18}O-depleted moisture from the sub cloud layer. Thus paleomonsoon proxies such as teak tree cellulose form Kerala may be interpretable in terms of the degree of large scale convective activity during the summer monsoon rather than the amount of monsoon rain.

Chapter 4

Water vapour- rain isotopic interactions over Kerala

This chapter presents a study of isotopic interactions between water vapour and rain in the southwestern peninsular India. The seasonal variability of the isotopic composition of water vapour and rainfall and their interaction are discussed first. The role of stratiform rain in the stronger heavier isotopic depletion observed in water vapour and rain of the large scale organised convective activity during the monsoon period is discussed next.

The stable oxygen and hydrogen isotopes of (δ_v) water vapour in the atmospheric boundary layer affect (i) the stable isotopic composition of evaporation flux [*Craig and Gordon*, 1965] from the ocean and (ii) modulate monsoon proxies such as the $\delta^{18}O$ and δD of tree ring cellulose through plant physiological cycle [*Managave et al.*, 2011; *Roden et al.*, 2000; *Sheshshayee et al.*, 2005]. Yet, perhaps because of the tedious sampling procedure for water vapor, measurements of its stable oxygen and hydrogen isotopic compositions ($\delta^{18}O_v$ and δD_v, respectively) are limited. As even the simplest of isotopic models necessarily require δ_v as an input, previous studies mostly assumed that the water vapor was in isotopic equilibrium with monthly mean rain and calculated it theoretically [*Jasechko et al.*, 2013; *Sheshshayee et al.*, 2010]. While this assumption may be valid for average values over longer time scales (months or years) , it could fail on shorter time scales (days or weeks) [e.g., *Deshpande et al.*, 2010; *Srivastava et al.*, 2015].

Though the major source of atmospheric water vapour is the evaporation from the oceans, its stable isotopic composition is significantly altered over land by transpiration [*Jasechko et al.*, 2013; *Moreira et al.*, 1997; *Wang and Yakir*, 2000], mixing [*Worden et al.*, 2007] and rain re-evaporation [*Berkelhammer et al.*, 2012; *Kurita et al.*, 2011; *Risi et al.*, 2008]. Recent studies reveal that the isotopic variations of rain and vapour during prominent tropical weather activities are mainly controlled by the rain-vapour interaction [*e.g., Berkelhammer et al.*, 2012; *Gedzelman et al.*, 2003; *Kurita*, 2013]. Rain-vapour interactions involve rain drop re-evaporation and isotopic equilibration of rain drop with the surrounding vapour [*Lee and Fung*, 2008; *Moore et al.*, 2014; *Risi et al.*, 2008]. The water vapour left behind after condensation of raindrops at higher altitudes of the atmosphere, more depleted in the heavier isotopes, is dragged down to the sub-cloud layer by strong downdrafts associated with large scale convective systems. Rain drop re-evaporation also contributes water vapor strongly depleted in ^{18}O and D to the sub-cloud layer. These recycled components of the vapour further feed into the systems; this acts as a feedback mechanism in large scale organized convective systems. This results in strong ^{18}O and D depletion in rainfall [*Berkelhammer et al.*, 2012; *Kurita et al.*, 2011; *Lawrence et al.*, 2002; *Moerman et al.*, 2013]. Rain drop re-evaporation and isotopic equilibration with the surrounding vapour are more effective during stratiform rain than during convective rain. Thus stratiform clouds can effectively produce vapour strongly depleted in ^{18}O and D and play a crucial role in the moisture recycling occurring in organized convective regime [*Kurita*, 2013; *Moore et al.*, 2014]. Isotopic measurements of atmospheric water vapour are still quite limited around the globe, and more measurements could help understand these processes better.

We set up 9 rain sampling stations over Kerala, southwestern India, where the monsoon onset begins around the end of May each year. Of these, two were hill stations: Ponmudi (8.76^{o}N, 77.12^{o}E; 780 m above m.s.l.) and Wayanad (11.51^{o}N, 76.02^{o}E; 800 m above m.s.l.). Monsoon vapour could be directly samples at these stations. These locations are characterized by seasonally reversing winds and thus the rain occurs from two different sources of moisture during the year. Both the stations are located at west of Western Ghats and obtain the majority of the annual rain during the Indian Summer Monsoon (ISM, June-September). North East Monsoon (NEM, October-December) also contributes significant amounts of rainfall at these stations (∼30% at Ponmudi and ∼14% at Wayanad).

4.1 Back trajectory analysis

5 days back trajectory analysis was done for every day of the collection using the Hybrid Single-Particle Lagrangian Integrated Trajectory (HYSPLIT). The relative humidity of the air parcels along their trajectory until they reach the sampling sites is also plotted in the top panels of Fig 4.1. The trajectories show distinct patterns during pre monsoon (April-May), ISM and NEM seasons ac-

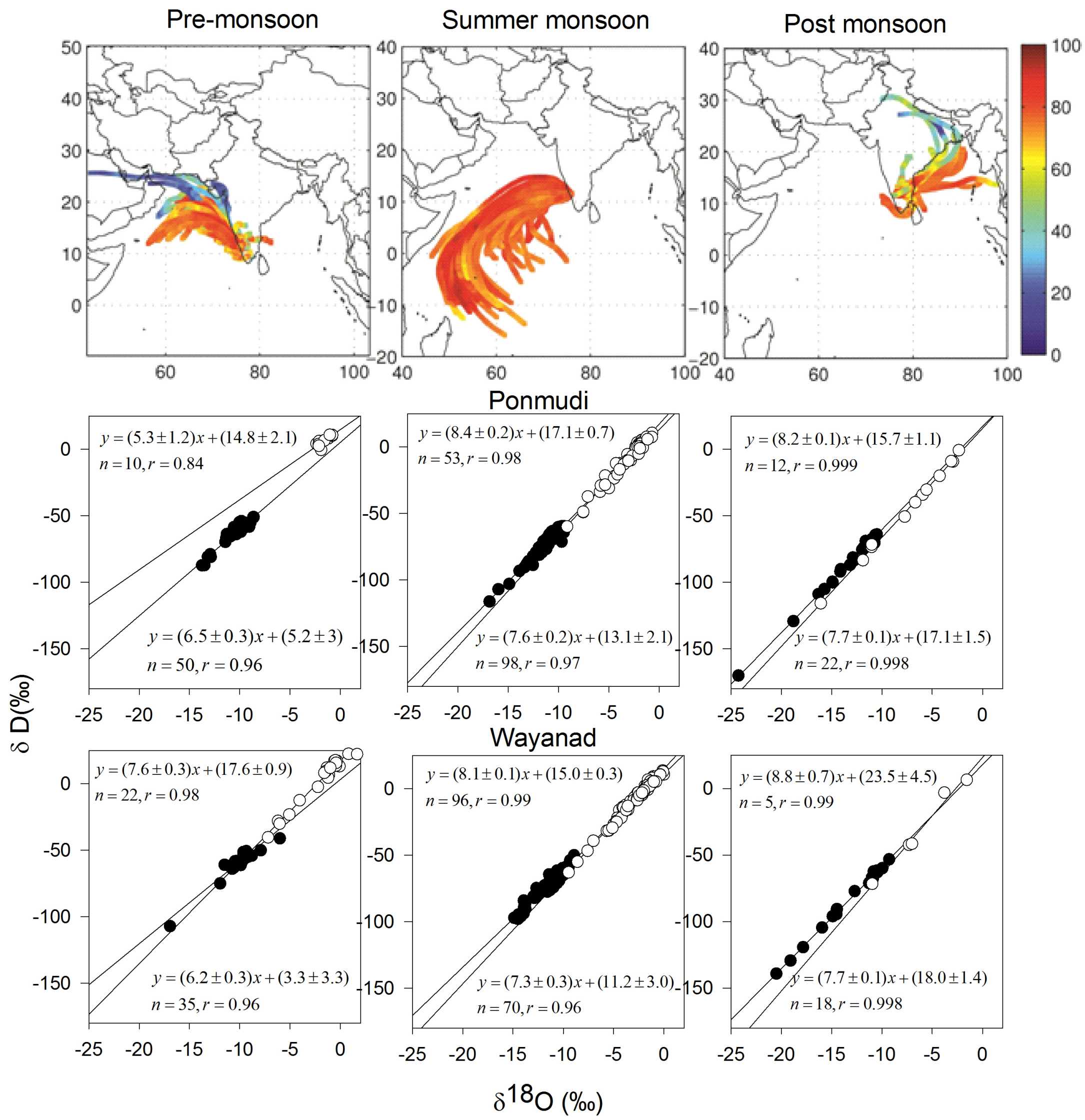

Figure 4.1: Top panel shows 5 days back trajectories of air parcel to Kerala (surface level) during the 3 seasons. The colour of the trajectory shows the relative humidity with the scale (legend) on the right. The six bottom panels show the local meteoric water and vapour lines of different seasons at Ponmudi and Wayanad. The open circles represent the $\delta^{18}O$ and δD measurements of the rain and the filled circles represent those of water vapour. Linear regression equation for rain $\delta^{18}O$ and δD are given in the top left of the graphs, while that for water vapour is given in the bottom right side in each figure.

cording to the prevailing wind. During the pre monsoon, the air parcels which reach Kerala mostly come from the Arabian Sea (track for the previous 5 days) with relative humidity $> 70\%$. Some air parcels show their trajectories from West Asia with very low relative humidity ($< 40\%$).

During ISM, the 5 day back trajectories show south westerly winds from the southern Indian Ocean reaching Kerala. The relative humidity along these back trajectories show that monsoon winds bring a great amount of moisture (RH > 70 %) from equatorial Indian Ocean. Though significant amount of rainfall occurs over the Arabian Sea during ISM [Fig 1.1, Climatological mean JJAS precipitation, GPCP data], the relative humidity of air parcels is high (irrespective of the height of the air parcel). A constant supply of moisture from the Arabian Sea leads to copious rainfall over Kerala (climatological annual ISM rainfall in Kerala is 2040 mm).

The NEM occurs after the withdrawal of south westerly winds with the establishment of north easterly winds. Back trajectory analyses show that air parcels travel from continental area (mainly from the Indian subcontinent) with low relative humidity until they reach the Bay of Bengal (BoB). Thereafter, significant moisture uptake takes place from the BoB, leading to NEM rainfall over Tamil Nadu before reaching Kerala. Continental recycle moisture (surface evaporation and transpiration) may also contribute vapour to these air parcels when they cross the Western Ghats.

Here we report simultaneous isotopic measurements of water vapour ($\delta^{18}O_v$ and δD_v) and rain ($\delta^{18}O_r$ and δD_r) from two tropical coastal stations in Kerala, western peninsular India during April- October, 2012. The temporal variation of rainfall and near surface $\delta^{18}O_v$, δD_v and the relationship between them, the influence of moisture dynamics on the rain and vapour isotopic compositions during the Indian Summer Monsoon (ISM) are discussed.

4.2 Variations of δD and $\delta^{18}O$ of Vapour

Figure 4.2 shows the time series of $\delta^{18}O_v$, δD_v of water vapour and $\delta^{18}O_r$, δD_r of rain. Ponmudi received less rain (a total of 1357 mm) than Wayanad (3903 mm). These can be compared with the climatological mean values of the respective, nearest meteorological stations: 1412 mm at Trivandrum and 2889 mm at Kozhikode, respectively (`http://www.imd.gov.in/`). The $\delta^{18}O_v$ at both the stations show a significant correlation (R) of 0.54; and $\delta^{18}O_r$ values, R= 0.62. The $\delta^{18}O_v$ (δD_v) of water vapour at Ponmudi and Wayanad varied from -8.6 to -24.3‰ (-51.0 to -170.0‰) and -7.9 to -20.5‰ (-50.0 to -139.1‰) respectively, while the $\delta^{18}O$ (δD) of rain water varied from -0.7 to -16.1‰ (10. 9 to -115.7‰) and 1.7 to -11.0‰ (22.4 to -71.6‰). Ponmudi values are slightly lower than the corresponding values at Wayanad for all these parameters, because although the former received less annual rainfall, it received a higher proportion of the NEM, more depleted in ^{18}O and D (see below). The d-excess of water vapour at Ponmudi and Wayanad varied from 6.3 to 26.5‰ and 13.3 to 31.2‰ and that of rain water varied from 9.0 to 23.1‰ and 8.9 to 27.3‰, respectively. However, individual seasons show distinct mean values for $\delta^{18}O$, δD and d-excess as in Table 4.1.

Very few rainfall events were recorded during the pre-monsoon, contributed by occasional thunderstorms and a low pressure cyclonic storm (during the last week of April). The $\delta^{18}O$ - δD relation for vapour during pre-monsoon shows significantly lower values of slope and intercept compared to those of the other two seasons [Fig 4.1]. The slope of Local Meteoric Water Line (LMWL) of pre monsoon rainfall at Wayanad is close to that of the GMWL (Global Meteoric Water Line) with higher value of intercept (at Wayanad only; the number of data points at Ponmudi is 10) [Fig. 4.2]. This is because the maximum temperatures ($\sim 32^oC$) exist during the pre-monsoon, which lead to evaporation of rain in the

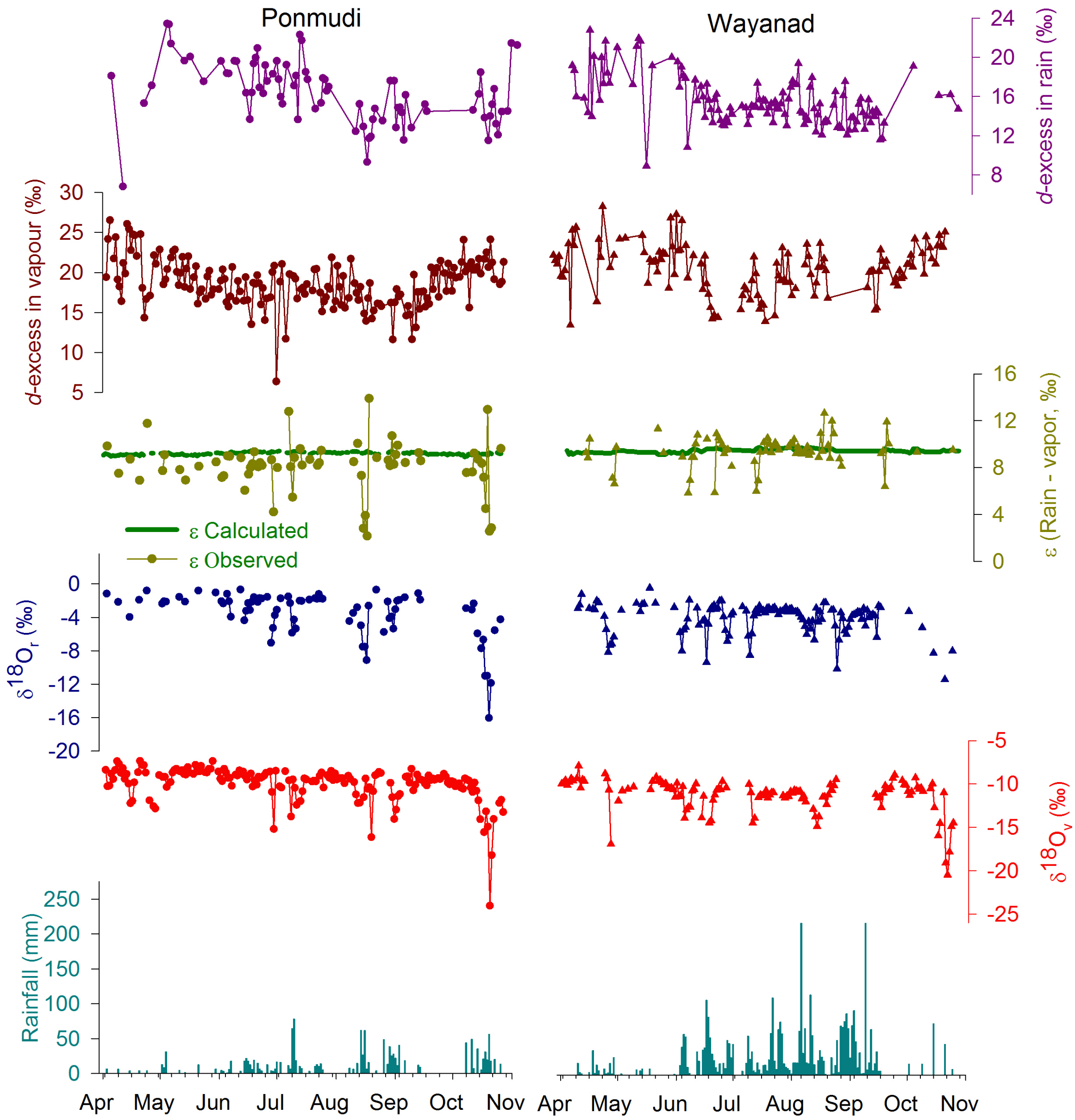

Figure 4.2: Time series of rainfall amount, $\delta^{18}O$ of vapour (whenever it is collected), $\delta^{18}O$ of rain, observed and the calculated equilibrium fractionation factor(ε),d-excess in water vapour and rain at Ponmudi (left) and Wayanad (right) in 2012.

Table 4.1: Seasonal mean $\delta^{18}O$, δD and $d-$excess values of water vapour and rain at Ponmudi and Wayanad during pre monsoon (April-May), ISM (June-September) and and NEM (October).

	Season	Amount of rain (mm)		Ponmudi		Wayanad	
		Ponmudi	Wayanad	Vapour	Rain	Vapour	Rain
	Pre monsoon	101.6	179.1	−10.2 ± 1.2	−1.9 ± 0.9	−10.1 ± 0.5	−1.8 ± 2.8
$\delta^{18}O$	ISM	935.7	3560.8	−11.0 ± 1.3	−3.1 ± 1.9	−11.4 ± 1.3	−2.5 ± 1.8
	NEM	319.6	163.6	−13.4 ± 3.2	−7.4 ± 4.3	−13.1 ± 3.4	−6.1 ± 3.6
	Pre monsoon	101.6	179.1	−61.4 ± 8.3	6.3 ± 3.8	−59.0 ± 10.0	3.6 ± 18.3
δD	ISM	935.7	3560.8	−70.5 ± 5.0	−9.1 ± 16.1	−71.8 ± 10.1	−5.1 ± 14.6
	NEM	319.6	163.6	−87.0 ± 25.1	−44.8 ± 35.1	−82.2 ± 26.2	−30.4 ± 31.9
	Pre monsoon	101.6	179.1	20.4 ± 2.9	19.3 ± 2.6	21.7 ± 4.0	18.3 ± 3.3
$d-$excess	ISM	935.7	3560.8	17.4 ± 2.5	16.1 ± 2.8	19.5 ± 3.1	14.8 ± 1.8
	NEM	319.6	163.6	20.6 ± 1.8	14.3 ± 1.9	22.3 ± 1.8	18.7 ± 5.1

atmosphere and a lower slope. The intercept is higher because of mixing with continental, evapotranspired vapour.

Water vapour and rain water during ISM are slightly depleted in ^{18}O and D compared to the pre-monsoon. But some individual events associated with large scale organized convection show comparatively stronger ^{18}O depletions in rain and vapour. The slopes of Local Meteoric Water and vapor lines are close to 8, signifying condensation at isotopic equilibrium. Higher values of intercept in rain compared to the vapour signify the locally derived moisture is much smaller than that advected by winds. This is confirmed by the slightly lower d-excess during ISM compared to the other two seasons. But, the seasonal d-excess values are not statistically different, as they show large variability within the season, confirming earlier observations [*Ramesh et al.*, 2012] based on data from the GNIP data (`http://www.univie.ac.at/cartography/project/wiser/`).

NEM rain and vapor show the lowest $\delta^{18}O$ and δD in the year (discussed later). The observed d-excess in rain and water vapour are slightly higher in this season. During this season too, at both the stations, the slopes of LMWL are close to 8 (condensation at isotopic equilibrium); the values of intercepts are higher compared to the other two seasons [Fig 4.1] because the component of re-cycled vapour is much higher as the air masses travel over larger distances over land [Fig. 4.4].

4.3 Rain-vapour isotopic interaction

$\delta^{18}O$ values of vapour in isotopic equilibrium with rain (calculated using $\delta^{18}O_r$ and ambient air temperature, *Majoube* [1971]) are significantly correlated with $\delta^{18}O_v$ at both the stations [Fig 4.3]. The observed difference (in ‰ units) between water vapour and rain water $\delta^{18}O_v$ are 8.3 ± 2.2‰ in Ponmudi and 9.4 ± 1.4‰ in Wayanad. These values are similar to the equilibrium fractionation factor (ϵ)

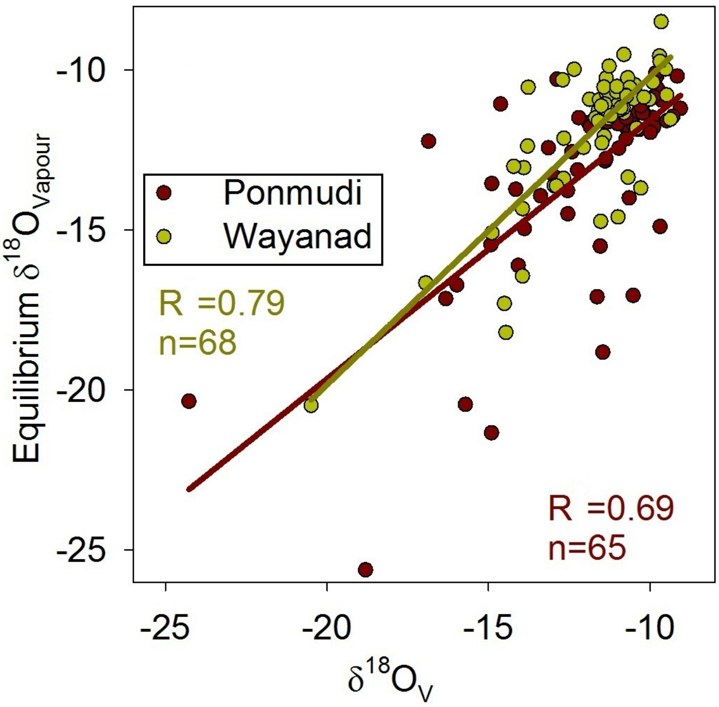

Figure 4.3: The relation between $\delta^{18}O$ of vapour and the $\delta^{18}O$ of vapour equilibrated with the rain (calculated for ambient temperature and $\delta^{18}O$ of rain).

calculated from the ambient air temperatures; 9.5 ± 0.1‰ and 9.4 ± 0.2‰ at Ponmudi and Wayanad, respectively. Though the average fractionation factor is similar to ϵ, it shows more deviations from ϵ mainly during some high rainfall events [Fig 4.2].

Fig 4.2 and Table 4.1 show that the rainfall and water vapour during NEM are more depleted in ^{18}O and D compared to the other seasons. This isotopic depletion of NEM rainfall was reported before [*Warrier et al.*, 2010; *Yadava et al.*, 2007] and can be seen in GNIP observations in peninsular India as well. We observe a higher ^{18}O depletion in rain (∼ 4 ‰) compared to the water vapour (∼ 2 ‰). Apparently the observed fractionation factor between rain and vapour is slightly less during NEM (7.9 ± 2.9‰, n = 13) compared to pre-monsoon (8.9 ± 1.4‰, n = 20) and ISM (9.0 ± 1.8‰, n = 100) periods. This could be because

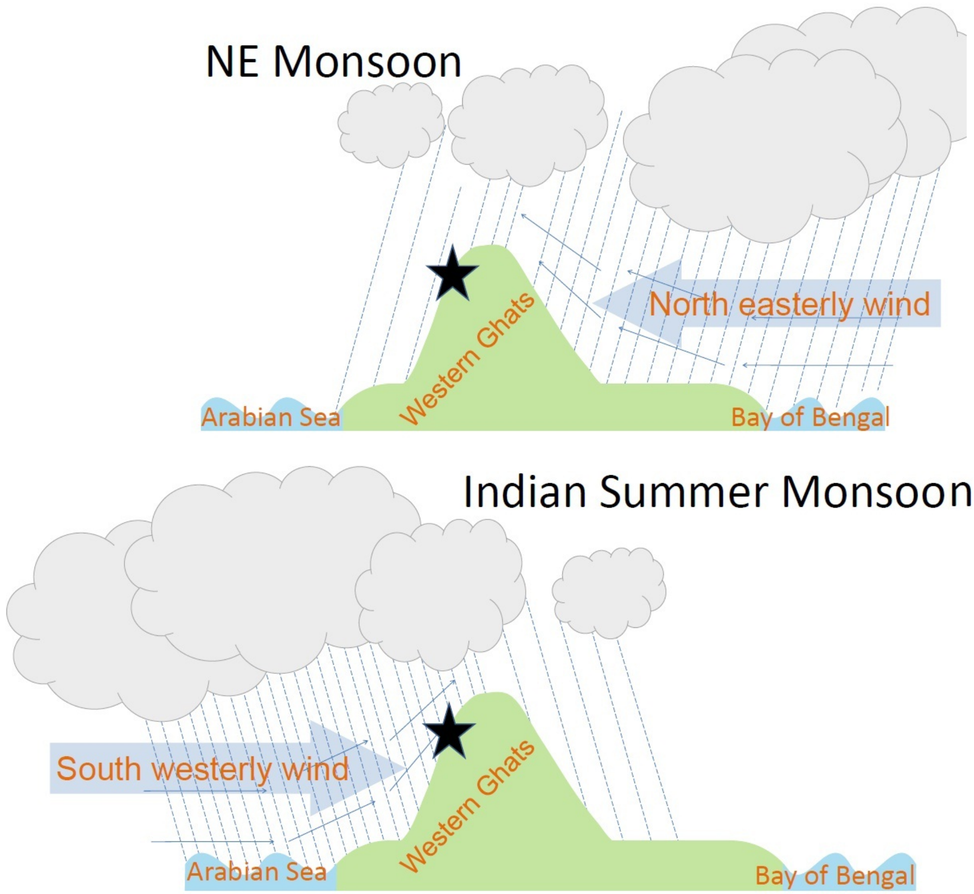

Figure 4.4: Schematic representation of wind pattern over Peninsular India during summer and NEM seasons. The star ($\star$) represents the location of sample collection.

the NEM rainfall at the sampling sites directly forms from the clouds, which are already depleted in ^{18}O and D. Since Kerala is located in the leeward side of the Western Ghats (for the northeasterly winds), locally derived moisture (evapotranspiration) also significantly contributes to the surface water vapour (Fig 4.4). And thus the rain and water vapour are not in isotopic equilibrium during the NEM season. Rain and moisture isotopic compositions of ISM are characterised by little alteration from locally derived moisture as the fractionation factor is close to the equilibrium values.

4.4 Moisture recycling during the Indian summer monsoon

During the ISM, the stable isotopic composition of rain and water vapour show strong intra-seasonal variations. *Lekshmy et al.* [2014] showed that, monsoon intra-seasonal variations of rainfall $\delta^{18}O$ in Kerala are associated with the large scale organized convection that occurs in the southeastern Arabian Sea, near the Kerala coast. Accordingly, we selected a grid box (8-12^{o}N and 70-75^{o}E) which includes in this region of large scale organized convection. The average convective and stratiform components of daily rainfall are then extracted from TRMM 3G68 data [`http://rain.atmos.colostate.edu/CRDC/datasets/TRMM_3G68.html`] for further analysis. Fig 4.5 shows the relation between rain /water vapour $\delta^{18}O$ and the calculated average daily rainfall and stratiform rain fraction in the grid box under consideration. On an average at both the stations, a linear correlation of R = -0.39 (R = -0.58) is observed between the total rainfall in the grid box and the average $\delta^{18}O_v$ (and $\delta^{18}O_r$) (both the relations are significant at P=0.01 level). ^{18}O depletion of rain from large scale organized convective systems is due to the intense moisture recycling occurring in the system; such as raindrop reevaporation, post condensation isotopic exchange, mixing with environmental air etc. The effects of these processes on rain and vapour isotopes vary according to the cloud type (convective or stratiform). The increase in the daily rain is reflected as an increase in both convective and stratiform rain. Thus the stratiform rainfall - $\delta^{18}O_v$ (and $\delta^{18}O_r$) relation is similar to the total rainfall - $\delta^{18}O_v$ (and $\delta^{18}O_r$) relation. It is also observed that, the increase in the total rainfall is characterized by increase in the stratiform rain fraction (i.e., the fraction of convective rain decreases during higher rainfall). The stratiform rain fraction shows a significant negative correlation (R = -0.35) with the $\delta^{18}O_v$ (and R = -0.65 with $\delta^{18}O_r$); this signifies the importance of stratiform clouds in moisture recycling in large scale organized convective systems. As reported before,

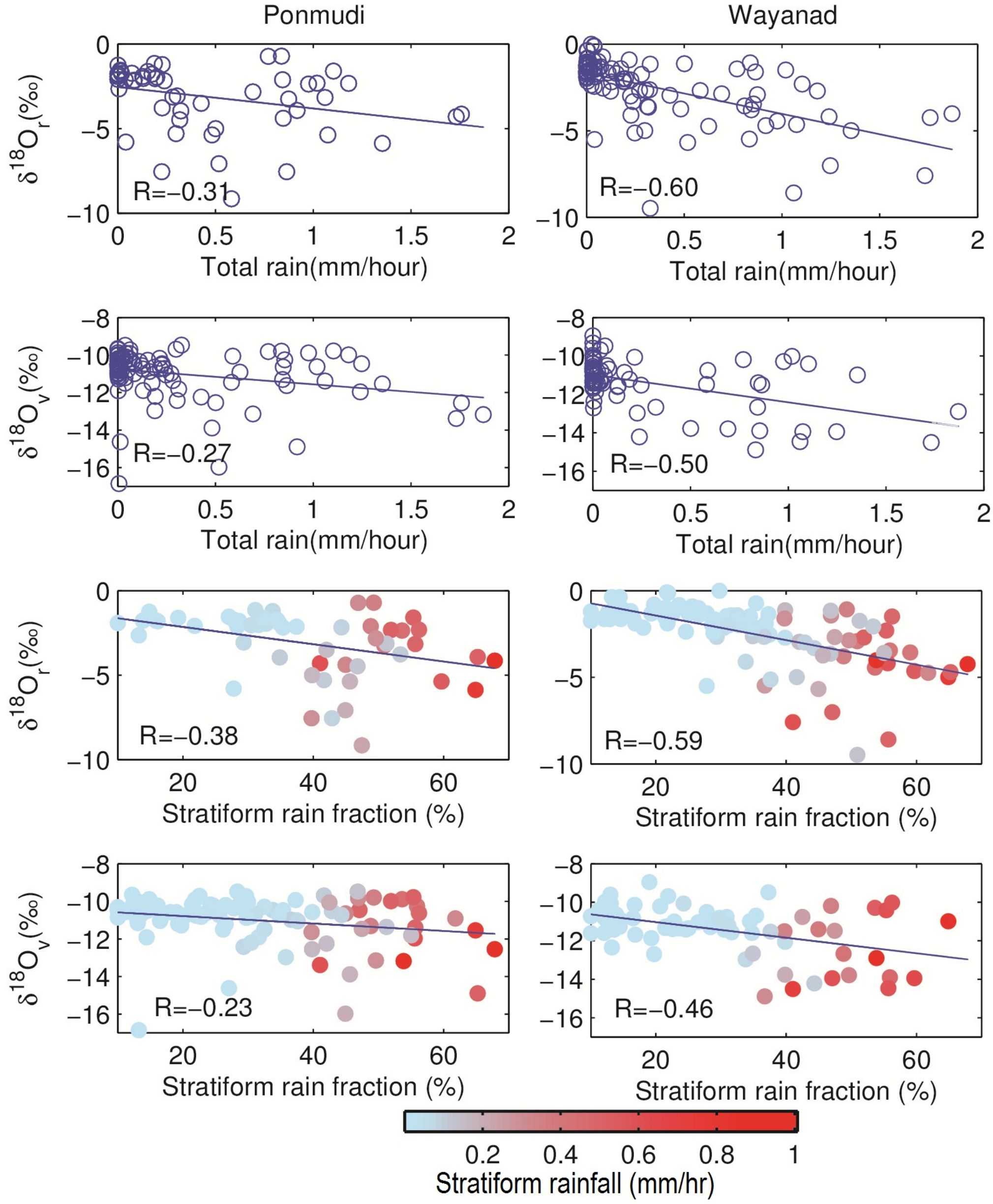

Figure 4.5: Relationship between daily $\delta^{18}O$ of vapour and $\delta^{18}O$ of rainfall with the daily total (top four) and stratiform rain fraction (bottom four) during ISM (June 1^{st} to September 30^{th}). The total and stratiform rain fractions are the average values over the grid box 8-12^{o}N and 70-75^oE. The colors of the symbols in the last 4 panels indicate the amount of stratiform rainfall (mm/hr) with respect to the total rainfall.

stratiform clouds and rain play an important role in the strong isotopic depletion observed during large scale rain events (eg., rain associated with Madden Julian oscillations, cyclones etc). Raindrop reevaporation and rain-vapour isotopic exchange are more for the smaller drops (generally during stratiform rain) due to their longer residence time in the atmosphere compared to larger rain (mainly from convective rain) drops. Thus our observations show that the presence more stratiform rain in large scale convective systems leads to higher ^{18}O depletion in the monsoon rainfall.

4.5 Conclusions

Our observations have provided high resolution stable isotope data on water vapour and rain isotopic data useful for studying tropical moisture dynamics. Distinct $\delta^{18}O$ and δD values during different seasons are due to (i) the variations in moisture sources, (ii) rain-vapour interactions and (iii) locally derived moisture (evapo-transpiration). Stable isotopic composition of ISM rain and water vapour are characterised by little alteration from locally derived moisture, but reflect the rain-vapour interactions occurring in the large scale organised convective clouds. Rain and vapour are observed to deviate from isotopic equilibrium mainly during the large scale organised convections that occur over the southeastern Arabian Sea. Stratiform rain fraction of this organised convective region plays a key role in moisture recycling and thereby rain and water vapour are depleted in the heavier isotopes during such events.

Chapter 5

'Amount effect' in peninsular India and Sri Lanka

This chapter mainly deals spatial and temporal variation of rainfall- $\delta^{18}O$ relation in peninsular India and Sri Lanka. Further the stronger ^{18}O depletion of north-east monsoon rain compared to the ^{18}O of summer monsoon rain is investigated.

Stable oxygen isotope ratios, measured as $\delta^{18}O$, of cave calcites and tree rings are utilised for the reconstruction of past monsoon rainfall. Some authors [*e.g., Managave et al.*, 2011; *Ramesh and Yadava*, 2005] interpret the $\delta^{18}O$ of proxies using the observed negative correlation between the monthly rainfall at the site and its $\delta^{18}O$; this amount effect, is typically $\sim -1.5‰/100$ mm of rain in the tropics [*Dansgaard*, 1964]. Others [*e.g., Wang et al.*, 2008] interpret in terms of monsoon intensity or regional scale convection [*e.g., Carolin et al.*, 2013]. The amount effect exhibits a large spatial variation; the causes include complex cloud-rainout processes [*Kurita*, 2013; *Moerman et al.*, 2013; *Moore et al.*, 2014; *Risi et al.*, 2008], seasonality of rain [*Cobb et al.*, 2007; *Yadava et al.*, 2007] and differences in the sources of moisture [*Xie et al.*, 2011].

Recently *Lekshmy et al.* [2014] showed that the local rainfall amount plays a weaker role in determining $\delta^{18}O$ of monsoon rain compared to moisture recycling associated with the large scale convective systems in south west India. The seasonal shift in the source of moisture and associated change in $\delta^{18}O$ of the incoming vapour further complicate the rainfall - $\delta^{18}O$ relation [*Araguás-Araguás et al.*, 1998; *Feng et al.*, 2009; *Warrier et al.*, 2010; *Yadava et al.*, 2007]. Peninsular India and Sri Lanka [Fig 5.1(a)] receive both the Indian summer monsoon (ISM, June-September) and north east monsoon (NEM, October-December); over the east peninsular Indian coast and Sri Lanka, NEM is the dominant source of rain, while over the rest of peninsular India ISM dominates. The seasonal wind fields and the moisture sources too differ significantly: during the ISM, driven by south westerly winds, the moisture source of rainfall lies in the Arabian Sea and southern Indian Ocean, while during the NEM, north easterly winds bring moisture mainly from the Bay of Bengal [*Wang*, 2006]. Here we investigate (i) the spatial variation of the amount effect and (ii) the causes for the seasonal difference in $\delta^{18}O$ of rainfall in NEM and ISM in peninsular India and Sri Lanka, with an aim to optimize the choice of ^{18}O based monsoon proxy sites from this region, rich in teak trees and limestone caves, so as to minimise noise in the reconstructed past monsoon signal.

5.1 The amount effect in peninsular India and Sri Lanka

Within the limited area (∼6 to 19^{o}N and 72.5 to 82.5^{o}E) considered, a significant spatial variation of the monthly rainfall- $\delta^{18}O$ correlation exists at GNIP stations in peninsular India and Sri Lanka [Table 5.1]. In peninsular India, observed correlations are not statistically significant (at P = 0.05 level), barring Kozhikode (GNIP with 92 monthly data) and Mangalore [*Yadava et al.*, 2007, with 7 monthly data], which show significant positive correlations. Although Kozhikode-Kavil in Table 5.1 (distinct from GNIP station Kozhikode, ∼30 km away) had only 15 months of data, it yields identical slopes and intercepts as GNIP data, albeit with higher standard deviation. In Sri Lanka, 8 of the 11 stations show highly significant negative correlations (–0.023 to –0.005‰ mm^{-1}), while at three GNIP stations the correlations are insignificant.

The relative contributions of ISM and NEM rainfall in peninsular India and Sri Lanka exhibit high spatial variability [Fig 5.1]. The ratio (r) of ISM (summer) rainfall to NEM (winter) rainfall was calculated using CRU climatological data. Barring Sri Lanka and south eastern peninsular India, which receive more NEM rainfall, the rest of the stations receive rainfall mostly from ISM. Further, NEM rainfall shows stronger ^{18}O depletion than ISM rainfall at most GNIP stations, reportedly the reason for the inverse amount effect [*Warrier et al.*, 2010; *Yadava et al.*, 2007], i.e., higher ISM rainfall with relatively enriched ^{18}O and lower NEM rainfall with relatively depleted ^{18}O. Our data for 9 stations in Kerala for 2013, reconfirmed [*Lekshmy et al.*, 2014] earlier inference that no amount effect exists, as was the case in 2012. Thus, we infer that the spatial variation of the slope of

Table 5.1: Monthly rainfall- $\delta^{18}O$ relations at different stations in peninsular India and Sri Lanka. Monthly rainfall below 5 mm is ignored. Correlations (R) which are significant at P = 0.05 level are highlighted (bold). GNIP stations (normal font);our stations and Mangalore [*Yadava et al.*, 2007] (*italics*). The average value of statistically significant amount effect is $-1.2‰$ per 100 mm of rain (barring Kozhikode and Mangalore). Table continued on next page.

Location(station number as in Fig. 1)	**Location** (^oN)	(^oE)	year	**R**	**n**	**Slope**	**Intercept**
Thiruvananthapuram (16)	8.53	76.99	2012-13	0.01	21	-0.0003 ± 0.0002	-3.6 ± 0.7
Ponmudi (15)	8.76	77.12	2012-13	0.09	17	0.001 ± 0.001	-3.9 ± 0.6
Idukki (13)	9.94	77.02	2012-13	0.31	15	0.002 ± 0.001	-4.2 ± 0.7
Ernakulam (14)	9.95	76.35	2012	-0.54	9	-0.009 ± 0.005	-1.5 ± 1.4
Thrissur (12)	10.45	76.12	2012-13	0.25	18	0.001 ± 0.001	-3.4 ± 0.5
Palakkadu (10)	10.76	76.27	2012-13	0.35	14	0.002 ± 0.001	-3.4 ± 0.6
Nilambur (9)	11.31	76.21	2012-13	0.57	12	0.003 ± 0.001	-3.6 ± 0.6
Kozhikode-Kavil (7)	11.49	75.77	2012-13	0.47	15	0.003 ± 0.002	-4.9 ± 0.8
Wayanad (8)	11.51	76.02	2012	0.01	7	0.004 ± 0.002	-3.1 ± 1.5
Tirunelveli (17)	8.7	77.7	2003-05	−0.25	12	−0.005 ± 0.006	−2.8 ± 0.5
Kozhikode (10)	11.2	75.8	1997-08	**0.29**	92	0.003 ± 0.001	−4.9 ± 0.5
Mangalore (6)	12.9	74.9	2000-02	**0.85**	7	0.008 ± 0.002	−5.8 ± 0.9
Bangalore (5)	13	77.6	2003-04	−0.31	13	−0.01 ± 0.01	−2.5 ± 1.7
Belgaum (4)	15.9	74.5	2003-05	0.18	12	0.003 ± 0.005	−3.1 ± 1.2

Table 5.2: Table 5.1 cont'd

Location(station number as in Fig. 1)	**Location** (^oN)	(^oE)	year	**R**	**n**	**Slope**	**Intercept**
Kakinada (3)	17	82.2	2003-06	−0.35	24	−0.006 ± 0.004	−3.9 ± 0.9
Hyderabad (2)	17.4	78.5	1997-2008	−0.24	55	−0.011 ± 0.005	−2.7 ± 0.8
Mumbai (1)	18.9	72.8	1960-78	0.16	50	0.001 ± 0.001	−2.0 ± 0.5
Mannar (18)	9	79.9	1983-86	**−0.48**	19	−0.006 ± 0.003	−4.2 ± 0.6
Anuradhapura (19)	8.4	80.4	1983-88	**−0.75**	37	−0.015 ± 0.002	−2.1 ± 0.4
Maha Illuppalla (21)	8.1	80.5	1992-93	**−0.85**	15	−0.009 ± 0.002	−2.4 ± 0.3
Puttalam (20)	8	79.8	1992-93	**−0.64**	15	−0.012 ± 0.04	−2.6 ± 0.6
Batticaloa (22)	7.7	81.7	1983-88	**−0.39**	49	−0.005 ± 0.002	−3.2 ± 0.39
Batalagoda (23)	7.5	80.5	1992-93	**−0.63**	16	−0.012 ± 0.004	−2.6 ± 0.7
Colombo (25)	6.9	79.9	1983-94	−0.06	53	−0.001 ± 0.002	−3.4 ± 0.5
Wellampittiya (24)	7	79.9	2009	**−0.74**	12	−0.023 ± 0.007	−0.87 ± 1.0
Nuwara Eliya (26)	7	80.8	1983-93	−0.14	61	−0.004 ± 0.004	−5.4 ± 0.7
Tanamalwila (27)	6.4	81.1	1983-86	−0.45	10	−0.010 ± 0.007	−3.5 ± 0.9
Hambantota (28)	6.1	81.1	1983-93	**−0.45**	39	−0.018 ± 0.006	−2.8 ± 0.5

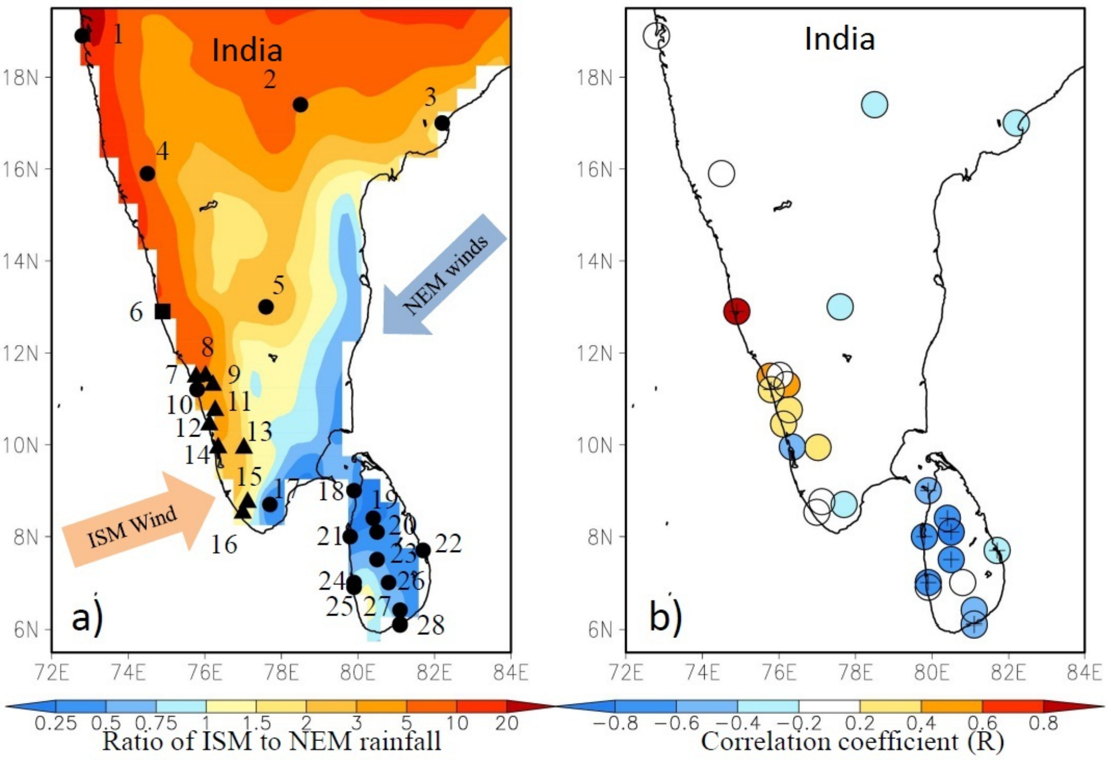

Figure 5.1: **a)** Spatial pattern of the ratio of ISM (JJAS) to NEM (OND) rainfall. Locations with heights above the mean sea level in parentheses are:- 1) Mumbai (10m), 2)Hyderabad (545m), 3) Kakinada (8m), 4) Belgaum (747m), 5) Bangalore (897m), 6) Mangalore (22m), 7) Kozhikode-Kavil (30m), 8) Wayanad (800m), 9) Nilambur (35m),10)Kozhikode (20m) 11) Palakkadu (26m), 12) Thrissur (12m), 13) Idukki (770m), 14) Ernakulam (6m), 15) Ponmudi (780m), 16)Thiruvananthapuram (53m), 17)Tirunelveli (4m), 18) Mannar (5m), 19)Anuradhapura (81m), 20) Puttalam (2m), 21) Maha Illuppallama (137m), 22) Batticaloa (5m), 23) Batalagoda (139m), 24) Wellampittiya(5m), 25) Colombo (7m), 26) Nuwara Eliya (1880m), 27) Tanamalwila (75m), 28) Hambantota (20 m). The wind vectors during ISM and NEM are schematically shown by arrows; circles are GNIP stations while triangles are our stations. Square represents the station of Yadava et al., [2007].**b)** Correlation coefficients between monthly rain and mean monthly $\delta^{18}O$. Values significant at 0.05 level are marked by a plus sign.

the monthly rainfall - $\delta^{18}O$ relation at peninsular India and Sri Lanka appears to be mainly determined by the spatial variation in the relative contributions of ISM and NEM: Significant negative correlations are observed only in regions where the NEM rainfall is higher than ISM rainfall. Weaker negative correlations are observed at stations where the summer and NEM rainfalls are comparable to each other (e.g., Tirunelveli, Bangalore, and Kakinada).

To check if this inference is robust and not an artefact of varying data lengths, we re-analysed the data of all the stations with more than 2 years of data. Correlations for as many consecutive two year periods as allowed by the data length were computed. Fig 5.2 shows a plot of the computed correlation coefficients as a function of the number of data points. It is clear that for stations with less than 14 months of data, the correlation coefficient is not significant. These stations have less data because they receive (a) only ISM rain for a few months; the rest of the year is dry (e.g. Mumbai; nine inverted triangles on the left region of Fig. 5.2) or (b) mainly ISM rain, with occasional pre-monsoon showers enriched in ^{18}O (e.g., Hyderabad; five triangles in the mid-region of Fig. 5.2). For stations with greater than 14 months of data, however, the significance or otherwise of the correlation appears to depends on r: lower this ratio, more significant are the negative correlations. This is also shown in Table 5.3: significant correlations do persist at Anuradhapura and Hambantota (stations 19 and 28). At Batticaloa (station 22), however, the correlation persisted only when r was 0.4. When r reduced further, the correlation deteriorated. This is because the NEM rain alone does not show any amount effect. The amount effect exists because of lower quantity of weakly ^{18}O depleted ISM rain followed by higher quantity of strongly ^{18}O depleted NEM rain. (data points are more at Batticaloa because it receives small amounts of pre-monsoon and ISM rains). There are interannual variations in the significance of the amount effect as revealed by Table 5.3. While we believe that this is mainly due to the relative dominance or otherwise of NEM, the robustness

Table 5.3: Correlation coefficients between monthly rainfall and its $\delta^{18}O$ calculated for every 2 consecutive years for GNIP stations with longer records. Values in bold font are significant at 0.05 level. Number of data points are given in parenthesis The ratios (r) of ISM to NEM rainfall are also tabulated.

Years	1997–98	1998–99	1999–00	2000–01	2001–02	2002–03	2003–04	2004–05	2005–06	2006–07	2007–08
Kozhikode Station,10	0.50 (16)	0.53 (14)	0.57 (14)	0.50 (16)	0.14 (14)	0.18 (13)	0.16 (15)	0.31 (17)	0.43 (18)	0.38 (17)	0.16 (16)
r	4.7	3.9	6.8	4.2	3.3	3.5	4.6	4.7	5.9	7.8	5.6
Hyderabad Station,2		−0.5 (15)	−0.36 (15)						0.00 (11)	0.30 (13)	−0.04 (14)
r		4.0	23.7						3.5	19.4	10.7
Years	1961–62	1962–63	1963–64	1964–65	1965–66	1973–74	1974–75	1975–76	1976–77		
Mumbai Station,1	−0.25 (10)	0.38 (10)	0.58 (9)	−0.09 (7)	−0.67 (8)	0.20 (9)	0.11 (9)	0.54 (10)	0.68 (9)		
r	22.8	46.1	31.3	31.4	142.0	23.1	17.1	19.5	8.9		
Years	1983–84	1984–85	1985–86	1986–87	1987–88	1992–93					
Anuradhapura Station 19	−0.79 (15)			−0.53 (18)							
r	0.5			0.2							
Hambantota Station,28	−0.88 (20)	−0.70 (16)									
r	0.7	0.6									
Batticaloa Station,22	−0.49 (18)	−0.33 (22)	−0.25 (20)	−0.24 (17)							
r	0.4	0.3	0.2	0.1							
Nuwara Eliya Station 26	−0.38 (18)	0.09 (22)	0.07 (16)	−0.50 (17)	−0.49 (16)	0.08 (12)					
r	1.9	2	2.8	1.2	1.3	1.12					
Colombo station 25	0.18 (18)	0.04 (16)	−0.26 (17)			−0.09 (16)					
r	1.19	1.11	0.91			0.99					

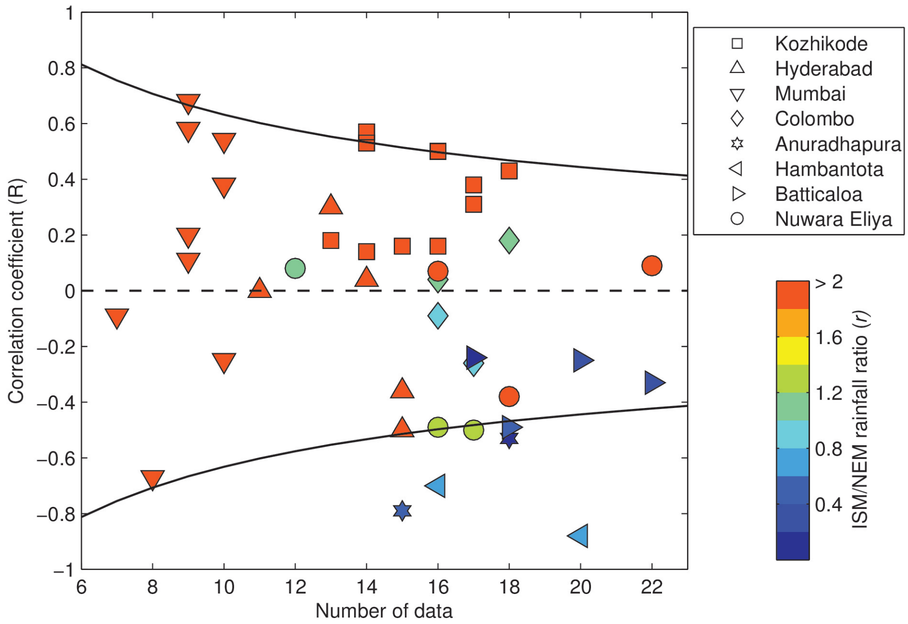

Figure 5.2: Linear correlation coefficient (R) between rainfall and $\delta^{18}O$ (calculated for every 2 consecutive years for GNIP stations with records longer than 2 years) plotted as a function of the number of monthly data. The black lines connect correlation coefficients that are significant at 0.05 level. Points falling outside these lines are significant at a level smaller than 0.05 (i.e., higher significance). Different symbols denote different stations, but with a common color coding based on the ratio (r) of ISM to NEM rainfall.

of our conclusion needs further validation with longer data sets.

5.2 Controls on NEM rainfall $\delta^{18}O$

A stronger ^{18}O depletion of NEM rain relative to ISM rain was explained earlier by i) seasonal runoff from the Ganga- Brahmaputra river system during and after ISM, which depletes the surface Bay of Bengal (BoB) water in ^{18}O, leading to ^{18}O depleted NEM vapour and consequent ^{18}O depletion of NEM rain [*Breitenbach et al.*, 2010; *Singh et al.*, 2010]; ii) ISM rain in western India tends to be the first condensate (even though the air masses travel a long distance over the Indian Ocean) and therefore relatively enriched in ^{18}O; whereas the NEM air mass travels a longer distance over land from its vapour source, the BoB [*Warrier et al.*, 2010], further depleting the ^{18}O of NEM rain over south-western India due to continuous rainfall occurring en route (the continental effect, for the western peninsular India) *Yadava et al.* [2007]. But these two factors appear to have less control on the stronger ^{18}O depletion of NEM than cyclonic activity over BoB, as discussed below.

5.2.1 ^{18}O depletion in BoB surface water

$\delta^{18}O$ value of surface seawater of BoB at the end of ISM is -0.4 ± 0.6 (n = 141, Sep-Oct, 2002 and Aug-Sep, 1988 [*Singh et al.*, 2010], Sept-Dec 2012-2013 [*Achyuthan et al.*, 2013]. We use the Craig and Gordon model (CG model) [*Craig and Gordon*, 1965] to calculate the $\delta^{18}O$ values of the evaporating vapour flux from the ocean during each season [Table 5.4]:

$$R_E = \alpha_{kin} \frac{\frac{R_{Ocean}}{\alpha_{eq}} - R_{atm} h}{1 - h}$$

where, R_E, R_{ocean} and R_{atm} are $\delta^{18}O$ of evaporative flux, sea surface water and the ambient atmospheric vapour, respectively. α_{kin} and α_{eq} are the kinetic and equilibrium fractionation factors and h is the relative humidity. Sea surface temperature (28^{o}C) and wind speed (5m/s) are taken as constants for both the seasons, as the variations are minor: SST climatology from NOAA optimum interpolated data [*Reynolds et al.*, 2002] and NCEP/NCAR reanalysis climatological average winds [*Kalnay et al.*, 1996] during the seasons are less than 7m/s , which is considered as a smooth ocean surface condition [*Merlivat and Jouzel*, 1979]. α_{kin} and α_{eq} were calculated using the equations of *Majoube* [1971] and *Merlivat and Jouzel* [1979]. The calculation of $\delta^{18}O$ values of the evaporating vapour flux was repeated assuming that the vapour over the BoB forms from the evaporating vapour flux alone, without interacting with advected vapour from elsewhere (local closure assumption, $R_{atm} = R_E$; entries 6 to 9 in Table 5.4).

Table 5.4: $\delta^{18}O$ of vapour flux from BoB under different ambient conditions of $\delta^{18}O$ of sea surface, $\delta^{18}O$ of ambient vapour, and relative humidity calculated using the *Craig and Gordon* [1965] model with (1-5) and without (6-9) closure assumption: Values in bold font pertain to observed ambient conditions. Data of $\delta^{18}O$ of ambient vapour and relative humidity are from *Midhun et al.* [2013] and *Srivastava et al.* [2015].

No:	$\delta^{18}O$(‰) Suraface water	$\delta^{18}O$ (‰) Ambient Vapour	RH(%)	$\delta^{18}O$(‰) Evaporative flux
1-ISM	**0.0**	**-11.0**	**80**	**-7.3**
2	0.0	-11.0	70	-10.5
3	-0.38	-11.0	80	-8.8
4	-0.38	-11.0	70	-11.5
5-NEM	**-0.38**	**-12.5**	**70**	**-8.0**
6	0.0	*Under*	70	-10.8
7-ISM	0.0	*closure*	**80**	**-10.2**
8-NEM	**-0.38**	*assumption*	**70**	**-11.2**
9	**-0.38**		80	-10.6

The first five entries of Table 5.4 indicate that the $\delta^{18}O$ of the evaporating vapour flux is not as sensitive to change in the $\delta^{18}O$ of the sea surface as it is to change in h. For the same values of h and $\delta^{18}O$ of vapour, a change of -0.38 ‰ in the $\delta^{18}O$ of the sea surface causes only a 1.3 (h = 70 %) to 1.9 ‰ (h = 80 %) decrease in $\delta^{18}O$ of the evaporating vapour flux. In contrast, the $\delta^{18}O$ of the evaporating vapour flux decreases by 2.6 to 3.2 ‰ when the h decreases from 80 (ISM) to 70 % (NEM) regardless of whether the $\delta^{18}O$ of the sea surface 0 (ISM) or -0.38 ‰ (NEM). On the other hand, a decrease of 1.5 ‰ in the ambient water vapour $\delta^{18}O$ (from -11.0 to $-12.5‰$) increases the $\delta^{18}O$ of evaporating vapour flux by 3.5 ‰ (at 70% relative humidity and -0.38 ‰ sea surface $\delta^{18}O$). Observations and unpublished data of *Midhun et al.* [2013] and *Srivastava et al.* [2015] over BoB during ISM and NEM show that the 0.38‰ decrease in the $\delta^{18}O$ of the sea surface is accompanied by reductions of h from 80 to 70 % and of the $\delta^{18}O$ of ambient water vapour from -11.0 to $-12.5‰$. Thus the $\delta^{18}O$ of evaporating vapour flux decreases only by a resultant of 1‰ (entries 1 and 5, Table 5.4). Repeating the calculation with the local closure assumption confirms this (entries 7 and 8 in Table 5.4). But the observed mean ^{18}O depletion of NEM rainfall is more than 3‰ relative to the ISM rainfall. Thus the reason for the higher ^{18}O depletion in NEM rain cannot be explained by the post-ISM ^{18}O depletion of BoB surface waters by river run-off alone.

5.2.2 Continental effect

The second possibility is that the continuous rainout from a moist air mass originating from BoB travelling westwards leads to a stronger ^{18}O depletion of NEM rain in the western peninsular India. But equally stronger ^{18}O depletion is observed in NEM rain at eastern coastal peninsular India too, where it reaches travelling a lesser distance. NEM shows an average $\delta^{18}O$ of $-5.9 \pm 2.5‰$ (Kozhikode and Mumbai, $-1.9 \pm 0.8‰$ for ISM) in the western peninsula and $-8.3 \pm 1.2‰$ (Kakinada and Hyderabad, $-3.9 \pm 1.4‰$ for ISM) in the eastern peninsula [Fig 5.3].

Interestingly the first condensate on NEM shows stronger ^{18}O depletion in the eastern peninsular India, and therefore the $\delta^{18}O$ difference between ISM and NEM rain is not just due to ISM rain being the first condensate in the western peninsula as stated by *Warrier et al.* [2010]. On the contrary, NEM rain is relatively more enriched in ^{18}O over the western peninsular India compared to the eastern side. This could be either due to the continental moisture recycling

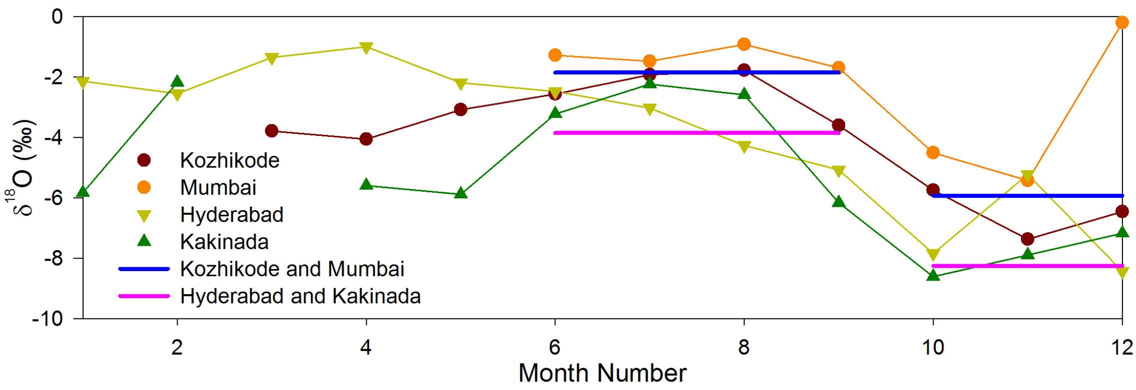

Figure 5.3: Monthly mean rainfall $\delta^{18}O$ at Kozhikode, Mumbai (Western peninsular India), Hyderabad and Kakinada (Eastern peninsular India). Seasonal averages (ISM-JJAS) and (NEM-OND) of stations in western and eastern peninsular India are marked as blue and magenta lines in the figure.

or the marine influence from the Arabian Sea, or both. Thus the continental effect also does not seem play a major role in the observed higher ^{18}O depletion of NEM rainfall.

5.2.3 Effect of cyclonic disturbances in BoB

NEM season is characterised by increased cyclonic activity over the BoB. It is reported that rainfall associated with tropical cyclones elsewhere too is more depleted in ^{18}O [e.g., *Fudeyasu et al.*, 2008; *Lawrence and Gedzelman*, 1996]. In organized convective systems, processes such as increased post condensation isotopic equilibration of rain drops with the ambient water vapour and rain drop re-evaporation occur. Such moisture recycling have been suggested to be responsible for stronger ^{18}O depletion of rain as well as the water vapour in the sub-cloud layer [*Kurita et al.*, 2011; *Risi et al.*, 2012]. Tropical cyclones and low pressure systems (depressions) in BoB during NEM, detected by the IMD are marked in Fig 5.4. The strongest ^{18}O depletion of NEM rainfall at Kozhikode co-occurs

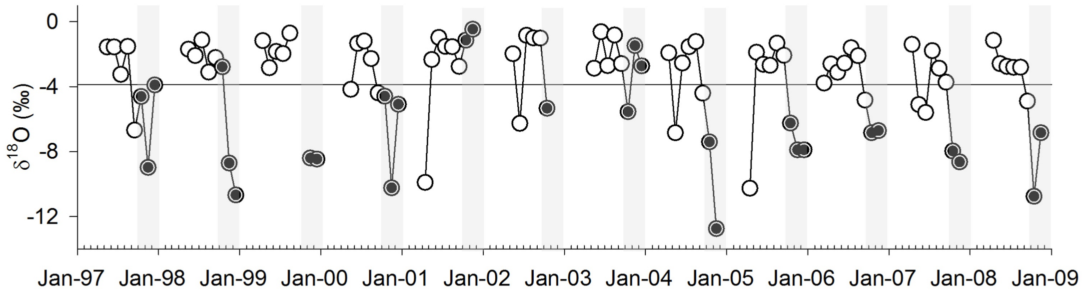

Figure 5.4: Time series of $\delta^{18}O$ of monthly rainfall at Kozhikode. Filled circles indicate the presence of cyclones in the Bay of Bengal during NEM.

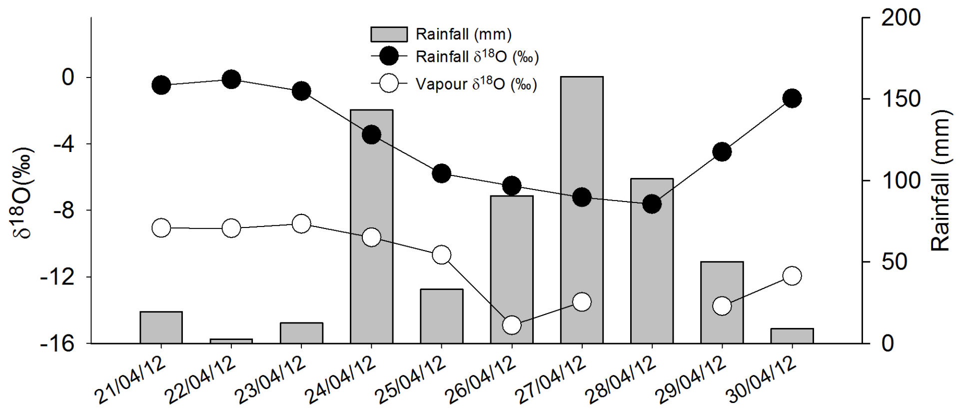

Figure 5.5: Variation of mean rainfall (vertical bars), its $\delta^{18}O$ (filled circle) (mean of 8 stations) and $\delta^{18}O$ of water vapour (mean of two stations, open circle) from stations in Kerala during a cyclonic storm that occurred during the last week of April 2012.

with cyclonic activities over BoB (18 out of 23 ^{18}O -depleted monthly events). Thus the stronger ^{18}O depletion of NEM rain could be due either to the rain caused by the low pressure systems or ii) the lateral advection and mixing of ^{18}O depleted remnant vapour of the immediate prior low pressure systems. Yet, a few cyclones are observed during some months with no depletion in ^{18}O (5 out of 23 events), possibly because the prevailing wind did not favour the advection of ^{18}O depleted vapour to the west.

In addition, there are a few months with higher ^{18}O depletion, which are not accounted by any cyclone or depression detected by IMD. Depressions and cyclones are determined according to the wind speed and pressure gradients. There are common occurrences of weak low pressure systems in the tropical Indian oceans during the pre-ISM (April, May) and NEM seasons, which do not intensify into depression or cyclones. A case study of a cyclonic storm that occurred over the southern peninsular India during April, 2012 shows [Fig 5.5] an ^{18}O depletion in rain (average of 8 stations) as well as in the ground level vapour (average of 2 stations). The typical strong depletion of ^{18}O in rain caused by depressions was also recorded over the Bay of Bengal [*Midhun et al.*, 2013]. Thus, the increased cyclonic activity over the Bay seems to play a significant additional role in the strong ^{18}O depletion of NEM rain.

5.3 Rainfall- $\delta^{18}O$ relation on a seasonal scale

Table 5.5 show the rainfall- $\delta^{18}O$ relation on different time scales; all monthly data, annual totals, monthly data of different seasons, viz., pre-ISM, ISM and NEM, and seasonal totals at Kozhikode (the GNIP station with the longest record in peninsular India/Sri Lanka). The monthly rainfall- $\delta^{18}O$ relation shows a significant inverse amount effect, while the monthly rainfall- $\delta^{18}O$ relations during the pre monsoon, ISM and NEM seasons are statistically insignificant. However,

Table 5.5: Slope, correlation coefficients and the statistical significance of rainfall - $\delta^{18}O$ relations at Kozhikode on different time scales. Ranges of monthly and seasonal rainfall variation are also given. Correlations which are statistically significant at P=0.05 level are given in bold.

Data		n	Slope (‰/mm)	R	Rainfall range Min:	Max:
All months		94	0.003±0.001	0.29	0	1383
Annual total		12	-0.0007±0.0004	-0.50	2131	4657
Monthly	Pre monsoon	18	-0.004±0.003	-0.29	0	864
	Summer monsoon	48	-0.0001±0.0007	-0.02	39	1383
	Post monsoon	28	0.001±0.004	0.03	0	579
Seasonal total	Pre monsoon	10	-0.003±0.002	-0.44	99	962
	Summer monsoon	12	-0.0007±0.0002	-0.76	1146	3744
	Post monsoon	12	-0.01±0.01	-0.36	377	617

the annual total rainfall and corresponding weighted mean $\delta^{18}O$ show a negative relation, significant at $P < 0.1$ level, while the ISM seasonal total rainfall and its $\delta^{18}O$ show a highly significant negative correlation ($P < 0.01$). This implies that the year to year variation of monsoon rainfall is almost well captured in the seasonal total rainfall $\delta^{18}O$, while the sub-seasonal (daily or monthly) rainfall amount and its $\delta^{18}O$ variation are random according to the processes occurring within the season. $\delta^{18}O$ of Kozhikode ISM rainfall also shows [Fig. 5.6] a weak negative relation with the ISM rainfall anomaly over south peninsular India and all India (i.e., with the regional rainfall amounts rather than the local rainfall). However, the seasonal total rainfall- $\delta^{18}O$ relations of pre monsoon and NEM seasons remain insignificant.

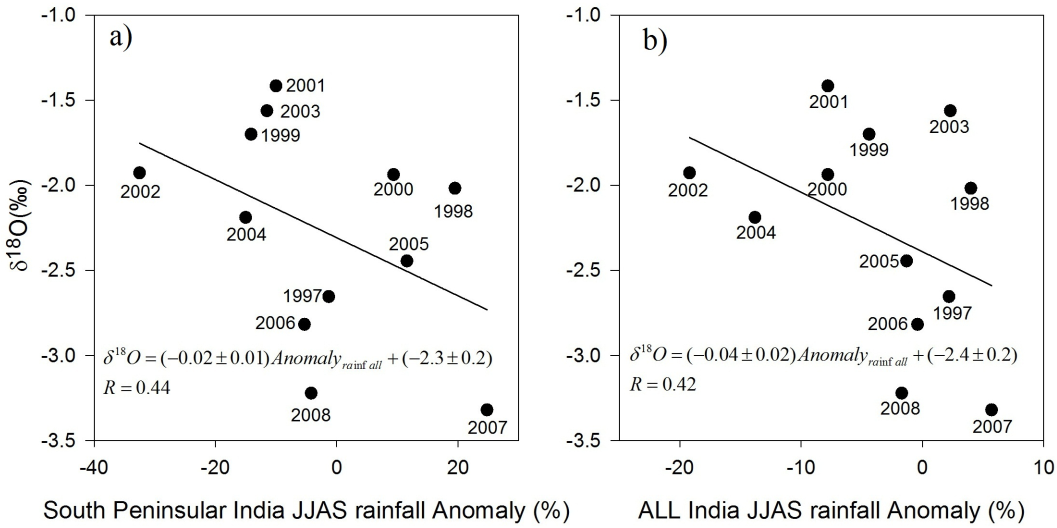

Figure 5.6: a) Relation between ISM rainfall anomaly at peninsular India and $\delta^{18}O$ of rain at Kozhikode. b) Relation between all India ISM rainfall anomaly and $\delta^{18}O$ of rain at Kozhikode.

5.4 Conclusion

Varying seasonal rainfall amounts in peninsular India and Sri Lanka lead to a large spatial variation in the slopes of the rainfall amount -$\delta^{18}O$ relations. The stronger ^{18}O depletion of NEM rainfall is likely affected by increased cyclonic activity over the Bay of Bengal, in addition to ^{18}O depletion of its surface waters. This leads to significant negative correlations between monthly rainfall and its $\delta^{18}O$ chiefly in regions where the North East Monsoon contributes more than, or at least as much rain as the Indian Summer Monsoon. The amount effect also vanishes when the ISM reduces significantly. There are year to year variations in the amount effect, again due to varying relative contributions of ISM and NEM rain. Our results show that a careful choice of sites for ^{18}O based monsoon proxies can be made so as to minimise noise in the paleomonsoon signal: from proxies capable of providing annual resolution (e.g., fast growing trees) past annual monsoon rainfall can be reconstructed at sites where the ratio of ISM to NEM rain is less than or comparable to unity, using the local amount effect.

Chapter 6

Summary and recommendations

Isotope hydrological studies in India deserve importance because of their potential in paleomonsoon reconstruction.The present study is a step towards understanding the hydrological cycle in the southern peninsular India, especially during the Indian Summer Monsoon (ISM). The major findings of this study are as follows

6.1 Results from the study of stable isotopes of monsoon rainfall

1. The daily monsoon rainfall shows a large spatial heterogeneity among the 9 sampling locations in Kerala, while their $\delta^{18}O$ and δD variations are highly coherent. This indicates that the monsoon rain at all these stations are formed from the same cloud system spread over the region; the rain amounts are different due to differences in orography.

2. The strongly ^{18}O depleted events observed during monsoon season are associated with large scale organized convection over the southeastern Arabian Sea, near the Kerala coast. In contrast, the weakly ^{18}O depleted events are observed to be formed from isolated clouds which are mostly located

along the Western Ghats. The TRMM rainfall and the Outgoing Longwave Radiation (OLR) shows significantly distinct spatial patterns during these events of stronger and weaker ^{18}O depleted rain events.

3. Analyses of proxies of convection such as OLR and vertical wind velocity show high moisture convergence and intense convection in the southern peninsular India, which can effectively take the recycled strongly ^{18}O-depleted moisture from the sub cloud layer into the cloud systems.

4. $\delta^{18}O$ of daily rain shows a strong negative correlation with the amount of rainfall over the southeastern Arabian Sea rather than with the measured local rain amounts. This signifies the importance of moisture recycling occurring in the area of large scale organised convection in determining the stronger isotopic depletions in rain, compared to areas of isolated local rain events.

6.2 Results from rain and vapour interaction studies

1. Water vapour and rain are comparatively enriched in ^{18}O and D during the pre monsoon period relative to ISM but they are more depleted in ^{18}O and D during NEM compared to ISM.

2. Rain and moisture isotopic compositions of ISM are characterised by little alteration from locally derived moisture. But rain-vapour interactions occurring in large scale organised convective clouds lead to intraseasonal variations in rain and vapour stable isotopic composition during ISM.

3. During NEM, ^{18}O depletion is stronger in the rain (by $\sim$4‰) compared to water vapour (by $\sim$2‰). This is because the NEM rainfall at the sampling

sites directly form from clouds, which are already depleted in ^{18}O and D, while the surface water vapour is altered by local evapo-transpiration.

4. The average isotopic fractionation factor (between rain and vapour) of all the samples (April- October) is close to the equilibrium value but it deviates more from the equilibrium values during the NEM.

5. The d-excess ($d = \delta D - 8\delta^{18}O$) in rain and water vapour shows a very weak seasonal cycle with lower values during ISM relative to NEM and the pre monsoon.

6. During ISM, stronger heavier isotopic depletion is observed in rain and water vapour in association with the large scale organized convective activity that occurs in the southeastern Arabian Sea, near the Kerala coast. The fraction of stratiform rain from the large scale convective cloud region shows a significant negative correlation with the $\delta^{18}O$ of vapour and $\delta^{18}O$ of rain; this signifies the importance of stratiform clouds in moisture recycling in large scale organized convective systems.

6.3 Results from studies on the rainfall-$\delta^{18}O$ relations in peninsular India and Sri Lanka

1. The rainfall-$\delta^{18}O$ relation shows large spatial variations over peninsular India and Sri Lanka.

2. Significant positive rainfall-$\delta^{18}O$ relations are observed at Kozhikode and Mangalore, where the ISM rainfall contributes more to the annual total rainfall compared to the NEM rainfall.

3. Significant negative rainfall-$\delta^{18}O$ relations are observed in most stations in Sri Lanka where the NEM rainfall contributes more to the annual total rainfall.

4. The spatial variation of the slopes of the rainfall-$\delta^{18}O$ relation over Peninsular India and Sri Lanka is decided by the spatial variation of ratio of ISM to NEM rainfall amounts. i.e., positive relations are observed mainly in regions where the ISM rainfall contributes more to the annual total rainfall. Significant negative relations are observed in regions where the NEM rainfall contributes either more than (or comparable to the ISM rainfall) to the annual total rainfall.

5. Strong isotopic depletion of NEM rainfall is not only due to the strong isotopic depletion of the Bay of Bengal surface water by the river water discharge from Ganga and Brahmaputra during the monsoon months.

6. Continental effect does not play any role in the observed stronger isotopic depletion of NEM rainfall over peninsular India.

7. Heavy isotopic depletion observed in the NEM monthly data at Kozhikode shows a co-occurrence with cyclonic activity (cyclones, depressions) in the Bay of Bengal. Stronger ^{18}O depletion of NEM rainfall relative to ISM rainfall could be due to (i) either their association with low pressure systems or ii) the lateral advection and mixing of ^{18}O depleted remnant vapour left by the immediately preceding low pressure systems.

8. Though the rainfall - $\delta^{18}O$ relation at Kozhikode shows a positive correlation in monthly data, a significant negative relation is observed between the annual total rainfall and the corresponding $\delta^{18}O$. This is a good news for paleoclimatologists who use tree ring $\delta^{18}O$ to reconstruct total monsoon rainfall.

9. The ISM seasonal total rainfall and its $\delta^{18}O$ show a highly significant negative correlation. This implies that the year to year variations of the ISM rainfall is almost well captured in the seasonal total rainfall $\delta^{18}O$, while

the sub-seasonal (daily or monthly) rainfall amount and its $\delta^{18}O$ variation could vary according to the processes occurring within the season.

6.4 Recommendations

In the recent years, though much work has been done on the present topic, continuous monitoring of rain and water vapour isotopic compositions are required to improve the understanding of the hydrological cycle and their potential in paleoclimate reconstructions. Future scope for such studies

1. We have identified the importance of large scale organised convection in the southeastern Arabian Sea, near the Kerala coast, in regulating the stable isotopic composition of ISM rainfall in southern peninsular India. This is likely due to the intense moisture recycling occurring in such systems. In this context, continuous monitoring of rain and water vapour isotopes from marine atmosphere from this region (Lakshadweep Islands) can provide better insight to the underlying processes.

2. The contribution from continental recycled moisture (soil evaporation and transpiration) to the hydrological cycle over India is not well understood. This has to be addressed using high resolution (spatio-temporal), simultaneous rain and vapour isotope observations.

3. A continuous monitoring of rainfall and water vapour stable isotopic composition is essential for understanding effect of interannual variations of monsoon on water stable isotopes. This will also help to understand the role of remote forcing through large scale circulations(e.g., El Nino) on ISM.

4. A strong intra-seasonal variation in rainfall and vapour stable isotopic compositions is observed. This is linked to the prevailing meteorological conditions. Hence the potential of the newly available satellite based δD observations to reveal the physical processes during monsoon intra-seasonal

oscillations can be assessed. Use of isotope enabled General Circulation Models (GCM) can also help in such studies.

5. Using the high resolution (sub-annual and sub-seasonal) sample analysis techniques, the potential of tree ring cellulose ^{18}O from Kerala in capturing the intra-seasonal variation of rainfall ^{18}O (owing the large scale organised convection occurring in this region) can be validated.

References

Achyuthan, H., et al. (2013), Stable isotopes and salinity in the surface waters of the Bay of Bengal: Implications for water dynamics and palaeoclimate, *Marine Chemistry*, *149*, 51–62.

Adler, R. F., et al. (2003), The version-2 Global Precipitation Climatology Project (GPCP) monthly precipitation analysis (1979-present), *Journal of hydrometeorology*, *4*(6), 1147–1167.

Ahmad, M., P. Aggarwal, M. v. Duren, L. Poltenstein, L. Araguas, T. Kurttas, and L. Wassenaar (2012), Final report on fourth interlaboratory comparison exercise for δ^2H and $\delta^{18}O$ analysis of water samples (WICO2011), *Tech. rep.*, International Atomic Energy Agency, Isotope Hydrology Laboratory, Division of Physical and Chemical Sciences, Department of Nuclear Sciences and Applications, Vienna (Austria).

Araguás-Araguás, L., K. Froehlich, and K. Rozanski (1998), Stable isotope composition of precipitation over southeast Asia, *Journal of Geophysical Research: Atmospheres (1984–2012)*, *103*(D22), 28,721–28,742.

Augustin, L., et al. (2004), Eight glacial cycles from an Antarctic ice core, *Nature*, *429*(6992), 623–628.

Berkelhammer, M., C. Risi, N. Kurita, and D. Noone (2012), The moisture source sequence for the Madden-Julian Oscillation as derived from satellite retrievals of HDO and H2O, *Journal of Geophysical Research: Atmospheres (1984–2012)*, *117*(D3).

Bhalme, H., S. Rahalkar, and A. Sikder (1987), Tropical Quasi-Biennial Oscillation of the 10-mb wind and Indian monsoon rainfall-implications for forecasting, *Journal of climatology*, *7*(4), 345–353.

Bhattacharya, S., K. Froehlich, P. Aggarwal, and K. Kulkarni (2003), Isotopic variation in Indian Monsoon precipitation: records from Bombay and New Delhi, *Geophysical Research Letters*, *30*(24).

Breitenbach, S. F., J. F. Adkins, H. Meyer, N. Marwan, K. K. Kumar, and G. H. Haug (2010), Strong influence of water vapor source dynamics on stable isotopes in precipitation observed in Southern Meghalaya, NE India, *Earth and Planetary Science Letters*, *292*(1), 212–220.

Carolin, S. A., K. M. Cobb, J. F. Adkins, B. Clark, J. L. Conroy, S. Lejau, J. Malang, and A. A. Tuen (2013), Varied response of western Pacific hydrology to climate forcings over the last glacial period, *Science*, *340*(6140), 1564–1566.

Chakraborty, S., and R. Ramesh (1993), Monsoon-induced sea surface temperature changes recorded in Indian corals, *Terra Nova*, *5*(6), 545–551.

Chapman, S., and T. G. Cowling (1951), *The Mathematical Theory of Non-uniform Gases*, Cambridge University Press.

Charles, C., D. Hunter, and R. G. Fairbanks (1997), Interaction between the ENSO and the Asian monsoon in a coral record of tropical climate, *Science*, *277*(5328), 925–928.

Chattopadhyay, R., B. N. Goswami, A. Sahai, and K. Fraedrich (2009), Role of stratiform rainfall in modifying the northward propagation of monsoon intraseasonal oscillation, *Journal of Geophysical Research: Atmospheres (1984–2012)*, *114*(D19).

Clark, I. D., and P. Fritz (1997), *Environmental isotopes in hydrogeology*, CRC press.

Cobb, K. M., J. F. Adkins, J. W. Partin, and B. Clark (2007), Regional-scale climate influences on temporal variations of rainwater and cave dripwater oxygen isotopes in northern Borneo, *Earth and Planetary Science Letters*, *263*(3), 207–220.

Craig, H. (1957), Isotopic standards for carbon and oxygen and correction factors for mass-spectrometric analysis of carbon dioxide, *Geochimica et cosmochimica acta*, *12*(1), 133–149.

Craig, H., and L. I. Gordon (1965), Deuterium and oxygen-18 variations in the ocean and the marine atmosphere.

Crowley, T. J. (2000), Causes of climate change over the past 1000 years, *Science*, *289*(5477), 270–277.

Dansgaard, W. (1964), Stable isotopes in precipitation, *Tellus*, *16*(4), 436–468.

Dansgaard, W., et al. (1993), Evidence for general instability of past climate from a 250-kyr ice-core record, *Nature*, *364*(6434), 218–220.

Datta, P., S. Tyagi, and H. Chandrasekharan (1991), Factors controlling stable isotope composition of rainfall in New Delhi, India, *Journal of Hydrology*, *128*(1), 223–236.

Deshpande, R., A. Maurya, B. Kumar, A. Sarkar, and S. Gupta (2010), Rain-vapor interaction and vapor source identification using stable isotopes from semiarid western India, *Journal of Geophysical Research: Atmospheres (1984–2012)*, *115*(D23).

Draxler, and G. Rolph (2003), HYSPLIT (HYbrid Single-Particle Lagrangian Integrated Trajectory) model access via NOAA ARL READY website (http://www. arl. noaa. gov/ready/hysplit4. html). NOAA Air Resources Laboratory, Silver Spring.

Epstein, S., and T. Mayeda (1953), Variation of O-18 content of waters from natural sources, *Geochimica et cosmochimica acta*, *4*(5), 213–224.

Esper, J., E. R. Cook, and F. H. Schweingruber (2002), Low-frequency signals in long tree-ring chronologies for reconstructing past temperature variability, *science*, *295*(5563), 2250–2253.

Fasullo, J. (2004), A stratified diagnosis of the Indian monsoon-Eurasian snow cover relationship, *Journal of climate*, *17*(5), 1110–1122.

Feng, X., A. M. Faiia, and E. S. Posmentier (2009), Seasonality of isotopes in precipitation: A global perspective, *Journal of Geophysical Research: Atmospheres (1984–2012)*, *114*(D8).

Forster, P., et al. (2007), Changes in atmospheric constituents and in radiative forcing. Chapter 2, in *Climate Change 2007. The Physical Science Basis.*

Fudeyasu, H., K. Ichiyanagi, A. Sugimoto, K. Yoshimura, A. Ueta, M. Yamanaka, and K. Ozawa (2008), Isotope ratios of precipitation and water vapor observed in Typhoon Shanshan, *Journal of Geophysical Research: Atmospheres (1984–2012)*, *113*(D12).

Gadgil, S. (2003), The Indian monsoon and its variability, *Annual Review of Earth and Planetary Sciences*, *31*(1), 429–467.

Gadgil, S., and S. Gadgil (2006), The Indian monsoon, GDP and agriculture, *Economic and Political Weekly*, pp. 4887–4895.

Gedzelman, S., J. Lawrence, J. Gamache, M. Black, E. Hindman, R. Black, J. Dunion, H. Willoughby, and X. Zhang (2003), Probing hurricanes with stable isotopes of rain and water vapor, *Monthly weather review*, *131*(6), 1112–1127.

Goswami, B. N., V. Venugopal, D. Sengupta, M. Madhusoodanan, and P. K. Xavier (2006), Increasing trend of extreme rain events over India in a warming environment, *Science*, *314*(5804), 1442–1445.

Goswami, P., and V. Mathew (1994), A mechanism of scale selection in tropical circulation at observed intraseasonal frequencies, *Journal of the atmospheric sciences*, *51*(21), 3155–3166.

Houze J R, R. A. (1997), Stratiform precipitation in regions of convection: A meteorological paradox?, *Bulletin of the American Meteorological Society*, *78*(10), 2179–2196.

Huffman, G. J., D. T. Bolvin, E. J. Nelkin, D. B. Wolff, R. F. Adler, G. Gu, Y. Hong, K. P. Bowman, and E. F. Stocker (2007), The TRMM multisatellite precipitation analysis (TMPA): Quasi-global, multiyear, combined-sensor precipitation estimates at fine scales, *Journal of Hydrometeorology*, *8*(1), 38–55.

Jasechko, S., Z. D. Sharp, J. J. Gibson, S. J. Birks, Y. Yi, and P. J. Fawcett (2013), Terrestrial water fluxes dominated by transpiration, *Nature*, *496*(7445), 347–350.

Joseph, P., A. Simon, V. G. Nair, and A. Thomas (2004), Intra-Seasonal Oscillation (ISO) of south Kerala rainfall during the summer monsoons of 1901–1995, *Journal of Earth System Science*, *113*(2), 139–150.

Kalnay, E., et al. (1996), The NCEP/NCAR 40-year reanalysis project, *Bulletin of the American meteorological Society*, *77*(3), 437–471.

Kumar, B., et al. (2010), Isotopic characteristics of Indian precipitation, *Water Resources Research*, *46*(12).

Kumar, K. K., B. Rajagopalan, M. Hoerling, G. Bates, and M. Cane (2006), Unraveling the mystery of Indian monsoon failure during El Nino, *Science*, *314*(5796), 115–119.

Kurita, N. (2013), Water isotopic variability in response to mesoscale convective system over the tropical ocean, *Journal of Geophysical Research: Atmospheres*, *118*(18), 10–376.

Kurita, N., D. Noone, C. Risi, G. A. Schmidt, H. Yamada, and K. Yoneyama (2011), Intraseasonal isotopic variation associated with the Madden-Julian Oscillation, *Journal of Geophysical Research: Atmospheres (1984–2012)*, *116*(D24).

Lawrence, J. R., S. D. Gedzelman, J. Gamache, and M. Black (2002), Stable isotope ratios: hurricane Olivia, *Journal of Atmospheric Chemistry*, *41*(1), 67–82.

Lawrence, R. J., and D. S. Gedzelman (1996), Low stable isotope ratios of tropical cyclone rains, *Geophysical Research Letters*, *23*(5), 527–530.

Lee, J.-E., and I. Fung (2008), "Amount effect" of water isotopes and quantitative analysis of post-condensation processes, *Hydrological Processes*, *22*(1), 1–8.

Lekshmy, P., M. Midhun, R. Ramesh, and R. Jani (2014), ^{18}O- depletion in monsoon rain relates to large scale organized convection rather than the amount of rainfall, *Scientific reports*, *4*.

Leuschner, D. C., and F. Sirocko (2003), Orbital insolation forcing of the Indian Monsoon–a motor for global climate changes?, *Palaeogeography, Palaeoclimatology, Palaeoecology*, *197*(1), 83–95.

Liebmann, B. (1996), Description of a complete (interpolated) outgoing longwave radiation dataset, *Bull. Amer. Meteor. Soc.*, *77*, 1275–1277.

Majoube, M. (1971), Fractionation of oxygen 18 and of deuterium between water and its vapor, *J. Chem. Phys*, *68*, 1423–1436.

Managave, S., M. Sheshshayee, A. Bhattacharyya, and R. Ramesh (2011), Intra-annual variations of teak cellulose $\delta^{18}O$ in Kerala, India: implications to the reconstruction of past summer and winter monsoon rains, *Climate dynamics*, *37*(3-4), 555–567.

Masson-Delmotte, V., et al. (2013), Information from paleoclimate archives, *Climate change 2013: The physical science basis*, pp. 383–464.

Merlivat, L., and J. Jouzel (1979), Global climatic interpretation of the deuterium-oxygen 18 relationship for precipitation, *Journal of Geophysical Research: Oceans (1978–2012)*, *84*(C8), 5029–5033.

Midhun, M., P. Lekshmy, and R. Ramesh (2013), Hydrogen and oxygen isotopic compositions of water vapor over the Bay of Bengal during monsoon, *Geophysical Research Letters*, *40*(23), 6324–6328.

Moerman, J. W., K. M. Cobb, J. F. Adkins, H. Sodemann, B. Clark, and A. A. Tuen (2013), Diurnal to interannual rainfall $\delta^{18}O$ variations in northern Borneo driven by regional hydrology, *Earth and Planetary Science Letters*, *369*, 108–119.

Mook, W. G. (2006), *Introduction to isotope hydrology*, Taylor & Francis.

Moore, M., Z. Kuang, and P. Blossey (2014), A moisture budget perspective of the amount effect, *Geophysical Research Letters*, *41*(4), 1329–1335.

Moreira, M., L. Sternberg, L. Martinelli, R. Victoria, E. Barbosa, L. Bonates, and D. Nepstad (1997), Contribution of transpiration to forest ambient vapour based on isotopic measurements, *Global Change Biology*, *3*(5), 439–450.

New, M., D. Lister, M. Hulme, and I. Makin (2002), A high-resolution data set of surface climate over global land areas, *Climate research*, *21*(1), 1–25.

Overpeck, J., D. Anderson, S. Trumbore, and W. Prell (1996), The southwest Indian Monsoon over the last 18 000 years, *Climate Dynamics*, *12*(3), 213–225.

Pang, H., Y. He, Z. Zhang, A. Lu, and J. Gu (2004), The origin of summer monsoon rainfall at New Delhi by deuterium excess, *Hydrology and Earth System Sciences*, *8*(1), 115–118.

Petit, J.-R., et al. (1999), Climate and atmospheric history of the past 420,000 years from the Vostok ice core, Antarctica, *Nature*, *399*(6735), 429–436.

Rajeevan, M., S. Gadgil, and J. Bhate (2010), Active and break spells of the Indian summer monsoon, *Journal of earth system science*, *119*(3), 229–247.

Rajendran, K., A. Kitoh, J. Srinivasan, R. Mizuta, and R. Krishnan (2012), Monsoon circulation interaction with Western Ghats orography under changing climate, *Theoretical and Applied Climatology*, *110*(4), 555–571.

Ramesh, R., and M. Yadava (2005), Climate and water resources of India, *Current Science*, *89*(5), 818.

Ramesh, R., S. Bhattacharya, and G. Pant (1989), Climatic significance of δD variations in a tropical tree species from India, *Nature*.

Ramesh, R., M. Tiwari, S. Chakraborty, S. Managave, M. Yadava, and D. Sinha (2010), Retrieval of south Asian monsoon variation during the Holocene from natural climate archives., *Current Science (00113891)*, *99*(12), 1771–1786.

Ramesh, R., S. Managave, P. Lekshmy, A. Laskar, M. Yadava, and R. Jani (2012), Comment on "Tracing the sources of water using stable isotopes: first results along the Mangalore-Udupi region, south-west coast of India", *Rapid Communications in Mass Spectrometry*, *26*(7), 874–875.

Reynolds, R. W., N. A. Rayner, T. M. Smith, D. C. Stokes, and W. Wang (2002), An improved in situ and satellite SST analysis for climate, *Journal of climate*, *15*(13), 1609–1625.

Rienecker, M. M., et al. (2011), MERRA: NASA's modern-era retrospective analysis for research and applications, *Journal of Climate*, *24*(14), 3624–3648.

Risi, C., S. Bony, and F. Vimeux (2008), Influence of convective processes on the isotopic composition ($\delta^{18}O$and δD) of precipitation and water vapor in the tropics: 2. Physical interpretation of the amount effect, *Journal of Geophysical Research: Atmospheres (1984–2012)*, *113*(D19).

Risi, C., et al. (2012), Process-evaluation of tropospheric humidity simulated by general circulation models using water vapor isotopic observations: 2. Using isotopic diagnostics to understand the mid and upper tropospheric moist bias in the tropics and subtropics, *Journal of Geophysical Research: Atmospheres*, *117*(D5).

Roden, J. S., G. Lin, and J. R. Ehleringer (2000), A mechanistic model for interpretation of hydrogen and oxygen isotope ratios in tree-ring cellulose, *Geochimica et Cosmochimica Acta*, *64*(1), 21–35.

Rozanski, K., L. Araguás-Araguás, and R. Gonfiantini (1993), Isotopic patterns in modern global precipitation, *Climate change in continental isotopic records*, pp. 1–36.

Sano, M., R. Ramesh, M. Sheshshayee, and R. Sukumar (2011), Increasing aridity over the past 223 years in the Nepal Himalaya inferred from a tree-ring $\delta^{18}O$ chronology, *The Holocene*, pp. 809–817.

Sengupta, S., and A. Sarkar (2006), Stable isotope evidence of dual (Arabian Sea and Bay of Bengal) vapour sources in monsoonal precipitation over north India, *Earth and Planetary Science Letters*, *250*(3), 511–521.

Sheshshayee, M. S., H. Rao Bindumadhava, R. Ramesh, T. Ganesh Prasad, M. R. Lakshminarayana, and M. Udayakumar (2005), Oxygen Isotope Enrichment

($\Delta^{18}O$) as a time averaged measure of transpiration rate, *Isotopes in environmental and health studies*, *56*(422), 3033–3039.

Sheshshayee, M. S., H. Rao Bindumadhava, R. Ramesh, T. Ganesh Prasad, and M. Udayakumar (2010), Relationship between ^{18}O enrichment in leaf biomass and stomatal conductance, *Isotopes in environmental and health studies*, *46*(1), 122–129.

Singh, A., R. Jani, and R. Ramesh (2010), Spatio-temporal variations of the $\delta^{18}O$-salinity relation in the northern Indian Ocean, *Deep Sea Research Part I Oceanographic Research Papers*, *57*, 1422–1431.

Singh, A., A. Mohiuddin, R. Ramesh, and S. Raghav (2014), Estimating the Loss of Himalayan Glaciers under Global Warming Using the $\delta^{18}O$–Salinity Relation in the Bay of Bengal, *Environmental Science & Technology Letters*, *1*(5), 249–253.

Sinha, A., G. Kathayat, H. Cheng, S. F. Breitenbach, M. Berkelhammer, M. Mudelsee, J. Biswas, and R. Edwards (2015), Trends and oscillations in the Indian summer monsoon rainfall over the last two millennia, *Nature Communications*, *6*.

Srivastava, R., R. Ramesh, N. Gandhi, R. Jani, and A. K. Singh (2015), Monsoon onset signal in the stable oxygen and hydrogen isotope ratios of monsoon vapor, *Atmospheric Environment*, *108*, 117–124.

Thompson, L., et al. (1997), Tropical climate instability: The last glacial cycle from a Qinghai-Tibetan ice core, *Science*, *276*(5320), 1821–1825.

Tiwari, M., R. Ramesh, B. Somayajulu, A. Jull, and G. Burr (2006), Paleomonsoon precipitation deduced from a sediment core from the equatorial Indian Ocean, *Geo-Marine Letters*, *26*(1), 23–30.

Wang, B. (2006), *The Asian Monsoon*, Praxis Publishing.

Wang, X. F., and D. Yakir (2000), Using stable isotopes of water in evapotranspiration studies, *Hydrological Processes*, *14*(8), 1407–1421.

Wang, Y., et al. (2008), Millennial-and orbital-scale changes in the East Asian monsoon over the past 224,000 years, *Nature*, *451*(7182), 1090–1093.

Warrier, C. U., M. P. Babu, P. Manjula, K. Velayudhan, A. S. Hameed, and K. Vasu (2010), Isotopic characterization of dual monsoon precipitation–evidence from Kerala, India, *Current Science*, *98*(11), 1487–1495.

Worden, J., et al. (2007), Importance of rain evaporation and continental convection in the tropical water cycle, *Nature*, *445*(7127), 528–532.

Xie, L., G. Wei, W. Deng, X. Zhao, et al. (2011), Daily $\delta^{18}O$ and δD of precipitations from 2007 to 2009 in Guangzhou, South China: Implications for changes of moisture sources, *Journal of Hydrology*, *400*(477-489), 207–220.

Yadava, M., R. Ramesh, and G. Pant (2004), Past monsoon rainfall variations in peninsular India recorded in a 331-year-old speleothem, *The Holocene*, *14*(4), 517–524.

Yadava, M., R. Ramesh, and K. Pandarinath (2007), A positive'amount effect'in the Sahayadri (Western Ghats) rainfall, *Current science*, *93*(4), 560–564.

Yonge, C. J., L. Goldenberg, and H. R. Krouse (1989), An isotope study of water bodies along a traverse of southwestern Canada, *Journal of Hydrology*, *106*(3), 245–255.

List of Publications

Papers in Refereed Journals

1. R Ramesh, SR Managave, **PR Lekshmy**, AH Laskar, MG Yadava, RA Jani (2012) Comment on "Tracing the sources of water using stable isotopes: first results along the Mangalore-Udupi region, south-west coast of India", *Rapid Communications in Mass Spectrometry* 26 (7), 874-875, doi: 10.1002/rcm.6174.

2. M Midhun, **PR Lekshmy** and R Ramesh (2013), Hydrogen and Oxygen Isotopic Compositions of Water Vapour over Bay of Bengal during Monsoon, *Geophysical Research Letters* 40, 6324-6328, doi:10.1002/2013GL058181.

3. **PR Lekshmy**, M. Midhun, R. Ramesh, and R. A. Jani (2014), ^{18}O depletion in monsoon rain relates to large scale organized convection rather than the amount of rainfall, *Nature Scientific Reports*, 1-5, doi:10.1038/srep05661.

4. **PR Lekshmy**, M. Midhun and R. Ramesh (2015), Spatial variation of amount effect over peninsular India and Sri Lanka: role of seasonality, *Geophysical Research Letters* 42, doi:10.1002/2015GL064517.

5. **PR Lekshmy**, M. Midhun and R. Ramesh (2015), Influence of stratiform clouds on δD and $\delta^{18}O$ of monsoon water vapour and rain in a tropical hill station ,*Journal of Atmospheric Chemistry* (under review).

Abstract presented in conferences

1. **P.R.Lekshmy**, M.Midhun, R.Ramesh, and R.A.Jani (2013) Is the Isotopic Composition of Rainfall of the South west coast of India Independent of Local Rainfall Amount? 12th ISMAS Triennial International Conference on Mass Spectrometry, March 4-8, Dona Paula, Goa..

2. M.Midhun, **P.R.Lekshmy**, R.Ramesh, and R.A.Jani (2013) Stable isotopic composition of atmospheric vapour over the Bay of Bengal and its relation with ocean surface conditions, 12th ISMAS Triennial International Conference on Mass Spectrometry, March 4-8, Dona Paula, Goa.

3. Band S, AH Laskar, **PR Lekshmy**, M Midhun, MG Yadava and R Ramesh (2014) Holocene monsoon variability derived from speleothems, Mini Symposium on Reconciliation of Marine and Terrestrial Records of Summer Monsoon Variability during the Holocene, 80^{th} INSA Anniversary General Meeting, December 19-21, Goa.

4. **Lekshmy, PR**, M.Midhun and R.Ramesh (2015),Rain- vapour isotopic interaction over the south-west coast of India, European Geophysical Union General Assembly, April 12-17,2015, Vienna, Austria.

5. Midhun M, **PR Lekshmy** and R.Ramesh (2015),Short-term Variability of Indian Summer Monsoon Rainfall $\delta^{18}O$, European Geophysical Union General Assembly, April 12-17,2015, Vienna, Austria.